THE AMERICAN MINERALOGIST

JOURNAL OF THE MINERALOGICAL SOCIETY OF AMERICA

Vol. 32 JANUARY–FEBRUARY, 1947 Nos. 1 and 2

SOME PROPERTIES OF MATERIALS USED FOR JEWEL INSTRUMENT BEARINGS

HERBERT INSLEY, H. F. McMURDIE, W. H. PARSONS AND B. L. STEIERMAN,
National Bureau of Standards, Washington, D. C.

ABSTRACT

Information on the physical properties of materials used for jewel bearings which was obtained in the course of tests by the National Bureau of Standards for the Bureau of Aeronautics, U. S. Navy, is summarized. Inherent properties of the material which affect the ease of fabrication and the performance in use are described for the principal materials used for jewel bearings in aviation instruments, namely, synthetic and natural corundum (sapphire and ruby), synthetic spinel, and glass. Some incidental observations on the properties of synthetic spinel in relation to its use as a possible optical material are also included.

I. INTRODUCTION

In the course of an investigation on jewel bearings for instruments, conducted under authorization of the Bureau of Aeronautics, United States Navy,[1] the National Bureau of Standards made a number of tests and examinations of various materials used for this purpose. The present report summarizes the results of these laboratory tests so far as they give information on the suitability of the materials for the use intended as well as for other possible technical uses. Data are provided on the hardness, strength, homogeneity and structural defects in these materials. No attempt has been made in this investigation to evaluate the dimensions, shape and bearing surfaces of the jewels or the quality of the finish on the bearing surfaces.

The principal bearing materials investigated were corundum (sapphire and ruby), spinel and glass.

II. CORUNDUM

Corundum (αAl_2O_3) is the only one of the several forms of alumina which is used, either as a naturally occurring mineral or as a synthetic product for making jewel bearings. Detailed descriptions of the properties and crystallography of corundum can be found in standard textbooks on mineralogy.[2] Strictly speaking, red varieties of corundum are called ruby, and blue varieties sapphire. Frequently, however, the name sapphire is given to any variety other than red and it is often used as a general name for all gem bearings made of corundum.

---

[1] This work was done under order NAer 00076, NBS Project no. 6324.

1. *Natural crystals*

The only natural corundum crystals submitted to this Bureau for examination and test were from a deposit in Montana and were submitted by the Defense Supplies Corporation. They were graded into sizes designated 5, 6 and 8, apparently corresponding to these sieve numbers. The crystals represented whole individuals or fragments in the form of partially waterworn, barrel-like prisms and thick plates. In color they were blue, green, pink, yellow, or lavender. No information was supplied by the Defense Supplies Corporation as to the source in Montana of these crystals. It is known that sapphire crystals have been obtained from at least two sources in that state, one at Philipsburg and the other at Yogo Gulch. It is understood that most of the supplies in recent years have come from Philipsburg.

The average percentage of stones rejected from purchased lots by the gem fabricators because of cracks, inclusions, etc., is not known. Two bearing manufacturers who appraised a lot of stones from the Defense Supplies Corporation at the request of the National Bureau of Standards agreed that about 60 per cent of these stones were suitable for bearing manufacture. As supplied to the bearing fabricators, natural corundum crystals are furnished in size grades depending on the size of the bearing to be cut. Even with size grading, however, the waste in cutting to size is probably at least as great as the waste in cutting synthetic boules of the conventional shape.

There is only one twinning plane in corundum, that parallel to the rhombohedral face $(10\bar{1}1)$. The twins produced may be of the interpenetration or repeated polysynthetic type. The crystals from the Montana source showed little external evidence of twinning.

While there is no good cleavage direction in corundum, there are two possible parting directions, one parallel to the base (0001) and the other parallel to the rhombohedron $(10\bar{1}1)$. The development of the parting along the rhombohedral plane appears to be greatly intensified by the presence of twinning along the same plane. The parting may affect the usefulness of the natural crystals for instrument bearings because it may increase the breakage in fabrication.

---

[2] Dana's Textbook of Mineralogy, E. S. Dana and W. E. Ford, 4th ed. (John Wiley & Sons, New York, 1932).

Gems and Gem Minerals, E. H. Kraus and C. B. Slawson, 4th ed. (McGraw-Hill Book Co. New York, 1941).

The hardness of natural corundum, which is designated as 9 on the Mohs scale of scratch hardness, is more precisely rated by the Knoop and Peters[3] method, using a wedge-shaped diamond indenter impressed into the test material by a definite load. By this method the hardness number of corundum is found to vary with the relation of the indenter direction to the crystallographic direction. Measurements[4] were made on the finished lower surface of Montana sapphire instrument bearings in random directions with respect to the crystallographic *c* axis. For the 100 gram load the hardness numbers were found to range from 1700 to 2000 and for the 500 gram load from 1450 to 1730. This is about the range of hardness numbers obtained by indentations made in surfaces of synthetic sapphires. The variation in hardness with crystallographic direction is appreciable and significant. The indenter marks parallel to the *c* axis, or to its projection on the surface tested, usually are perfect, whereas those oblique or perpendicular to the *c* axis usually show fracture marks perpendicular to the *c* axis extending from the ends of the long axis of the indenter. These are probably cracks parallel to the basal parting plane caused by the pressure of the indenter.

Natural corundum may contain inclusions of liquid or of crystals such as rutile or hematite, but in general these are not a major cause of loss in the fabrication of gem bearings and such inclusions are rarely found in the finished bearings.

2. *Artificial Corundum*

As far as is known, all artificial corundum or artificial sapphire used for gem bearings is manufactured by methods which are basically the same as that of Verneuil.[5] By this method powdered raw material is introduced through the pipe of an oxyacetylene or oxyhydrogen blowtorch which is surrounded axially by a cylindrical furnace with insulated refractory walls. The raw material is usually very pure ammonium alum which is introduced into the blowpipe after reduction to a very fine powder by calcination. The raw material, melted in the flame of the blowtorch, impinges on a fire clay or other refractory base and there solidifies, building up from a small tip into a cylindrical or elongated pearshaped form called a boule. As the boule grows, the fire-clay base is lowered by a mechanical or hand-operated screw until the required length is reached, when the flame is turned off and the boule is allowed to cool in the furnace for some time before removal to the open air.

---

[3] A sensitive pyramidal-diamond tool for indentation measurements. Frederick Knoop, Chauncey G. Peters and Walter B. Emerson: *J. Research NBS*, **23,** 39 (1939); *RP* **1220.**

[4] Made by C. G. Peters, of the National Bureau of Standards.

[5] Verneuil, A. V. L., *Comptes rendus*, **150,** pp. 185–187. *Idem.*, U. S. Patents 988,230 and 1,004,505 (1911). Kraus and Slawson, *op. cit.*, pp. 124–134.

With the exception of twinning bands in some boules, the corundum made by the process just described is essentially a single crystal and even the rod forms, which may be several feet long, are a single crystal from end to end.

To color artificial corundum, small amounts of other oxides are added to the aluminum oxide in the raw material, one or two per cent of chromium oxide for ruby, and a mixture of iron oxide and titanium oxide for sapphire.

After removal from the furnace the elongated pear-shaped corundum crystals either split spontaneously or may be readily split into halves along the longitudinal axis (Fig. 1) by nipping off the small tip with a pair of pliers or by rapping the boule sharply on the tip with a hammer. The *c* axis almost without exception lies in the split plane.

The splitting of boules on the plane containing the *c* axis may be explained by the differences in the coefficient of thermal expansivity in different crystallographic directions in corundum. As determined by J. B. Austin[6] for a blue Indian sapphire, the mean linear coefficient is 8.2×10^{-6} for the direction parallel to the principal axis (the crystallographic *c* axis) and 7.2×10^{-6} for the direction perpendicular to this axis over the temperature range 20° to 1,000°C. Preliminary determinations on oriented slices of an artificial corundum boule by A. S. Creamer, of the National Bureau of Standards, gave values which are essentially in agreement with those of Austin. Since the thermal expansivity of a crystallographically uniaxial crystal (such as corundum) may be represented by an ellipsoid of revolution with the *c* axis as the revolution axis, and since the boule shape also is a figure of revolution, the cooling of any boule in which the *c* axis is oblique to the boule axis results in a concentration of strain in the plane containing these axes, the release of which takes place by splitting along this plane.

The orientation has been determined by *x*-rays at the National Bureau of Standards on a number of specimens of artificial corundum. Of the 56 boules of the pear-shaped type on which the orientation has been determined, 55 had the *c* axis lying in the split plane. Of the latter, 15 (or 27 per cent) had orientations such that the *c* axis made an angle of 80° or more with the boule axis, and 29 (or 53 per cent) had orientations such that the *c* axis made an angle of 70° or more with the boule axis. The number of specimens decreased with decrease in the angle and only one

---

[6] *J. Am. Ceram. Soc.*, **14,** 795 (1941).

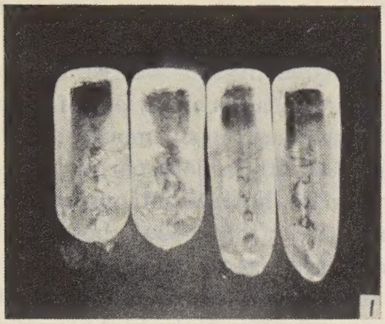

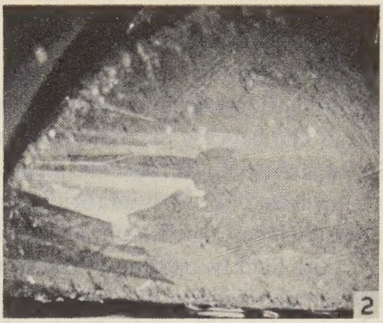

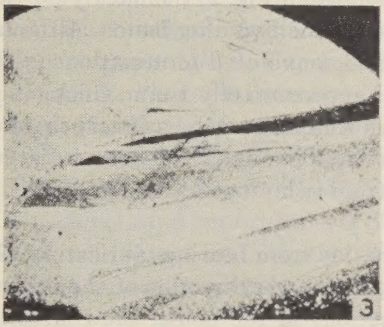

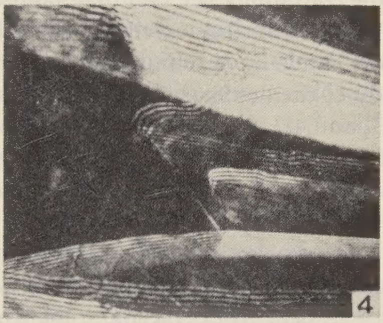

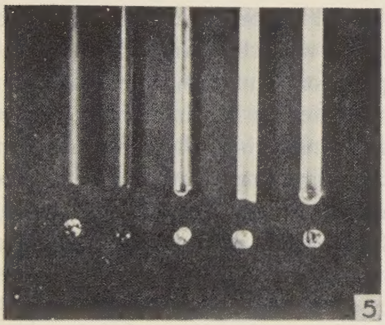

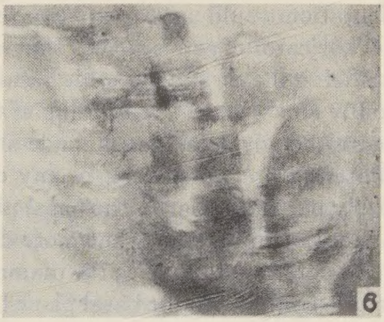

FIG. 1. Two artificial sapphire boules showing the split surface. ⅔ natural size.

FIG. 2. A transverse slice from a split corundum boule showing twinning bands and folds. Polarized light. Crossed nicols. Mag. 5½×.

FIG. 3. Cross-section of a sapphire boule showing banding and inhomogeneities. Polarized light. Crossed nicols. Mag. 5×.

FIG. 4. Same specimen as Fig. 3 at a higher magnification. Polarized light. Crossed nicols. Mag. 27×.

FIG. 5. Rod-shaped synthetic corundum and spinel boules. ⅔ natural size.

FIG. 6. Split surface of a sapphire boule showing striations and banding. Ordinary light. Mag. 7×.

was found with an angle of less than 20° between the *c* axis and the boule axis.

Winchell[7] has made a much more detailed analysis on a larger number of boules and has correlated the orientation with the behavior of the material in the process of manufacture of jewel bearings. Among other results of his work, he observed that boules with smooth parting planes gave lower loss in bearing fabrication than did those with rough or hackly parting surfaces. Our examination of only two or three of such boules indicates that hackly parting surfaces are related to areas in the boules in which repeated twinning takes place in the rhombohedral plane. In the boule containing the twinning bands shown in Fig. 2, the hackly portion of the split surface extends only as far as the twinning bands. Although these bands have rounded, irregular and convoluted terminations in the body of the boule as observed in slices approximately 1 mm. thick (Figs. 2, 3, and 4), alternate bands extinguish simultaneously, as in repeated or polysynthetic twinning, and the extinction angles between adjacent bands have the values to be expected from twinning on the rhombohedral twinning plane of corundum.

If, as appears probable from information from bearing fabricators, the ease and perfection of boule slicing depend on the direction of the saw cut with respect to crystallographic directions in the boule, the control of orientation would appear to be of practical importance. It is claimed by one fabricator of gem bearings that cutting with the diamond saw exactly parallel to the crystallographic basal plane of corundum takes place more rapidly and with less splintering of the material than in any other direction, although if the cut is made slightly off this plane, fracturing and splintering are worse than in any other direction. Cuts made approximately perpendicular to the basal plane take place with little fracturing, but the cutting is somewhat more difficult. This opinion is corroborated by the determination with the diamond indenter, which shows the softest direction parallel to the basal plane but with flaws extending out from the indenter mark parallel to this plane. In order to have easier control of orientation as well as to obtain a sample which gives less waste in cutting bearings, a domestic producer has modified the furnace operation so that long, thin rods $1\frac{1}{2}$ to 4 mm. in diameter are produced (Fig. 5) instead of the usual pear-shaped boule. The orientation is controlled by starting the formation in the furnace on a slice of corundum whose orientation has been determined. The new rod builds up on the "seed" with the same orientation. The manufacturer of the rod forms provides[8] the following information concerning the most favorable orientation. Corundum rods which are to be worked thermally for such uses as thread guides should have orientations of from 30° to 75° between the *c* axis and the rod axis and preferably between 40° and 50°. Moreover, the plane of bending for such rods should coincide as nearly as possible with the plane containing the *c* axis and the rod axis. "For cutting and grinding operations synthetic corundum rods wherein the angle is between 30° and 80°, and preferably between 40° and 80°, are recommended for the maximum yield of usable products such as jewel bearing blanks."

---

[7] Winchell, Horace, Orientation of synthetic corundum for jewel bearings: *Am. Mineral.*, **29**, 399–413 (1944).

[8] Personal communication from M. H. Barnes, of the Linde Air Products Co.

While determination of the relation of crystallographic directions to the boule axis can be made most precisely by means of *x*-rays, there are some visual indications of the crystallographic orientation of the split surfaces of some boules. Figure 6 shows the split surface of such a boule at a magnification of 7 diameters. The fine parallel oblique striations (not to be confused with the nearly horizontal, broad bands) lie in the direction of the *c* axis. After a little practice these lines can be found with the unaided eye on the majority of boules having split surfaces.

The defects and impurities in artificial corundum are unlike those found in the natural material. Foreign crystals are rarely, if ever, observed in artificial corundum although gas bubbles are sometimes found. The gas bubbles, when present, are usually arranged in a zone paralleling one of the surfaces of the boule. Structure lines consisting of numerous fine parallel striations can sometimes be seen in artificial corundum, especially in the colored varieties. The cause of these striations is unknown, but they are probably due to an uneven distribution of the pigment.

Hardness determinations on synthetic corundum crystals made by the Knoop indenter agree quite well with those made on natural corundum crystals. A typical set of hardness numbers by the Knoop indenter as determined by C. G. Peters,[9] of the National Bureau of Standards, is given in the table below:

	100 grams	500 grams
Artificial corundum		
Indentation parallel to *c* axis	2000 P[1]	1670 P
Indentation perpendicular to *c* axis	1660 P	1525 F[2]

[1] P = perfect indentation.

[2] F = light fracture.

Although these values are within the range of those found by Winchell,[10] there are some discrepancies between the two sets of observations as to the relation of the Knoop number to orientation. In part, the discrepancies may be the result of the apparent low hardness number parallel to the basal plane caused by the tendency to part along this plane. It is obvious, nevertheless, that experiments are necessary in which the direction of the indenter and the orientation of the plane on which the indentations are made are carefully controlled.

---

[9] Personal communication.

[10] Winchell, Horace, The Knoop microhardness tester as a mineralogical tool: *Am. Mineral.*, **30**, 583–595 (1945).

Optically, artificial corundum is not significantly different from natural corundum. The indices of refraction are practically identical and the colored varieties of artificial corundum, like the natural type, are pleochroic.

The specific electrical resistance of a single crystal of artificial corundum as measured at the National Bureau of Standards[11] was found to be 1 megohm at 1214°C. parallel to the *c* axis and 1 megohm at 1231°C. perpendicular to the *c* axis.

3. *Corundum as Instrument Bearings.*

Corundum (sapphire and ruby) has long been used as a bearing material in watches, chronometers, compasses, watt-hour meters and other instruments. As such, corundum has the advantage of its considerable hardness, toughness and resistance to impact. It has the disadvantage, however, that it is much harder than the metals commonly used for pivots. In bearings of the Vee type (having a conical surface) for instruments subject to vibration, this causes wear and deformation of the pivot. The accumulation of iron oxide resulting from the abrasion and rusting causes an increase in friction. Since the pivot with its attached parts is usually more difficult and expensive to replace than the bearings, there is a belief among some engineers that the bearing material should have approximately the same hardness as the pivot material. In ring bearings differential hardness may cause ellipticity in the opening, with consequent increase in frictional resistance.

III. SPINEL

Another material having properties which make it suitable for use as gem bearings is the mineral spinel. While spinel in pieces large enough for gem bearings occurs in nature less abundantly than corundum, it can readily be made artificially.

Although the chemical formula of true spinel is $MgO.Al_2O_3$ with a composition by weight of 28.3 per cent MgO and 71.7 per cent Al_2O_3, Rankin and Merwin[12] have found that the composition of homogeneous spinels may be extended by solid solution of alumina to a limiting composition of 7 per cent MgO, 93 per cent Al_2O_3. Rinne[13] has shown that spinels made by the Verneuil process show a continuous variation in physical properties up to a molecular composition of about $MgO.4Al_2O_3$. It has been found in commercial production that excess of magnesia over the composition $MgO.Al_2O_3$ causes the crystallization of periclase (MgO) with the spinel, which gives rise to the disruption of the boule during cooling. For this reason spinels are generally made with excess alumina.

---

[11] Geller, R. F., Yavorsky, P. J., Steierman, B. L., and Creamer, A. S., *J. Research NBS*, **36**, 277 (1946); *RP* **1703.**

[12] *J. Am. Chem. Soc.*, **38**, 568–588 (1916).

So far as is known, natural spinel has not been used for instrument or meter bearings although it is well known as a decorative gem material.

Artificial spinel has been made for a number of years. It is produced with the same apparatus as artificial corundum. The raw material used is a mixture of magnesia and alumina, of magnesium carbonate and ammonium alum, or of similar materials which will give the required ratio of magnesia to alumina. The solidified material, like artificial corundum, occurs in the form of a pearshaped boule with a narrow stem below and a broad top. Artificial spinel boules, unlike artificial corundum, often have fairly well developed crystal faces corresponding to those of the cube, octahedron and dodecahedron. As the boule forms in the furnace, the rounded upper portion and the vertical sides are generally cube faces (Fig. 7) and the octahedral faces constitute the pyramidal planes (Figs. 7 and 8). The velvety matte appearance of the top surface of the boule is caused by the projecting pyramidal surfaces of microscopic crystals (Fig. 9).

Spinel boules in the rod-shaped forms similar to those of corundum (Fig. 5) have also been manufactured in this country. These grow spontaneously with the fourfold axis (the cube axis) coincident with the rod axis.

Blue spinels and green spinels are produced by the addition of small amounts of cobalt oxide and chromium oxide, respectively, to the batch mixture.

A detailed description of the artificial spinels, including the crystal faces observed as well as other physical and chemical properties, has been published by F. Rinne.[14]

Since spinel is a compound, the crystals of which belong to the isometric (cubic) system, it should have no double refraction and, therefore, should show no interference effects between crossed polarizing prisms. As a matter of fact all synthetic spinels made and cooled in the usual manner in the furnace show marked double refraction and heterogeneous interference patterns. The double refraction appears to be due in part to

---

[13] *Neues Jahr. für Mineral., Geol.,* und *Pal.: Beilage Band* **58,** Abt. A, 43–108 (1928).

[14] *Op. cit.*

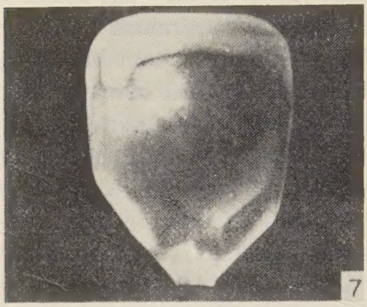

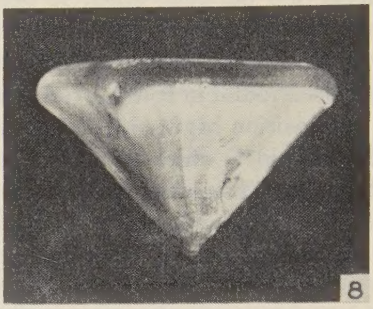

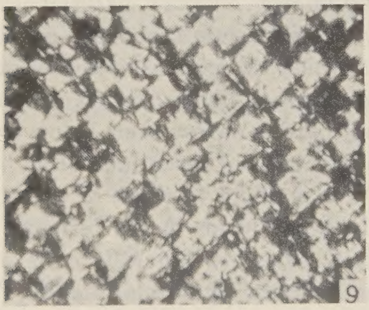

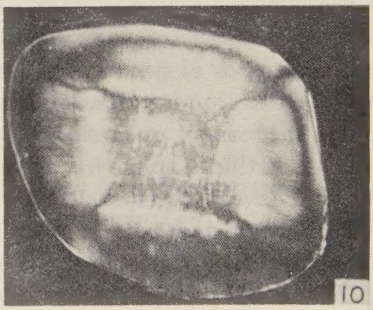

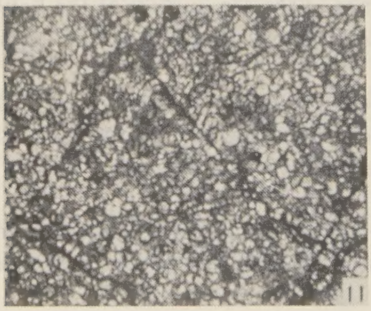

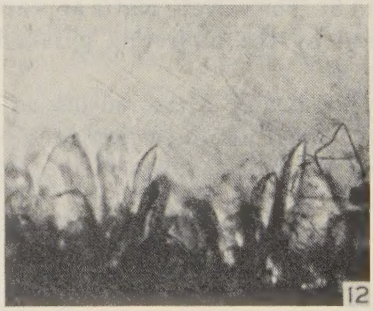

FIG. 7. Spinel boule showing crystal faces. Mag. about $1\frac{1}{3}\times$.

FIG. 8. Spinel boule showing crystal faces. $\frac{2}{3}$ natural size.

FIG. 9. Crown of a spinel boule showing projecting surfaces of microscopic crystals. Mag. 33×.

FIG. 10. Cross section of a spinel boule showing distribution of birefringent elements. Polarized light. Crossed nicols. Mag. $2\frac{1}{2}\times$.

FIG. 11. Crystallization in a slice from a spinel boule after heating at 1725°C. for one-half hour. Polarized light. Crossed nicols. Mag. 33×.

FIG. 12. Same slice as shown in Fig. 11 viewed on edge. Ordinary light. Mag. 80×.

the strain developed by rapid cooling. In part, however, it is related to the alumina content of the boule, the double refraction increasing with increase in the alumina content. The distribution and form of the strain patterns were studied at this Bureau on slices from a spinel boule which was furnished by a domestic manufacturer. This boule is understood to contain about 10 per cent MgO and 90 per cent Al_2O_3. It has a central core in which the birefringent components are distributed in a grating arrangement and an outer portion with a radiating fibrous structure (Fig. 10).

Determinations of hardness[15] made with the diamond indenter in the same manner as those made on the sapphire gave the following values:

Sample	*100 g*	*500 g*
Spinel #1, parallel to boule axis	1380 P[1]	1205 P
Spinel #1, 45° to boule axis	1339 P	1340 P
Spinel #2, parallel to boule axis	1339 P	1179 F[2]

[1] P = perfect indentation

[2] F = light fracture

Hardness is not significantly different for spinels of different colors or for different directions in a spinel crystal.

Because spinel has a hardness between that of sapphire and that of the hardest glass so far tested, it appeared to be promising for use as jewel Vee bearings. It was considered that the use of spinel would cause less deformation and fragmentation of the pivots than sapphire bearings and at the same time would provide a bearing less likely to fracture than glass. While preliminary tests appear promising, the only spinel bearings available for vibration testing with steel pivots had bearing surfaces so rough and so full of "blowholes" that data useful for comparison with data on glass and sapphire could not be obtained.

During examination of spinel for use as a bearing material, it was observed that spinel was a material with such high index of refraction and such low dispersion that it would be exceptional for use in certain optical installations provided other properties were satisfactory. The table below[16] gives the refractive index (n) for certain wave lengths of light, the Abbe value for the relative dispersion

$$\left(V=\frac{n_D-1}{n_F-n_C}\right)$$

and the mean dispersion (n_F-n_C).

---

[15] Made by C. G. Peters, of the National Bureau of Standards.

[16] Rinne, *op. cit.*, Tables 5 and 6.

Substance		$\lambda(A)$	n	V	$n_F - n_C$
$MgO \cdot Al_2O_3$	(C)	6563	1.7143		
(spinel)	(D)	5893	1.7182	60.86	0.0118
	(F)	4861	1.7261		
$MgO \cdot 5Al_2O_3$	(C)	6563	1.7243		
(spinel)	(D)	5893	1.7280	61.70	0.0118
	(F)	4861	1.7361		
Quartz (ω)	(D)	5893	1.5442	69.8	0.0078
Crown Glass	(D)	5893	1.5181	59.0	0.0088
Flint Glass	(D)	5893	1.6199	36.3	0.0171
Flint Glass	(D)	5893	1.727	28.8	0.0252

Unfortunately, the strain birefringence of artificial spinel is sufficient to destroy its optical homogeneity and to make it useless for most optical purposes. In consideration of the possibility of removing the strain by annealing, it was noted that a heat treatment of a boule at 1050°C. for a long period of time by Rinne[17] had resulted in the crystallization of corundum. An attempt at the National Bureau of Standards to remove the strain by annealing at 1750°C. also caused the crystallization of corundum as shown in Figs. 11 and 12. In a further attempt, annealing experiments were carried out on pieces of spinel rods furnished by the manufacturer, composed of MgO 10 per cent, Al_2O_3 90 per cent, and on a spinel prism of unknown composition and origin. They were heated by R. F. Geller, of the National Bureau of Standards, in a high-temperature resistor furnace of his design[18] at a temperature of 1950°C. for about 20 minutes. For the composition of the rod boule this temperature is close to the solidus as indicated by the diagram of Rankin and Merwin.[19] The heat treatment caused a very marked reduction in the birefringence (Figs. 13 and 14) of the rod specimens. The spinel prism was badly warped by heating at about the same temperature and there was considerable surface crystallization of corundum. Either the temperature distribution in the furnace was such as to cause partial melting of the spinel or the prism contained even more alumina than did the rods. These preliminary experiments indicate that suitable heat treatments can reduce the birefringence of artificial spinels very markedly without causing the crystallization of excess alumina and it seems probable that more can be done in this direction by further experiments. With the strain birefringence removed, spinel should have many advantages for optical uses.

---

[17] *Op. cit.*

[18] *J. Research NBS*, **27**, 555–566 (1941); *RP* **1443.**

[19] *Op. cit.*

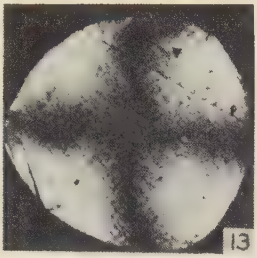

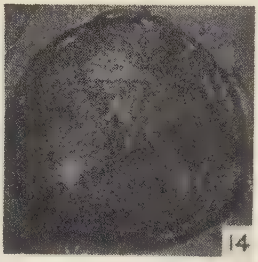

FIG. 13. Cross section of rod-shaped artificial spinel boule, as received. Polarized light. Crossed polaroids. Mag. 11×.

FIG. 14. Cross section of same boule as shown in Fig. 13 after annealing at 1950°C. for 20 minutes. Polarized light. Crossed polaroids. Mag. 11×.

IV. GLASS

For some time glass has been a recognized substitute for sapphire bearings in certain aviation installations where the weight of the pivot and indenter is kept below a specified maximum. Five types of glass used for this purpose have been tested by the National Bureau of Standards: an ordinary commercial soda-lime glass, two types of glass containing boric oxide (Pyrex brand) and two high-alumina glasses.

Of all the glasses tested the alumina glasses had the best performance records as Vee bearings. An approximate analysis of one of the latter was made at the National Bureau of Standards. The results are:

	Per cent	
SiO_2	57.0	
Al_2O_3	20.5	(including small amounts of Fe_2O_3 and P_2O_5)
CaO	5.5	
MgO	12.0	
B_2O_3	4.0	
Na_2O	1.0	

This is an unusually high Al_2O_3 content.

Using the same indenter method as that used on sapphire and spinel bearings, some measurements were made on glass bearings. The results are given below:

Material	*Hardness value*
Soda-lime glass (bottle glass)	440
Pyrex	400
High-alumina glass	560

For comparison, fused quartz has an indenter hardness value of 490.

Although all glass-bearing material is less resistant to fracture under impact than either sapphire or spinel, glass has the advantage that it is less liable to injure the pivot by abrasion. Even with molded surfaces, glass jewels are less abrasive than sapphires and spinels with polished surfaces.

Other properties of glass bearings that may affect their service are the presence of bubbles and the degree of strain. Bubbles when small in size, few in number and distant from the bearing surface probably have little or no effect on the life of the bearing. When abundant and large, however, (Fig. 15), they are very likely to intersect the bearing surface, thus increasing the friction of the pivot by providing rough surfaces to abrade the pivot. Glass put under high compressive stresses by quenching is known to be tougher under some conditions than well annealed glass, but when subjected to impact by a sharp instrument (such as a pivot), it may shatter completely. Consequently it is considered better from a practical point of view to use well annealed rather than highly strained glass jewels. Other inhomogeneities such as striae (cords) and small "stones" (crystalline nuclei) are probably not of importance unless they produce high localized strain in the glass or unless the crystalline material occurs at the bearing surface.

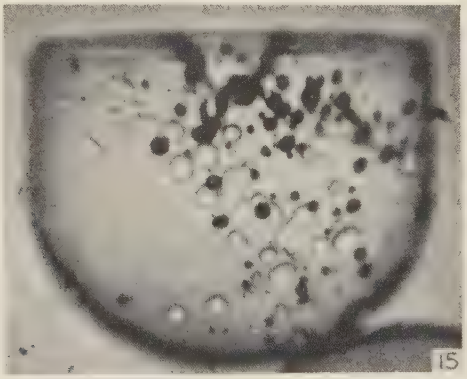

FIG. 15. Glass Vee jewel showing distribution of bubbles in glass. Mag. 29×.

V. OTHER BEARING MATERIALS

Other nonmetallic bearing materials than those described above have been proposed, including vitrified porcelain and organic plastics. One sample of porcelain and one of organic plastic were examined at the

National Bureau of Standards. The surface of the porcelain even when well polished was still too rough to afford a satisfactory bearing surface. The organic plastic was too soft and too weak to be a satisfactory bearing material.

VI. SUMMARY

This report provides a brief compilation and comparison of the significant properties of the three principal nonmetallic instrument bearing materials, corundum (sapphire), spinel and glass. Of the three, corundum has the greatest hardness and strength, but its hardness is so much greater than the usual steel instrument pivots that under continued vibration the pivots tend to deform, rust accumulates in the bearing and friction increases. Glass has about the same hardness as the steel pivots, but glass bearings may break under vibration and impact. Spinel is intermediate between corundum and glass in strength and hardness and, therefore, should have advantages as a bearing material, but sufficient data on actual vibration and wear tests of spinel bearings have not yet been accumulated to draw conclusions as to its service behavior. Some incidental observations on the physical properties of artificial spinel in relation to its use as a possible optical material are also included.

SOME COMPUTATIONS ON SVANBERGITE, WOODHOUSEITE AND ALUNITE

A. PABST, *University of California, Berkeley, California.*

ABSTRACT

Computations have been carried out to correct the indexing of a powder diffraction pattern of svanbergite found in the literature. Similar computations lead to the first published indexing of powder patterns of woodhouseite. Parameters are obtained for the structures of these two minerals. Less extended computations for alunite, using the parameters given by Hendricks, afford a basis for evaluating the results. They also afford a check on the reliability of standard patterns recorded on ASTM cards.

Incidentally the transformation from hexagonal to rhombohedral axes is discussed.

INTRODUCTION

Svanbergite is a rare member of the alunite-beudantite group. Its composition may be written $SrAl_3(SO_4)(PO_4)(OH)_6$. In a recent paper Ygberg[1] has reported on a powder diffraction of svanbergite and has calculated lattice dimensions and density.

Minerals of the alunite-beudantite group have been shown by Hendricks[2] to have a rhombohedral lattice. Ygberg also assigns svanbergite to a rhombohedral space group but in his indexing of part of a powder pattern, in which he gives indices for 26 planes, 8 planes fail to meet the criteria for a rhombohedral lattice. It follows that either the assignment of the space group, or the indexing of the pattern must be in error.

Specimens of svanbergite were not available, but it was found that Ygberg's observations could be checked directly without new experimental data. Once these computations had been carried out it was a simple matter to extend them to the related mineral woodhouseite, $CaAl_3(SO_4)(PO_4)(OH)_6$, for which Ygberg reported lattice dimensions and density though his tabulation of the powder pattern is not indexed, and to check them against new observations.

An alunite-like structure was assumed for these minerals and so it has seemed desirable to calculate the theoretical intensities and positions of lines in an alunite powder pattern using the parameters given by Hendricks, who did not report on such a pattern, and to compare these with published patterns and a new pattern obtained from alunite from the type locality. In the following the results on these three minerals will be reported in the order in which they have just been mentioned.

---

[1] Ygberg, Erik R., Svanbergite from Horrsjörberg: *Arkiv för Kemi, Mineralogi och Geologi*, **20A,** no. 4, 1–17 (1945).

[2] Hendricks, S. B., The crystal structure of alunite and the jarosites: *Am. Mineral.*, **22,** 773–784 (1937).

SVANBERGITE

Since no new observations were made on svanbergite the cell dimensions given by Ygberg, $a_0=6.96\pm0.03$ Å and $c_0=16.8$ Å, were accepted. The stated dimensions correspond to an axial ratio, c/a, 2.414, which is close to twice the value assigned from goniometric measurements. The observed density is given as 3.20 and the calculated density corresponding to three formular units in the hexagonal cell as 3.18.

Ygberg correctly gives the dimensions of the corresponding rhombohedral cell as $a_{rh}=6.89$ Å and $\alpha=60°\ 38'$, but states that these were found to be "the dimensions of the rhombohedral unit cell $\{40\bar{4}1\}$." This is rather puzzling. A cell of the stated dimensions would, if referred to the hexagonal axes found by x-ray diffraction have the indices $10\bar{1}1$ or $01\bar{1}1$. If referred to axes with half the axial ratio, as chosen from the morphology, the indices would be $20\bar{2}1$ or $02\bar{2}1$.

Reports on a powder pattern of svanbergite are given by Ygberg in two tables. In the first of these (his table 2) he gives intensity, $\sin^2\theta$ (obs), $\sin^2\theta$ (calc) and hexagonal indices for 22 lines whose $\sin^2\theta_{Cu}\leqq 0.420$. In another table (his table 5) intensities and spacings (presumably observed spacings) are given for 33 lines of svanbergite together with similar data for woodhouseite. At the base of the former table the value of $\lambda^2/3a^2$ is given as 0.0162 though the calculated values of $\sin^2\theta$ given for $11\bar{2}0$, $22\bar{4}0$ and $41\bar{5}0$ correspond to 0.0160, whereas the stated length of a_h leads to 0.0163.

Disregarding these difficulties, spacings were calculated from the stated cell dimensions for all rhombohedral planes with spacings greater than 1.3. This alone was not quite sufficient for assured indexing of the pattern because many coincidences or near coincidences occur. Assuming that the structure of svanbergite is similar to that found for alunite by Hendricks, that the content of the hexagonal cell is three formular units, and that interionic distances are limited by known ionic radii, a search was made for parameters that would yield intensities accounting for Ygberg's observations.

Hendricks assigned alunite to the space group C_{3v}^5–$R3m$, having observed it to be pyroelectric. The structure he described for alunite may, however, be considered to be in the space group D_{3d}^5–$R\bar{3}m$.[3] In this structure all atoms lie in symmetry planes. For this reason it is a rather simple matter to picture possible atomic arrangements by constructing, say, a $1\bar{2}10$ section through the cell as has been done for another member of the group (woodhouseite) in Fig. 1. From such a diagram either hexagonal or rhombohedral coordinates of atoms may be read off directly and by a system of overlapping grids (not shown in the figure) it is possible to make a quick graphical transformation of coordinates. It will be noted that for the hexagonal cell the a_1 axis does not lie in the plane of projection but the coordinates of atoms in this plane along an axis normal to c are the same as their a_1 coordinates. For the rhombohedral cell an equally convenient situation exists. The outline of this cell in the plane in question is a parallelogram whose edges are a_{r1} and the face diagonal of the unit rhombohedron. This face diagonal is vectorially $a_{r2}+a_{r3}$. All atoms in this plane will have equal coordinates along a_{r2} and a_{r3} which will be the same as the coordinate of such an atom along the face diagonal as can be seen in the lower part of Fig. 1.

---

[3] The group $R\bar{3}m$ arises from $R3m$ by addition of a center of symmetry at 000. From Hendricks' table of parameters it can be seen that all atoms in his structure are centrosymmetrically disposed in pairs on opposite sides of K at 000.

A choice of parameters was first made from ionic radii. This was then modified with the help of intensity calculations. In addition to trials for isolated planes several extended series of intensity calculations were carried out. The parameters used for the reported intensity calculations are set forth in Table 1. In this table P and S share the rhombohedral positions xxx and $\bar{x}\bar{x}\bar{x}$, leaving the structure in space group $R\bar{3}m$. If they did not share the two positions but each occupied one of them the symmetry centers would be lost and the space group would be $R3m$.

TABLE 1. PARAMETERS AND INTERATOMIC DISTANCES FOR SVANBERGITE

	Parameters			
All Trials	Sr		Al	
	Rh	Hex	Rh	Hex
	1: (*a*) 000	3: (*a*) 000	3: (*d*) ½00	9: (*d*) 1/6 1/6 $\overline{1/6}$

	S, P		O_1		O				OH			
	Rh 2: (*c*) xxx	Hex 6: (*c*) $00z$	Rh 2: (*c*) xxx	Hex 6: (*c*) $00z$	Rh 6: (*h*) zxx		Hex 18: (*h*) $x\bar{x}z$		Rh 6: (*h*) zxx		Hex 18: (*h*) $x\bar{x}z$	
Trial	x	z	x	z	x	z	x	z	x	z	x	z
A	.30	.30	.39	.39	.15	.51	.12	.27	.27	−.18	−.15	.12
B	.30	.30	.39	.39	.15	.51	.12	.27	.28	−.14	−.14	.14
C	.29	.29	.38	.38	.14	.50	.12	.253	.28	−.14	−.14	.14

	Interatomic Distances		
All Trials	$(S, P)-O_1=1.512$	$O-O=2.51$	
Trial C	$(S, P)-O=1.57$ $O_1-O=2.58$ $O_1-OH=2.80$	$Sr-O=2.90$ $Sr-OH=2.89$	$Al-O=1.71$ $Al-OH=1.97$

TABLE 2. OBSERVED AND CALCULATED SPACINGS AND INTENSITIES FOR LINES IN A POWDER DIFFRACTION PATTERN OF SVANBERGITE

Calculated from E. Ygberg's Cell Dimensions				Calculated Intensity			Quoted from E. Ygberg's Table 2				Table 5
$hk\bar{i}l$	hkl	$\sin^2\theta_{cu}$	d_{hkl}	Trial A	Trial B	Trial C	I	$\sin^2\theta$ (obs.)	$\sin^2\theta$ (calc.)	$HI\bar{K}L$	d_{hkl}
$10\bar{1}1$	100	.0184	5.67	300	321	264	s	.018	.0181	$10\bar{1}1$	5.73
0003	111	.0189	5.60	22	1	3			.0189	0003	
$01\bar{1}2$	110	.0247	4.90	0	9	28	w−	.024	.0244	$10\bar{1}2$	4.96
$11\bar{2}0$	$10\bar{1}$	.0489	3.48	171	189	189	s	.048	.0480	$11\bar{2}0$	3.51
$10\bar{1}4$	211	.0499	3.44	61	70	56					
$02\bar{2}1$	$11\bar{1}$	.0675	2.965	54	40	37	s+	.067	.0661	$20\bar{2}1$	2.97
$11\bar{2}3$	210	.0678	2.955	725	749	750					
$01\bar{1}5$	221	.0688	2.930	2	4	9					
$20\bar{2}2$	200	.0736	2.835	22	41	46	w	.077	.0756	0006	2.77
0006	222	.0756	2.800	13	60	38					
$02\bar{2}4$	220	.0988	2.435	144	70	102	w†	†	†	†	2.47
$21\bar{3}1$	$20\bar{1}$	.1162	2.260	71	92	143	s+	.120	.1204	$21\bar{3}2$	2.22
$20\bar{2}5$	311	.1177	2.250	72	73	72					
$10\bar{1}7$	322	.1193	2.230	203	217	176					
$12\bar{3}2$	$21\bar{1}$	.1225	2.198	77	90	70					
$11\bar{2}6$	321	.1245	2.181	41	23	17					
$30\bar{3}0$	$2\bar{1}\bar{1}$	.1467	2.010	16	14	14	w	.145	.1440	$30\bar{3}0$	2.02
$21\bar{3}4$	310	.1477	2.008	12	34	17			.1456	$21\bar{3}4$	
$01\bar{1}8$	332	.1507	1.982	15	22	56					
$03\bar{3}3$	$22\bar{1}$	.1656	1.891	198	211	273	s	.163	.1629	$31\bar{3}3$‡	1.91
$30\bar{3}3$	300			19	24	24					
$12\bar{3}5$	320	.1676	1.883	14	7	3			.1645	$21\bar{3}5$	
$02\bar{2}7$	331	.1681	1.877	1	1	4					
0009	333	.1701	1.866	2	16	11					
$22\bar{4}0$	$20\bar{2}$	.1956	1.740	235	215	215	s	.193	.1920	$22\bar{4}0$	1.75
$20\bar{2}8$	422	.1996	1.723	43	19	21	w−	.202	.2004	$22\bar{4}2$*	1.71
$13\bar{4}1$	$21\bar{2}$	.2140	1.663	13	12	11					
$22\bar{4}3$	$31\bar{1}$	.2145	1.662	12	1	1					
$21\bar{3}7$	421	.2170	1.652			37	w	.220	.2196	$30\bar{3}6$	1.64
$11\bar{2}9$	432	.2190	1.645			10			.2210	000·10*	
$31\bar{4}2$	$30\bar{1}$	.2203	1.640			0					
$03\bar{3}6$	330	.2223	1.633			5					
$30\bar{3}6$	411					11					
$10\bar{1}\cdot 10$	433	.2263	1.618			4	w−	.230	.2269	$31\bar{4}3$*	1.60
$13\bar{4}4$	$32\bar{1}$	.2455	1.553			2					
$12\bar{3}8$	431	.2485	1.543			0					
$40\bar{4}1$	$3\bar{1}\bar{1}$	.2629	1.501			0					
$31\bar{4}5$	410	.2644	1.496			26	w	.265	.2644	$40\bar{4}2$	1.49
$01\bar{1}\cdot 11$	443	.2684	1.486			24					
$04\bar{4}2$	$22\bar{2}$	.2692	1.483			15					
$22\bar{4}6$	420	.2712	1.478			68	w	.276	.2749	$40\bar{4}3$*	1.46
$02\bar{2}\cdot 10$	442	.2752	1.466			108	m	.281	.2821	$21\bar{3}9$*	1.45
000·12	444	.2924	1.423			4					
$40\bar{4}4$	400	.2944	1.418			29	w	.295	.2949	$22\bar{4}7$*	1.41
$32\bar{5}1$	$30\bar{2}$	.3118	1.378			23	w	.316	.3148	$32\bar{5}2$	1.37
$04\bar{4}5$	$33\bar{1}$	.3133	1.375			0					
$13\bar{4}7$	430	.3148	1.372			68					
$03\bar{3}9$	441	.3168	1.367			3					
$30\bar{3}9$	522					21					
$23\bar{5}2$	$31\bar{2}$	.3181	1.365			1					
$20\bar{2}\cdot 11$	533	.3183	1.364			1					
$21\bar{3}\cdot 10$	532	.3251	1.350			19					
$41\bar{5}0$	$3\bar{1}\bar{2}$	.3423	1.316			28	w−	.337	.3360	$41\bar{5}0$	1.32
$32\bar{5}4$	$41\bar{1}$	.3433	1.314			7					
$31\bar{4}8$	521	.3463	1.308			19					

* Indices thus marked denote planes not conforming to rhombohedral criteria.

† Intensity and spacing for this line taken from Ygberg's Table 5. It is omitted in his Table 2.

‡ Impossible indices.

Since S^{+6} and P^{+5} have practically the same scattering power discrimination by x-ray diffraction is not feasible.

Intensity calculations were made by the well known formula

$$I_{\mathrm{calc}} \sim \mathrm{j} \cdot F^2 \cdot \frac{1 + \cos^2 \theta}{\sin^2 \theta \cdot \cos \theta}$$

using ionic scattering factors from the ITDCS for all ions except Sr^{+2}. For Sr the atomic scattering factors of the ITDCS were slightly modified for low angles to correspond to expected ionic scattering. For the sake of simplicity intensity calculations were made from the rhombohedral parameters. In Table 1 all parameters are given for both cells.

In Table 2 the results of three series of intensity calculations are shown together with rhombohedral and hexagonal indices, calculated spacings and Ygberg's data from two of his tables for the range here covered. It can be seen that trial C for intensities best accounts for the observations, especially on 111, 200 and 222, 220 and on 422. Accordingly, calculations for this trial were extended to the first 55 planes as an additional check. The margin for choice between trials B and C is, however, not large. Comparison of calculations with observations further shows that even a number of lines to which Ygberg assigned permissible indices are to be attributed to other planes if svanbergite has an alunite structure. For instance, the strong line for spacing 2.97 to which he gave the indices $20\bar{2}1$ must be attributed largely if not entirely to $11\bar{2}3$.

In the range covered by calculations, the seven lines for which Ygberg gave indices that are non-rhombohedral or impossible have been explained as due to diffraction from planes in a rhombohedral lattice. In addition to these Ygberg also listed $32\bar{5}6$ ($\sin^2\theta$ (obs) = .378). No doubt this observation as well might be accounted for by rhombohedral indices but present calculations were not carried so far. It may now be asserted with greater assurance that svanbergite does indeed have a rhombohedral lattice.

As will be seen more clearly in the discussion of woodhouseite, the intensity designations w and s, as used by Ygberg each cover a wide range of intensities, whereas the designation m is but sparingly used by him. Under these circumstances no close determination of the parameters is possible but the fit of calculated intensities for trial C and reported intensities over a rather large range shows that a fair approximation has been reached.

Rhombohedral Indexing

Since indices of planes and coordinates of atoms in this paper are referred to both hexagonal and rhombohedral cells it is necessary to make a statement about the conventions adopted. The writer has not followed the ITDCS in these matters. It is pertinent to quote Donnay[4] in this connection. He has written:—"If the lattice is rhombohedral (hexagonal-R), and is referred to the smallest R-centered cell, there are still two alternatives. The dominant rhombohedron may have a face sloping forward, in which case it is symbolized $\{10\bar{1}1\}$, or backward, in which case it is indexed $\{01\bar{1}1\}$. The second setting may be obtained from the first by a 180° (or 60°) rotation about the c axis. In the first setting, the cell (which is here a triple cell) has its additional nodes at $\frac{2}{3}\,\frac{1}{3}\,\frac{1}{3}$ and $\frac{1}{3}\,\frac{2}{3}\,\frac{2}{3}$; in the second setting, at $\frac{2}{3}\,\frac{1}{3}\,\frac{2}{3}$ and $\frac{1}{2}\,\frac{2}{3}\,\frac{1}{3}$. The extinction criterion of the faces ($hk\bar{\imath}l$) is, in the first setting $2h+k+l=3n$ or $h+i+l=3n$; in the second setting $2h+k-l=3n$ or $h+i-l=3n$. It is unfortunate that the *International Tables* should recommend the adoption of the second setting. The dominant rhombohedron has always been indexed $\{10\bar{1}1\}$ by mineralogists."

With all this the writer is in agreement except that the sign before the i in the alternative forms of the criteria should be negative in each case.[5]

This matter is taken up at two points in the ITDCS. The transformation γ given on page 74 in volume I corresponds to Donnay's "first setting," whereas in volume II under "Indices Transformations," page 471, both settings are described. In the space group tables the second setting is used consistently as indicated by Donnay.

Under "Rhombohedral centering" a transformation corresponding to the "first setting" is discussed by Buerger[6] and an equivalent transformation formula [88] is given in the new seventh edition of *Dana's System of Mineralogy*.[7] Neither of these authorities hint at the possibility of a "second setting."

The writer follows mineralogical usage in making the transformation according to the "first setting." Then $(10\bar{1}1)$ becomes (100) and the criteria for hexagonal indices which correspond to planes in the rhombohedral lattice may be taken to be:

$$\begin{gathered} h-i+l=3n, \\ k-h+l=3n \\ \text{or } i-k+l=3n. \end{gathered}$$

---

[4] Donnay, J. D. H., Rules for the conventional orientation of crystals: *Am. Mineral.*, **28**, 313–328 (1943).

[5] This slip corresponds to the statement found at the foot of page 77 in Rogers' "Introduction to the study of minerals," 3rd. ed. 1937, that $h+k=i$. Though this is stated as a conclusion from a detailed proof it is incorrect.

[6] Buerger, M. J., *X-ray Crystallography*, New York, (**1942**), pp. 68–70.

[7] Palache, Berman and Frondel, *Dana's System of Mineralogy*, 7th ed., vol. I, New York (1944), p. 25. This is taken from C. W. Wolfe's "Crystallographic Procedures," *Am. Mineral.*, **26**, 55–91 (1941), where the transformation here referred to is stated as formula [94].

These are also the transformation formulas and may be applied to the correlated indices of tables 2, 5 and 7 in this paper.

The relations of the two lattices thus chosen may be seen from Fig. 1 showing that the coordinates of atoms which give rhombohedral centering to the hexagonal lattice are $\frac{2}{3}$, $\frac{1}{3}$, —, $\frac{1}{3}$, and $\frac{1}{3}$, $\frac{2}{3}$, —, $\frac{2}{3}$.

WOODHOUSEITE

Thanks to the courtesy of Professor C. D. Woodhouse, Santa Barbara College, University of California, Santa Barbara, California, the writer was able to obtain specimens of woodhouseite from the type locality. The specimens consist of small clusters of woodhouseite crystals a millimeter or two in diameter implanted on much larger quartz crystals. It proved quite easy to detach uncontaminated material suitable for density determination or *x*-ray powder study.

TABLE 3. LATTICE DIMENSIONS AND DENSITY OF WOODHOUSEITE

	Hexagonal axes			Rhombohedral axes		Density	
	a_h	c_h	c/a	a_r	$\angle\alpha$	$d_{\text{obs.}}$	$d_{\text{calc.}}$
Lemmon	—	—	1.170 ($\frac{1}{2}\times 2.340$)			3.012	—
Ygberg	6.93	16.3	2.352	6.75	61° 75′*	—	3.024
Pabst	6.961	16.27	2.338	6.75	62° 4′	3.003	3.003†

* The value given for α here is quoted from Ygberg. This was obviously a misprint. The value corresponding to his dimensions for the hexagonal cell would be 61° 48′.

† The calculated density given at this point is based on the assumption of a cell content corresponding to the ideal formula. The analysis reported by Lemmon, however, shows 1.00% BaO and other contaminants. It must be assumed that these constituents enter into the lattice. On this basis the density would be 3.029 using my dimensions or 3.051 using Ygberg's dimensions.

The density of woodhouseite was determined by the Berman balance using toluene of density 0.862 at 26° C. The lattice dimensions were determined from a powder pattern made in a camera of 360 mm. circumference with copper radiation and nickel filter. The wave length of the unresolved copper K_α radiation was taken to be 1.539 kX. In calculating density from cell content the value of Avogadro's number was taken as 60.594×10^{22} for consistency with the kX units.[8] The results of these measurements and calculations are given in Table 3 together with earlier values reported by Lemmon and Ygberg.

---

[8] Schlecht, Wm. G., Calculation of density from *x*-ray data: *Am. Mineral.*, **29**, 108–110 (1944).

If my dimensions for the woodhouseite cell are rounded off to three significant figures, like Ygberg's, they become 6.96 and 16.3. This leaves us with a correction for a_0 and so it may be well to state precisely the basis for this change. The cell dimensions were determined from 16 lines free from disturbing coincidences in the powder pattern. They are indicated by asterisks in Table 5. From these lines one obtains 14 values for each of the necessary constants. The average values are:—

$$\sin^2 \theta_{10\bar{1}0} = 0.016296 \qquad \text{and} \qquad \sin^2 \theta_{0001} = 0.002237.$$

The standard errors,

$$S_{\bar{x}} = \sqrt{\frac{\Sigma(X - \bar{x})^2}{n(n-1)}},$$

are respectively 0.00000615 and 0.00000335. They correspond to 0.0015 kX and 0.013 kX. The maximum errors calculated from the maximum values of $(X - \bar{x})$ correspond to 0.012 kX and 0.10 kX, respectively. They may be assumed to be well beyond the limits of probable error. A further check was obtained from the alunite pattern discussed below. Lattice dimensions obtained from this showed no significant difference from those given by Hendricks.

TABLE 4. PARAMETERS AND INTERATOMIC DISTANCES FOR WOODHOUSEITE

Parameters							
Rh Ca 1: (*a*) 000		Hex 3: (*a*) 000	Rh Al 3: (*d*) $\frac{1}{2}$00			Hex 9: (*d*) 1/6 1/6 1/6	
	2: (*c*) xxx	6: (*c*) 00z		6: (*h*) zxx		18: (*h*) $x\bar{x}z$	
	x	z		x	z	x	z
S, P	.31	.31	O	.16	.52	.12	.28
O_1	.405	.405	OH	.27	−.12	−.13	.14

Interatomic distances

(S, P)−O = 1.53
(S, P)−O_1 = 1.55

O−O = 2.51
O_1−O = 2.50
O_1−OH = 2.69
OH−OH = 2.71

Ca−O = 2.71
Ca−OH = 2.77
Al−O = 1.93
Al−OH = 1.88

Parameters were found for woodhouseite in the same manner as described for svanbergite. Several sets of intensity calculations were made with various parameters. In Table 4 are given only the parameters finally chosen together with the corresponding interatomic distances. These are in close accord with accepted values but no great weight should be laid on this since the parameters are stated only to two figures for most atoms and a small shift may make substantial changes in interatomic distances. For instance, changing z for O_1 by only 0.005 would change the $S-O_1$ distance by a little more than 0.08 kX.

Table 5 shows the observed and calculated spacings for woodhouseite down to 1.293 kX. The observed intensities for the new woodhouseite pattern are recorded by the heights of peaks on a photometer curve. Except that the heights of the first two peaks which lie within the central halo of fog seem low (in the direct estimate of intensities made before the photometer curve was run they were assigned the same value as that of the third line) the agreement with calculated intensities is rather satisfactory, being just as good as that shown for alunite in Table 7. Even so, no high accuracy is claimed for the adopted parameters.

Records of powder patterns of woodhouseite have previously been published by Ygberg[9] and by McConnell.[10] The latter gave no cell dimensions; neither gave indices. Their data are included in Table 5. The record is carried a little farther in Table 5*a* in which are given lines of woodhouseite patterns between 1.29, the limit of intensity calculations, and 0.90, the line of smallest spacing recorded by Ygberg. McConnell's published record does not extend into this region. Measurement of my pattern was not carried beyond 0.90 kX.

Though there is substantial agreement among the several patterns some notable differences occur. The new pattern shows a few more lines. In the indexed part these are all satisfactorily accounted for except the weak line 2.56. Ygberg's pattern shows a few marked departures in spacing, for instance for his 2.99 line, whereas McConnell records two or more lines not observed by the writer and not explained by the supposed structure of woodhouseite. These discrepancies can hardly be explained by differences in material since we all worked with woodhouseite from Inyo County, the only known locality.

The structure of woodhouseite is shown in section in Fig. 1. Since all atoms lie in symmetry planes this may be considered to be a full representation of the structure. In the diagram all atoms within one rhombohedral cell are shown in the side view, whereas only atoms at the corners of such a cell are shown in the top view. The hexagonal parameters of Table 4 must be taken with x along the a_1 and a_3 axes to give correct positions corresponding to the labelled atoms or ions in the drawing.

---

[9] *Op. cit.* p. 15.

[10] McConnell, Duncan, *X*-ray data on several phosphates: *Am. J. Sci.*, **240**, 649–657 (1942).

TABLE 5. CALCULATED AND OBSERVED SPACINGS AND INTENSITIES IN POWDER DIFFRACTION PATTERNS OF WOODHOUSEITE

Calculated Lines				Observed Lines					
Radiation		Cu		Pabst		Ygberg (1946)		McConnell (1942)	
				Cu		Cu		Fe	
$hk\bar{i}l$	$h_rk_rl_r$	I	d_{hkl}	I	d_{hkl}	I	d_{hkl}	I	d_{hkl}
$10\bar{1}1$	100	74	5.652	.30‡	5.66−	m	5.73	<½	5.61
0003	111	6	5.427						
$01\bar{1}2$	110	79	4.854	.40	4.84+	m	4.86	½	4.81
								<½	3.83
$11\bar{2}0$*	$10\bar{1}$	87	3.479	.90	3.48+	s	3.51	1	3.46
$10\bar{1}4$	211	0	3.373						
				.20	3.27‖			2	3.21
$02\bar{2}1$	$11\bar{1}$	0	2.963					2	2.960
$11\bar{2}3$*	210	436	2.929	2.45	2.93−	s+	2.99	6	2.908
$01\bar{1}5$	221	8	2.865	.15	2.84				
$20\bar{2}2$	200	0	2.825						
0006*	222	32	2.714	.45	2.70−	w	2.72	1	2.683
				.15	2.56§				
$02\bar{2}4$*	220	13	2.423	.40	2.42	w	2.40	1	2.418
								2	2.370
$21\bar{3}1$	$20\bar{1}$	6	2.257						
$20\bar{2}5$	311	21	2.213						
$12\bar{3}2$	$21\bar{1}$	41	2.195	2.10†	2.19+	s+	2.18	3	2.198
$10\bar{1}7$	322	147	2.171		2.16−			4	2.152
$11\bar{2}6$	321	2	2.141						
				.20	2.09+‖			2	2.068
$30\bar{3}0$	$2\bar{1}\bar{1}$	1	2.009						
$21\bar{3}4$	310	14	1.987	.20	1.99−	w−	2.01		
$01\bar{1}8$	332	0	1.930						
$03\bar{3}3$*	$22\bar{1}$	144	1.884	2.30	1.885	s+	1.89	2	1.918
$30\bar{3}3$	300	6						5	1.886
$12\bar{3}5$	320	1	1.867						
$02\bar{2}7$*	331	6	1.842	.10	1.844				
0009*	333	15	1.810	.20	1.804				
$22\bar{4}0$*	$20\bar{2}$	138	1.740	1.90	1.741	s	1.73	4	1.740
$20\bar{2}8$*	422	5	1.687	.20	1.685	w−	1.68		
$13\bar{4}1$	$21\bar{2}$	0	1.663						
$22\bar{4}3$	$31\bar{1}$	0	1.657						
$31\bar{4}2$*	$30\bar{1}$	4	1.638	.40 B	1.638			1	1.638
$21\bar{3}7$	421	10	1.628			w−	1.62		
				?	1.621			1	1.619
$03\bar{3}6$	330	2	1.615						
$30\bar{3}6$	411	0							
$11\bar{2}9$*	432	18	1.605	.40	1.602	w−	1.60	1	1.600
$10\bar{1}.10$	433	4	1.572	.10	1.568			1	1.573
$13\bar{4}4$	$32\bar{1}$	4	1.547	.10	1.546				
$12\bar{3}8$*	431	13	1.521	.45	1.519	w−	1.51	1	1.515
$40\bar{4}1$	$3\bar{1}\bar{1}$	7	1.501						
$31\bar{4}5$	410	12	1.487	.60	1.487	w	1.48	2	1.486
$04\bar{4}2$	$22\bar{2}$	13	1.482						
$22\bar{4}6$*	420	49	1.464	.90	1.466	w	1.46	2	1.464
$01\bar{1}.11$	443	0	1.438						
$02\bar{2}.10$*	442	80	1.433	1.55	1.432	m	1.43	3	1.426
$40\bar{4}4$*	400	13	1.414	.25	1.416				
$32\bar{5}1$	$30\bar{2}$	5	1.378						
$04\bar{4}5$	$33\bar{1}$	2	1.367	.55B	1.366	w−	1.36		
$23\bar{5}2$	$31\bar{2}$	12	1.363						
$13\bar{4}7$	430	29	1.357						
000.12	444	1	1.357						
$03\bar{3}9$*	441	22	1.344	.40	1.345	w−	1.34		
$30\bar{3}9$	522	2							
$20\bar{2}.11$	533	5	1.328	.40B	1.322	w	1.31		
$21\bar{3}.10$	532	3	1.325						
$41\bar{5}0$	$3\bar{1}\bar{2}$	7	1.315						
$32\bar{5}4$	$41\bar{1}$	0	1.310						
$31\bar{4}8$	521	1	1.293						

* Lines used to determine cell dimensions.

† Photometer curve shows common peak for two lines whose intensities were estimated at 4 and 8 (intensity of strongest line being 10), in agreement with calculated intensities.

‡ Observed intensities given by heights of peaks on photometer curve.

§ Unidentified line, probably due to unknown contaminant, not quartz.

‖ β lines.

Table 5a. Observed Lines in Woodhouseite Powder Diffraction Patterns for the Interval 1.29 to 0.90 kX

Pabst		Ygberg		Pabst		Ygberg	
I	d_{hkl}	I	d_{hkl}	I	d_{hkl}	I	d_{hkl}
4*	1.282	m	1.27	2	1.036		
1	1.262			2	1.031		
2	1.225			3	1.007		
5	1.192	m	1.19	3	1.003	w	1.00
4	1.164	w+	1.16	2−	0.962		
3−	1.138−	w	1.13	5	0.953	w+	0.95
2	1.124			4	0.945	w	0.94
2	1.106			5	0.935	w+	0.93
4	1.098	w−	1.10	2−	0.930		
4	1.078	w+	1.07	3+	0.913	w−	0.91
2+	1.067			5	0.903	w	0.90
2+	1.056						

* Intensities given by arbitrary serial numbers from 1 for very faint lines to 10 for the strongest line.

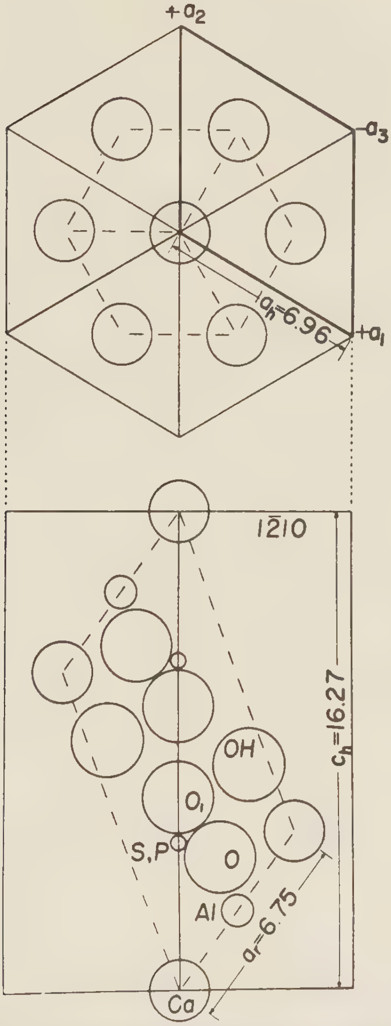

FIG. 1. Atomic arrangement of woodhouseite. Dashed lines in both views outline rhombohedral unit cell. Heavy full lines outline hexagonal unit cell in top view only.

ALUNITE

Alunite from Tolfa, Italy, taken from the collections of the Department of Geological Sciences, University of California, Berkeley, originally obtained through Ward's Natural Science Establishment, was used for a powder pattern. This may be considered to be from the type locality since the mineral was known at Tolfa from early times, before it received its present name.

The density was determined with the Berman balance on three small fragments of this material consisting of compact fine-grained crystal aggregates. Single crystals were not available. The resulting value, 2.70 is slightly lower than the observed and calculated values, 2.75 and 2.80, given by Hendricks,[11] as might be expected.

The dimensions of the hexagonal cell were determined from a powder pattern taken under just the same conditions as that of woodhouseite. The results checked closely with the dimensions given by Hendricks. These, together with the constants calculated for the corresponding rhombohedral cell, are:—

a_h	c_h	c_h/a_h	a_{rh}	α
6.96	17.35	2.492	7.058	59° 5′.

The parameters found for alunite by Hendricks are given in Table 6 in the same form in which parameters have been given for svanbergite

TABLE 6. PARAMETERS USED IN INTENSITY CALCULATION FOR ALUNITE. ADAPTED FROM HENDRICKS

Rh K 1: (a) 000		Hex 3: (a) 000	Rh Al 3: (d) ½00			Hex 9† (d) 1/6 $\overline{1/6}$ 1/6	
	2: (c) xxx	6: (c) 00z		6: (h) zxx		18: (h) $x\bar{x}z$	
	x	z		x	z	x	z
S	.305	.305	O	.157	.512	−.213	−.058‡
O_1	.393	.393*	OH	.276	−.174	−.150	.126

* The O_1 parameter is given by Hendricks as .06. This is obviously a slip as it would make the $K-O_1$ distance only 1.04. The value given in the table herewith is obtained by adding .333 to the value given by Hendricks (*op. cit.*, p. 777). From his figure 2 it is clear that he intended the value here given.

† There are 9 aluminums in the hexagonal unit, not 3 as suggested by Hendricks' tabulation (*op. cit.*, p. 777).

‡ The hexagonal parameters for O here given are the same as tabulated by Hendricks. By adding .333 to each it will be seen that these parameters are very close to those found for svanbergite and woodhouseite stated in Tables 1 and 4.

---

[11] *Op. cit.*, p. 775.

and woodhouseite. Using these parameters and the dimensions cited, the intensities and positions for the first twenty five possible lines in an alunite powder pattern were calculated. Table 7 shows the results of

TABLE 7. COMPARISON OF CALCULATED AND OBSERVED SPACINGS AND INTENSITIES FOR ALL POSSIBLE LINES IN AN ALUNITE POWDER DIFFRACTION PATTERN FOR WHICH d_{hkl} IS GREATER THAN 1.69

Calculated				Observed† (Pabst)		ASTM—ASXRED‡			
						card 2155		card II-1459	
$hk\bar{i}l$	$h_rk_rl_r$	d_{hkl}	I	d_{hkl}	I	d_{hkl}	I	d_{hkl}	I
0003	111	5.783	1						
$10\bar{1}1$	100	5.69	38	5.75	.30	5.70	.25	5.70	.2
$01\bar{1}2$	110	4.946	59	4.98	.65	4.94	.50	4.92	.4
								3.97	.½
$10\bar{1}4$	211	3.52	3						
$11\bar{2}0$	$10\bar{1}$	3.481	62	3.50	1.05	3.49	.41	3.50	.2
				3.33+*	.40	3.34	.03		
$01\bar{1}5$	221	3.01	16	3.00−	2.80	2.98	1.00	2.96	1.0
$11\bar{2}3$	210	2.985	424						
$02\bar{2}1$	$11\bar{1}$	2.97	138						
0006	222	2.892	23	2.89+	.55	2.88	.06	2.85	.½
$20\bar{2}2$	200	2.848	0						
$02\bar{2}4$	220	2.474	54	2.48+	.65	2.47	.09	2.47	.¼
$10\bar{1}7$	322	2.292	148	2.29+	2.40	2.29	.50		
$20\bar{2}5$	311	2.276	28	2.26	.95				
$21\bar{3}1$	$20\bar{1}$	2.259	14						
$11\bar{2}6$	321	2.227	5	2.21+	.25			2.24	.5
$12\bar{3}2$	$21\bar{1}$	2.204	35			2.20	.19		
				2.11+*		2.13	.03		
$01\bar{1}8$	332	2.042	12	2.04−	.20	2.02	.03		
$21\bar{3}4$	310	2.018	0						
$30\bar{3}0$	$2\bar{1}\bar{1}$	2.010	2						
0009	333	1.928	9						
$02\bar{2}7$	331	1.914	18	1.90+	3.30	1.893	.59	1.89	.5
$12\bar{3}5$	320	1.904	0						
$03\bar{3}3$	$22\bar{1}$	1.897	133						
$30\bar{3}3$	300		4						
$22\bar{4}0$	$20\bar{2}$	1.740	145	1.750	2.90	1.74	.50	1.735	.5
$20\bar{2}8$	422	1.699	1						

* β lines. See text.

† Cu radiation. Intensities given as heights of peaks on photometer curve. The calculated intensities are also for Cu radiation.

‡ Presumably the patterns recorded on both ASTM cards were made with Mo radiation.

these calculations together with observations on the powder pattern. Included in the table are also parts of the records of alunite patterns that are available on ASTM-ASXRED cards.

The observed lines include several that do not correspond to calculated spacings. When the lines at 3.33 and 2.11 kX were noted on the pattern of alunite from Tolfa, Italy, they were at first suspected of being due to quartz contamination. Quartz has strong lines at 3.35 and 2.11.[12] Microscopic examination, however, revealed no quartz in the sample and it proved to be completely soluble upon prolonged treatment with sulphuric acid. These two lines are Cu-K_β lines corresponding to $11\bar{2}3$ and $03\bar{3}3$, the strongest α lines observed. Such Cu K_β lines ought to simulate Cu K_α lines for spacings 3.315 and 2.119, very close to the observed positions.

On card 2155 lines are also recorded near the positions just discussed, namely at 3.34 and 2.13. It may be assumed that this pattern, from the first ASTM set, was made with Mo radiation. Due to the different ratio of β to α wave lengths for this radiation the β lines for $11\bar{2}3$ and $03\bar{3}3$ would simulate α lines corresponding to spacings 3.382 and 2.152 respectively, in this case. Thus it seems probable that the alunite used for the pattern of ASTM card 2155 carried a little quartz contamination, though one might again attribute the lines to β radiation if one allowed about a one per cent error in the reporting of the positions of these particular lines.

No explanation has been found for the 3.97 line on card II—1459.

---

[12] ASTM-ASXRED card II—1007.

EXPERIMENTS IN *X*-RAY IRRADIATION OF GEM STONES

FREDERICK H. POUGH, *The American Museum of Natural History, New York City,*
AND
T. H. ROGERS, *Machlett Laboratories, Inc., Springdale, Connecticut.*

ABSTRACT

Irradiation of gemstones with a new and powerful beryllium windowed *x*-ray tube effects, in a few minutes, color changes which with previous tubes either gave negative results or required hours of exposure. Some of the effects appear to be permanent, some disappear slowly upon exposure to light, and some revert without other stimulation. The anticipated availability of this treatment to temporarily improve commercial gems makes it important that jewelers be informed of the possibility so that they may be on their guard against frauds of this nature.

The recent development of a new and extremely intense source of *x*-rays (Rogers, 1945–1946) by the Machlett Laboratories suggested the possibility that irradiation experiments with this equipment might materially shorten the time required for producing coloration effects, long studied by physicists, in various minerals and reveal colors which had not previously been affected by *x*-rays produced by ordinary tubes.

In the early days of experimentation with various energy sources, it was noted that both radium and *x*-rays affected the coloration of various minerals. Doelter, 1912, lists a number of such changes: in diamond, spodumene, quartz and topaz, among others. The mineralogists of that day had no explanation for this, or for some of the other phenomena, like fluorescence, all of which were recorded on a basis of observation.

On the other hand, in more recent years, physicists working with transparent mineral materials have observed various color changes as incidental phenomena in the course of other experiments, such as photoconductivity. For purposes of comprehensive explanation and the working out of theories, however, they have concentrated in a few fields of simple compounds, especially the alkali halides.[1] The more complex phenomena involved in crystals with a large number of constituents still require explanation, although it is natural to suppose that similar mechanisms will operate in these cases.

The nature of the changes induced by *x*-ray radiation, however, as they are explained at present by the physicists, makes it unlikely that any permanent results will be obtained from this type of attack. The slight disruption of the electronic structure depends upon the existence of structural defects, into which electrons freed from halogen ions can migrate and become trapped when released by the x-ray bombardment. However, since this irradiation results in an unstable structure within the affected crystals with unsatisfied positive and negative charges, comparatively little energy is required to move the electrons back into a stable combination with the consequent elimination of the electrons trapped at the lattice defects, and a return to the normal state.

---

[1] For an introduction into the physicists' explanations of these phenomena, consult Mott & Gurney, *Electronic Processes in Ionic Crystals*, Oxford (1940).

DeBoer, J. H., *Electron Emission and Absorption Phenomena*, Cambridge (1935).

Some substances, those that fluoresce and phosphoresce, for example, are in an easily excited state when they crystallize. Others are more stable, and while they may be colored by the irradiation, they show little or no luminescence. A third group appears to be entirely unaffected by the bombardment; though no experiments have ever been performed with most of them to see whether or not they became conductors during such an irradiation, and consequently had been affected, even though it had not subsequently shown up as a color change.

The irradiation of gem stones, and the possibility that some day a method may be found for making permanent the temporary effects now observed is, of course, an intriguing problem and one which naturally immediately presents itself when a new powerful source of x-rays becomes available. The radiation output of the Machlett beryllium window tube is equivalent to several hundred times the output of tubes previously available. This means that effects can be obtained in one minute that would require several hours with a conventional x-ray apparatus.

The stones selected for the study were dictated by previous experience with especially sensitive material, such as gem spodumene; by commercially desirable changes, if they could be made permanent, such as those found to occur in the corundum gems; and by various other interests. The results of the exposures will be found in the table. Special phenomena observed in the several stones will be discussed under those headings.

The specimens listed in Table 1 were all subjected to radiation from a Machlett Type AEG-50 x-ray tube (Fig. 1) having a focal spot approximately 5 mm. wide. The tube was energized by a full-wave rectified non-filtered power supply, in accordance with the circuit diagram of Fig. 2. The voltage applied to the tube was 50 kilovolts peak, as measured by the spark-over distance between standard 12.5 cm. spheres. The current through the tube was adjusted to 50 milliamperes as measured by a d.c. milliammeter.

The Type AEG-50 tube is provided with a beryllium window approximately 1 mm. in thickness, located 2 cm. from the center of the focal spot. The target is of tungsten, positioned at an angle of 20° to the cen-

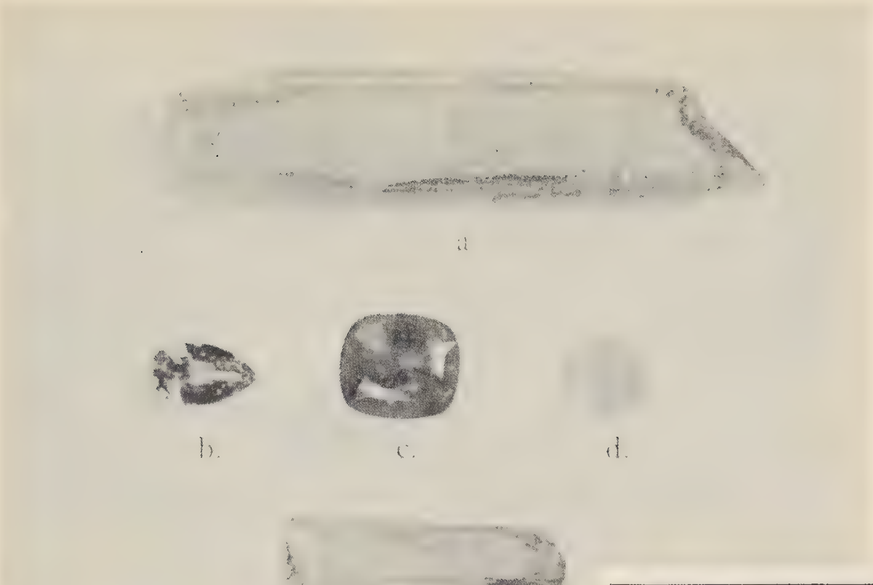

FIG. 1. (*above*) Untreated specimens; a, spodumene; b, ~~scapolite~~; c, yellow sapphire; d, ~~cut kunzite~~; e, kunzite.
cut kunzite scapolite

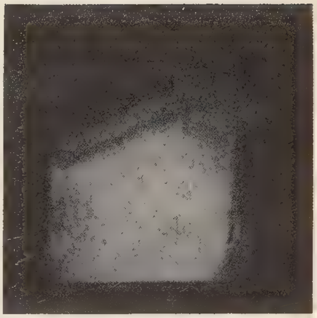

FIG. 2. (*right*) Phosphorescent specimen of spodumene after irradiation, illuminated only by its own phosphorescence.

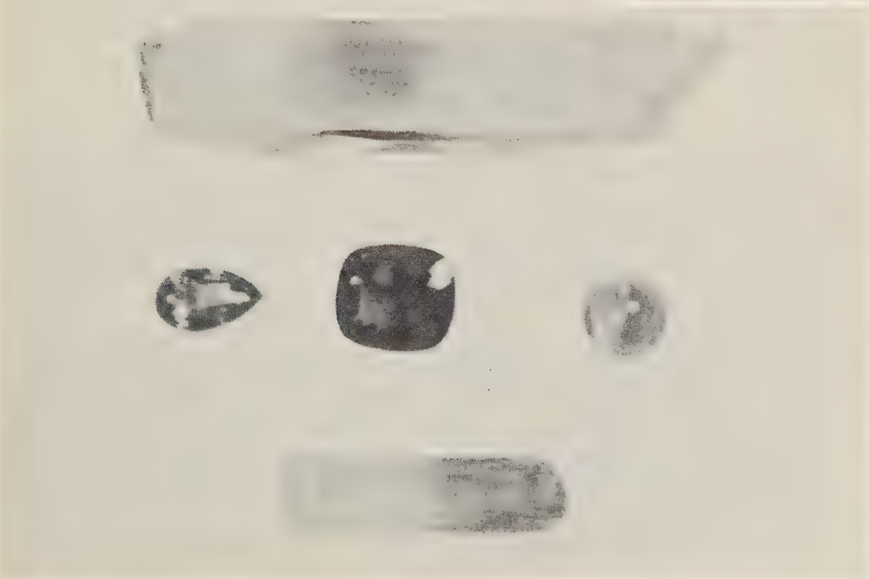

FIG. 3. Specimens of Fig. 1 after treatment, in whole or in part, by five minutes irradiation from new x-ray tube.

(Courtesy Machlett Laboratories, Inc.)

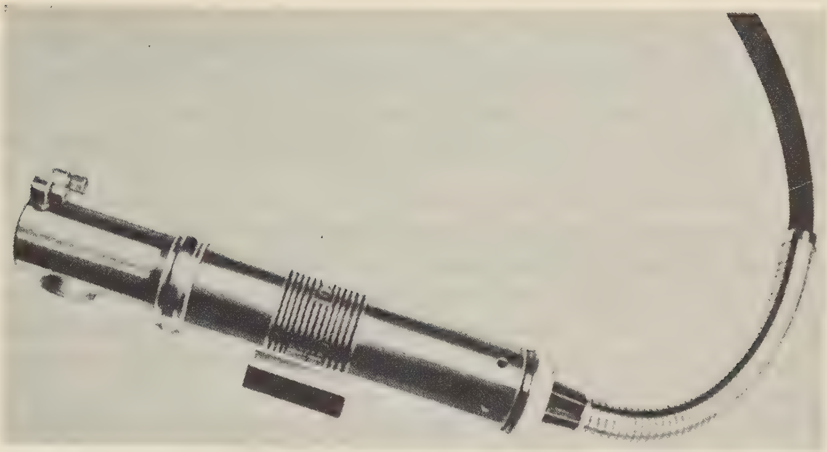

(Courtesy of Machlett Laboratories, Inc.)

FIG. 1. Type AEG-50 x-ray tube.

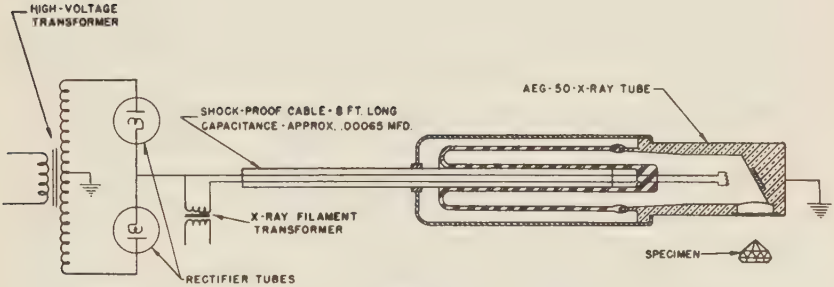
HIGH-VOLTAGE TRANSFORMER
AEG-50-X-RAY TUBE
SHOCK-PROOF CABLE-8 FT. LONG
CAPACITANCE-APPROX. .00065 MFD.
X-RAY FILAMENT TRANSFORMER
SPECIMEN
RECTIFIER TUBES

FIG. 2. Schematic diagram of circuit used to energize x-ray tube used for irradiation tests herein described.

tral axis of the x-ray beam, which covers a conical solid angle of 40°. The specimens were placed approximately 0.5 cm. from the window.

The x-ray intensity at this point was not measured directly, its order of magnitude being estimated with a sufficient degree of accuracy from data given by Rogers (1945–1946) for measurements made on a similar tube of 50 MA and 50 KV constant potential, under which conditions a value of 2,330,000 r per minute was obtained at the window. A correction for the fact that in the present case the voltage is pulsating rather than constant potential, plus the correction for the additional distance from the focal spot, is estimated to be approximately one-half, indicating a dosage at the surface of the specimens in the order of one million r

per minute. The quality of these rays (see Fig. 3) is such that they are very readily absorbed, even by low atomic number materials such as comprise most of the mineral specimens studied. The color changes observed in the larger specimens indicated a penetration of the radiation to a depth of approximately 1 cm. in sufficient intensity to produce perceptible reaction.

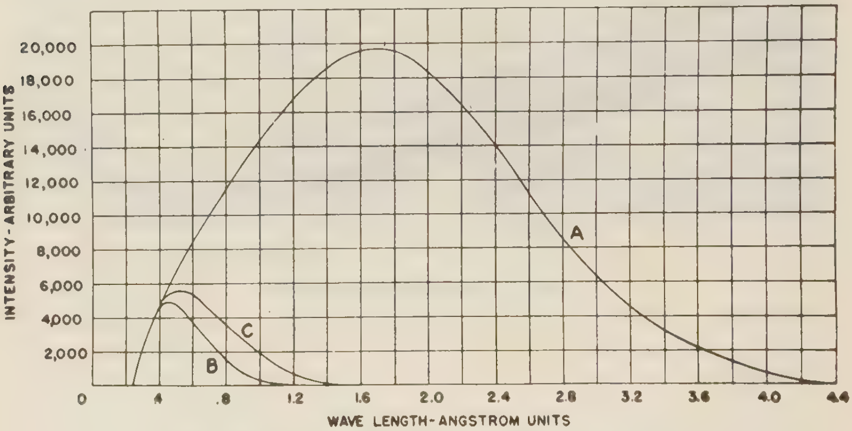

Fig. 3. Calculated spectral distribution of x-radiation generated at 50 KV:
A—with 1 mm. beryllium filtration
B—with 1 mm. aluminum filtration
C—with 1 mm. pyrex glass filtration.

DISCUSSION OF MINERALS TESTED

Spodumene

Various specimens derived from several sources were treated and comparable results were obtained, no matter what the source. The light green coloration is very intense but soon fades when exposed to sunlight or on heating, and the stone reverts to its original appearance. Treated stones kept in the dark appear to retain their color indefinitely. The coloration is rapid, but appears for a time to progress through the crystal at a definite rate, a five minute exposure, for example, produces a colored layer a little more than 1 mm. thick. The most remarkable feature in the change in spodumene (the kunzite type was the variety treated most frequently), was the customary intense and persistent orange phosphorescence, which made it look like a glowing coal when it was removed from the tube and which could be seen for as much as an hour. The appearance of a green coloration was directly related to this phosphorescence, for immediately after the cessation of irradiation, the stone observed had a brownish hue in the light, and the green did not become visible until the phosphorescence had ended. Heating renewed the phosphorescence, and removed the green coloration. One specimen, a white Brazilian crystal, showed in one area no phosphorescence but the irradiated area was green when it was removed from the window of the tube. The portion which phosphoresced was sharply separated from the non-phosphorescent part immediately following the exposure, but no such demarcation was observable after the phosphorescence had ceased and the stone assumed a uniform green. It is surprising to note that Doelter obtained no color change in this mineral by x-ray irradiation.

Beryl

A series of differently colored stones were treated and found to be affected but slowly by the irradiation. The first, a pale aquamarine, showed no change after eight hours of exposure. This stone was given prolonged treatment, a total of forty-one hours, and at the end of that time the stone was a light green color, and was a very attractive gem. All of the very pale blue stones became light green after treatment, but this color change was attained only after long exposures and was relatively light. A deep blue aquamarine became moderately green after prolonged (50 hrs.) treatment. In fading experiments the color became somewhat lighter and yellower, but could not be entirely removed. The stone has not been heated and remains green. An emerald given a short exposure was not affected and a pale colorless beryl became light brown after sixteen hours of exposure. There was no fluorescence or phosphorescence accompanying or following these exposures, though the calcite on a Colombian emerald matrix specimen phosphoresced. On heating, the irradiated stones reverted to their original color, without heat they appear to have been permanently colored.

Corundum

The most unexpected results were those obtained with various corundum gems, most marked in the case of the pale natural Ceylon sapphires. Previous reports had not indicated that sapphire would be particularly susceptible to changes induced by irradiation, but it was found that sapphires were, with spodumene, the most easily altered of all the gem stones tested, and that the effects disappeared on exposure to light more slowly than might have been expected from the rapidity of the coloration.

The color added by the x-rays was the same in each case, but variations in the original color naturally affected the result. The actual induced color is a rich golden or amber hue, in the case of colorless or pale sapphires this would be a most desirable change if it could be made permanent. Completely colorless sapphires become a rich amber in an exposure of five or ten minutes; usually the beam was directed at the culet so that the effect on the facetted gem would be most pronounced. Viewed horizontally, these stones are seen to be deeply colored near the surface where the radiation first struck the gem, but fade out to colorless a few millimeters toward the crown. White and pale yellow stones become, briefly, very handsome gems. Blue sapphires naturally become a sort of muddy green, while light lilac stones become a rosy orange, near to *pacparatum*. Common gray star sapphires turn yellow brown. Natural sapphires show the change much more distinctly than the synthetics, though these too show changes which differ only in degree, not in hue.

Prolonged exposure to sunlight gradually causes a reversion to the original hue; though it is rather difficult to get the last trace of color out of the originally colorless stones without some application of heat. In the dark, the color appears to remain the same indefinitely. Pale yellow stones fade more slowly and color more deeply than stones which are originally white. The fading of natural yellow sapphires in the same sort of sun lamp exposure as that to which the x-ray colored stones were tested was tried, and they were found to fade only slightly, the fading being not at all comparable to the fading of the color induced by the x-ray. If a method could be found which would make this color more permanent, it would be of considerable commercial importance. As it is, the color might last for years if gems so tinted were used only occasionally and where they would not be exposed to sunshine. Naturally deep yellow stones should be carefully scrutinized and subjected to fading tests before purchase when the tubes become generally available.

The ubiquity of the amber coloration, regardless of any other pigmentation, suggests that the discoloration under x-rays is caused by a constituent universally present, regardless of the other pigmentation, but since it is weakest in the purest synthetics, it is due to an impurity or structural defect not abundant in the synthetic material, but universally present in natural Ceylon stones.

No fluorescence or phosphorescence was observed in the corundum gems during and after exposure, with the single exception of a pale salmon-colored stone which fluoresced a brilliant orange during the radiation. In other respects this stone did not differ from experience with the other sapphires. Blue Australian sapphires were unaffected.

Synthetic Corundun

The synthetic corundums of various colors showed varying responses to the irradiation. Blue stones showed a slight greening, or, like synthetic ruby, no change at all. A deep pink stone became deeper red in

TABLE 1

Mineral	Composition	Original Color	After Radiation	Experiment Time	Phosphorescence and remarks
Spodumene (kunzite) (Cal.)	$LiAlSi_2O_6$	Lilac	Green	5 min. to 1½ hrs.	Bright orange
Spodumene (Brazil)	$LiAlSi_2O_6$	White	Green	10 min.	Zoned
Spodumene (Madagascar)	$LiAlSi_2O_6$	White	Green	5 min. to 4 hrs.	Orange
Beryl (aquamarine)	$Be_3Al_2Si_6O_{18}$	Pale blue	Light green	41 hrs.	None
Beryl	$Be_3Al_2Si_6O_{18}$	White	Pale brown	16 hrs.	None
Beryl (emerald)	$Be_3Al_2Si_6O_{18}$	Green	Green	1 hr.	None. No change
Beryl (morganite)	$Be_3Al_2Si_6O_{18}$	Pink	Muddy pink	1 hr.	None. Restored color removed by heat.
Corundum (Ceylon)	Al_2O_3	White and blue	Amber and dark green	5 min.	None
Corundum (Australia)	Al_2O_3	White and blue	Light brown and blue	5 hrs.	None
Corundum (Ceylon)	Al_2O_3	Pale yellow	Amber	10 min.	None. Paled in 5 hrs. sun.
Corundum (Ceylon)	Al_2O_3	Blue violet	Amber	10 min.	None
Corundum (Ceylon)	Al_2O_3	Lavender	Amber	Up to 23 hrs.	None. No change on prolonged exposure.
Corundum (Ceylon)	Al_2O_3	Blue gray (Star sapphire)	Amber	10 min.	None
Corundum Synthetics	Al_2O_3	Blue Rose red Pink rose Green Pink White	Slight greening No change Red amber Dirty amber Red amber Slightly brown	2 hrs. 2 hrs. 15 hrs. 10 min. 5 hrs. 1 hr.	None None None None None None
Corundum (Ceylon)	Al_2O_3	Pale salmon	Amber	10 min.	Bright yellow fluorescence
Tourmaline	Complex silicate	Pink	Dark rose purple	10 hrs.	None
Tourmaline	Complex silicate	Dark green	Dark rose purple	8½ hrs.	None
Tourmaline	Complex silicate	Light green	Light yellow	1½ hrs.	None
Quartz	SiO_2	White	Smoky	1 hr.	None
Quartz	SiO_2	Purple	Darker purple	15 hrs.	None
Quartz	SiO_2	Brown	Purple	5 hrs.	None
Topaz	$Al_2SiO_4 \cdot (F, OH)_2$	White	Brown purple	15 min.	None
Topaz	$Al_2SiO_4 \cdot (F, OH)_2$	Pale blue	Brown purple	1½ hrs.	None
Topaz	$Al_2SiO_4 \cdot (F, OH)_2$	Pale blue	Amber	27 min.	None
Topaz	$Al_2SiO_4 \cdot (F, OH)_2$	Pale brown (Utah)	Smoky brown	15 min.	None
Topaz	$Al_2SiO_4 \cdot (F, OH)_2$	Yellow brown	Amber	15 min.	None
Topaz	$Al_2SiO_4 \cdot (F, OH)_2$	Pinked	Orange brown	15 min.	None

TABLE 1 *Continued)*

Mineral	Composition	Original Color	After Radiation	Experiment Time	Phosphorescence and remarks
Diamond	C	White	White	4½ hrs.	None
Diamond	C	Light yellow	Lighter yellow	19 hrs.	None
Diamond	C	Pale brown	Gray brown	19 hrs.	None
Diamond	C	Yellow (skin)	Yellow	19 hrs.	None. Change is very slight, if any.
Spinel	$MgAl_2O_4$	Gray blue to red	Slight darkening	½ hr.	None
Phenakite	Be_2SiO_4	White	Yellow brown	40 min.	Weak
Apatite	$Ca_5(F, Cl)(PO_4)_3$	Green	Yellow green	1 hr.	None
Fluorite	CaF_2	Yellow and blue	Banded blue and no change	10 min.	None. Blue bands in yellow area parallel to crystal face.
Opal	$SiO_2 \cdot nH_2O$	Colorless	No change	20 hrs.	None
Opal	$SiO_2 \cdot nH_2O$	Orange	No change	18 hrs.	None
Scapolite	Complex silicate	White	Purple	10 min.	None. Strongly dichroic.
Scapolite	Complex silicate	Yellow	Gray purple	10 min. to 1½ hrs.	Orange. Strongly dichroic.
Brazilianite	$Na_2Al_6P_4O_{14} \cdot 4H_2O$	Yellow	Slightly darker	1½ hrs.	None
Simpsonite	$Al_{10}Ta_6O_{20}$	Yellow brown	No change	40 min.	None
Dioptase	H_2CuSiO_4	Green	No change	1 hr.	None
Hackmanite	$nNaAlSiO_4 \cdot NaNaSO_4$	White	Raspberry red	10 min.	Orange fluorescence
Cancrinite	$(Ca, NaH)CO_3 \cdot 3NaAlSiO_4$	White	Blue veins	10 min.	None
Lapis Lazuli	Complex Na silicate	Blue and white	Bluer	2 hrs.	None
Zircon	$ZrSiO_4$	Brown	No change	????	None
Zircon	$ZrSiO_4$	Blue (heated)	Grayer	????	None
Chrysoberyl	$BeAl_2O_4$	Yellow	No change	½ hr.	None
Oligoclase	Na, Ca aluminum silicate	White	Orange and green	1 hr.	Green fluorescence. Strongly pleochroic. White phosphorescence.

color and a light pink became a rich red amber, much like the color produced in natural stones. A green sapphire became a dirty amber hue, and a colorless stone turned slightly brown. The exposures of all these synthetics were longer than those given the natural stones, and ranged up to fifteen hours. However, as with the natural stones, the changes induced seem to take place quickly, and further irradiation has little effect. A white American boule was slightly yellowed where the beam fell.

Tourmaline

A number of stones of different colors were treated, but no marked results were obtained. In general there was a darkening of color but it was very slight. The darkening in a deep rose-purple stone was accomplished by a ten hour exposure, though the total effect may have been attained much earlier, while a green stone showed no change after eight and a half hours. A pale green gem, on the other hand, turned light yellow with a treatment lasting but one hour and twenty minutes.

Quartz

(a) *Rock Crystal:* It has been reported that quartz oscillators turn dark on exposure to *x*-rays, but in our experiments colorless quartz appeared quite resistant to color changes. A series of tests on a single prism face of a crystal showed appreciable discoloration only after an hour or more of exposure. In this substance, individual quartz crystals will undoubtedly vary, for Frondel, 1944, reports the development of banding parallel to growth faces in the irradiated plates and is also able to detect twinning by differential coloration. This was noted by us in a large crystal which was irradiated. In this connection, Frondel notes that "the sensitizing factor apparently depends on the growth history of the mother crystal." Similar banding was noted in fluorite, and it seems likely the explanation lies in a varying percentage of lattice defects caused by variations in conditions during crystal growth, rather than an impurity included during growth. The color can be removed by heating as are the other stone colorations, but Frondel reports that the effect on oscillation frequencies appears to be permanent below 175° C.

(b) *Amethyst:* Violet stones seem to be relatively unaffected by irradiation, though in some there was a suggestion of darkening. Heated amethysts, so-called "topaz," which had been changed to brown, became much darker, the result of the imposition of a smokiness on the yellow brown coloration. Here, as in brown topaz we find the two colorations unrelated and independent. Natural citrine also became smoky in the treatment.

(c) *Other Quartz Varieties:* Rose quartz became very dark under irradiation, as reported by Frondel. Chalcedony was weakly affected, and the banding was accentuated by variations in response.

Scapolite

Scapolites of two types were tested and showed similar responses, with some variation. A white scapolite cat's-eye from Burma became deep violet after a brief (10 minute) exposure to the radiation. Penetration was not deep and best results were obtained by exposing different areas of the stone in succession. The induced color was strongly dichroic, ranging from deep violet parallel to the *c*-axis to almost colorless across it, and across the parallel inclusions which make the "eye." Because of this strong dichroism, the coloration of the gem is less intense than might be expected. This color fades rapidly on moderate heating or on exposure to light, and, unlike the other stones treated, it fades in the dark. Within one month of the treatment, a very deeply colored stone had become almost white again, although it had been kept in the dark all of the time. Of all the stones tested, this showed the most marked fading with time alone; some of the others may have faded but certainly none was as noticeable.

A transparent pale yellow stone from Brazil was similarly treated and this likewise changed to violet. A comparable stone was treated by exposure to radium by Mr. Grant Waite of Toronto and both acquired a pale violet color, with pronounced dichroism. The coloration of the yellow gems appears to be no more permanent, the radiated stone likewise faded rapidly on exposure to light, but it was less sensitive than the white Burmese gem. A bright orange fluorescence and phosphorescence was observed, continuing for some minutes after the exposure.

Opal

A Mexican opal was subjected to radiation in the hope that darkening of the clear material of the back might make the color stand out better, but no change was noted in the stone after twenty hours of treatment. Similarly negative results were obtained in the treatment of a fire opal from Mexico.

Topaz

Specimens of blue and white topaz became smoky brown on exposure. This color did not resemble any natural topaz coloration. It was easily removed by heat treatment. On the other hand, pale yellow and pale pink Brazilian topaz had a definite brownish coloration added, of a type which, if permanent, would greatly enhance the value of the stone. Eight hours of exposure to sunlight removed most of the induced color.

Zircon

Several stones were treated, including blue heat-treated zircons and natural brown ones. The heat-treated blue partly reverted to a brown stone, a layer about 1 mm. thick became very brown, while the brown crystals were unaffected. On exposure to sunlight, one irradiated stone became blue again.

Diamond

A few stones were treated, off-color yellows and browns having been selected to begin with. No particularly remarkable results were obtained and most of the diamonds appeared unaffected. One of a matched pair of yellow brown stones was treated and after fifteen hours of irradiation it appeared to be somewhat lighter in color than its mate. Another pale brown stone appeared to have darkened a little. Since these stones were so small, it was difficult to judge colors, and further work in this field might be advisable. Certainly any process which could reduce yellow in diamonds is worth investigating further, for if the change is temporary there is a danger of treatment just before a sale; and if permanent, worth considering as a gem treatment.

Other Experiments

Heating and chilling: A number of other experiments were tried, with the thought that extreme temperatures coupled with *x*-ray bombardment might produce more spectacular or more permanent results. No particularly interesting results were obtained; but further work along those lines might be profitable. Sapphires which were heated above 300° C. at the time of the exposure to the radiation failed to color at all deeply. Below that temperature progressively deeper colorations down to 100° C., were obtained and below that the results were the same as at room temperature. Supercooled stones, immersed in liquid air just before treatment, were colored in the same way and to the same degree as a stone at room temperature.

Electrical tests: Experiments with strong magnetic fields made no difference in the color of the sapphires: likewise with strong electrostatic fields. Apparent conductivity was noted in a strong electric field, a current of 5.5 microamperes being obtained. However, this was caused by ionization of the air between the high voltage plates and not by any conductivity of the gem, as was shown by a test run without the stone in place.

Fading by light and/or heat: Tests for fading due to sunlight were made on an accelerated basis by using a Westinghouse Mazda-Type RS 275 W type sunlamp, the fading effect of which on treated stones at a six inch distance was found to be approximately equivalent in one hour to two hour's exposure to mid-summer midday sun, in the latitude of New York. An ultraviolet germicidal lamp, having very little visible or infra-red output, produced no perceptible fading. An hour's treatment under the sun lamp resulted in the removal of most of the induced color in the case of treated sapphires. Fading tests on natural yellow sapphires showed that under the same conditions of light as were found to be sufficient to fade irradiated stones, comparatively little fading took place. On the other hand, irradiated stones which were originally light yellow, rather than colorless, assumed a deeper hue and faded more slowly in light than the originally colorless stones. Heating to a temperature of 300° C. for five minutes was sufficient to drive the last vestige of color from the originally colorless stones, but did not do this to the naturally yellow stones though there was some fading. Prolonged *x*-ray treatment had no effect upon depth of color or rate of fading, variations were found to be due to differences in the individual stones.

X-ray quality effects: It was desired to test the influence of different quality *x*-rays upon the colors; it having been noted that the bright green obtained in spodumene by the treatment described above seemed to be more intense than in the case of stones previously treated by other experimenters, whose crystals appear gray-green. A kunzite was exposed to irradiation from a Machlett Thermax tube (a conventional Pyrex glass, oil-immersed tube) for thirty minutes at 155 PKV and 8 MA, and the stone became about the same green as already noted, after about an hour required for the disappearance of the phosphorescence. However, the high voltage rays had a greater penetrating power and gave an even coloration to the spodumene. In the previous experiments high surface absorption of spodumene had been noted, when the phosphorescence after ten minutes' treatment was seen to be very close to the surface. Probably the grayer green noted in stones colored some years ago, for example some seen in the Goldschmidt collection in Heidelberg a number of years ago, had partly reverted to their original hue, or were incompletely colored in the first place, retaining much of the inner lilac hue, which naturally reduced the richness of the new color.

A pale yellow sapphire treated for ten minutes at 125 PKV×10 MA and followed thirty minutes of 150 PKV×8 MA became a rich amber, possibly somewhat darker than the color obtained with the AEG-50 tube. This again indicates greater penetration of the high voltage *x*-rays, producing a more uniform coloration throughout the entire mass of the larger stones. In the experiments with the Thermax tube, the specimens were laid directly against the plastic window in the shockproof tube enclosure, and approximately 8 cm. from the focal spot.

Supplementary note: In the course of the heating experiments, an interesting color phenomenon was observed on a lilac sapphire. This stone was irradiated to produce an orange color. On heating to 300° C. it was observed to become a blue-green. As it cooled after treatment, the original color reappeared. This color change with temperature was found to be independent of the irradiation, it was a temperature phenomenon, much like that which has been described for gillespite (Lee,

1936) and which jewelers have noted in working with rubies. Further thermal experiments with this type of stone should prove interesting.

ACKNOWLEDGMENTS

The authors wish to express their appreciation to Mr. R. R. Machlett for making the new AEG-50 tube available for the tests; to Mr. H. M. Paskow for the loan of gem material and to Mr. Joseph D'Agostino for his cooperation in initiating the experiments. The authors also wish to express their appreciation to Machlett Laboratories, Springdale, Connecticut, for supplying the color plate.

REFERENCES

DEBOER, J. H., *Electron Emission and Absorption Phenomena.* Cambridge (**1935**).

DOELTER, C., *Handbuch der Mineralchemie.* Vol. 1–4 (**1912**).

FRONDEL, CLIFFORD, Frequency adjustment of quartz oscillator-plates by *x*-rays. *Reeves Sound Laboratories* (July, **1944**).

LEE, O. IVAN, Reversible photosensitivity in hackmanite: *Am. Mineral.*, **21,** 771 (1936).

MOTT AND GURNEY, *Electronic Processes in Ionic Crystals.* Oxford (**1940**).

ROGERS, T. H., A high intensity source of long wave-length *x*-rays: *Industrial Radiography,* **4** (no. 3), 35–39 (1945–46).

ANALYSES OF THE MINOR CONSTITUENTS IN POLLUCITE

L. H. Ahrens, *University of the Witwatersrand, Johannesburg, South Africa.*

Contents

Introductory 44
Analytical
(a) Qualitative 45
(b) Quantitative 48
Results and Discussion:
(a) Qualitative 48
(b) Quantitative 48
1. Abundance of rubidium 49
2. Abundance of thallium 49
3. Ratio of rubidium to thallium 50
(c) Presence of strontium and the radioactivity of rubidium 50
Acknowledgments 51
References 51

Abstract

Three specimens of pollucite (Greenwood, Maine, U.S.A.; Tin Mountain, S. Dakota, U.S.A.; and Varuträsk, Sweden) have been examined qualitatively for Pb, Sn, In, Ag, Cb, Y, La, Sr, Ba, W and Be and quantitatively for Rb, Tl, K, Li and Ga, using the spectrograph.

From the available data it appears that Rb and Tl are enriched in pollucite to a considerable extent. The mean Rb_2O content is 0.53% (seven analyses) and the mean Tl_2O content is 0.0028% (five analyses).

The mean weight ratio Rb_2O/Tl_2O is 150 (five ratios), which is very similar to the mean ratio of about 110 in potassium minerals, indicating that Rb^+ and Tl^+ replace Cs^+, and K^+, with the same relative facilities.

In general the spectra of the different specimens of pollucite indicate that the mineral is relatively free from the presence of several of the rarer elements commonly found in pegmatitic minerals. A trace of strontium was found in each specimen of pollucite; the quantity of strontium present in each case suggests that it is largely radiogenic.

A brief outline is given of the qualitative method of analysis.

Introductory

Shortly after publishing quantitative analyses of the minor constituents in two specimens of pollucite (Ahrens, 1), three more specimens of this rare and fascinating mineral were very kindly sent by Dr. Michael Fleischer of the U. S. Geological Survey. After cleaning each mineral from possible sources of contamination, the specimens were examined qualitatively and quantitatively using the spectrograph, and the results of the analyses are given and discussed in this paper.

ANALYTICAL

(*a*) *Qualitative analysis:*

Several of the rarer elements were sought which are frequently found in pegmatitic minerals, particularly in those which have been formed from later residual emanations. These elements were:

Pb: All feldspars and several specimens of mica that have been examined contain Pb; other investigators have reported the presence of Pb in feldspar.

Sn: Many specimens of muscovite and lepidolite have been found to contain Sn.

In: This rare element has been detected in about fifteen per cent of the muscovite and lepidolites that I have examined.

Ag: Many specimens of feldspar and also of mica contain traces of silver.

Cb: Cb is invariably found in granite, probably entering the mica lattice, and this element has been found in all lepidolites (0.005–0.2% Cb_2O_5), and some muscovites that have so far been analysed by the author. Although tantalum is invariably associated with columbium and is found in mica (Rankama, 2), it was not sought because its spectral sensitivity is extremely poor.

Y, La, Be, W: All are relatively common in pegmatites.

Sr: Strontium was sought because its presence was expected as a result of the radioactive decay of rubidium, relatively large quantities of which may be found in pollucite.

Ba: The presence or absence of barium would serve as a rough indicator as to the genesis of strontium.

For the analyses of lead, tin, silver and indium (volatile elements in the arc) a low amperage was employed (2–3 amps) and only the first minute of arcing was recorded. For the detection of the relatively involatile elements such as columbium, yttrium, lanthanum, strontium, barium and beryllium, each specimen of pollucite was treated with hydrofluoric acid and the residue taken to dryness, prior to arcing. All fluorides are readily volatilised from the arc: this renders the detection of traces of the involatile elements more sensitive and simple than by analysing without prior acid treatment, even if care has been exercised to arc the untreated mineral to completion so as to record the spectra of the involatiles.

Each fluoride residue was arced for 30 seconds at 6–7 amps, and in each case the mineral was volatilised from the anode.

Figure 1 shows the spectrum of pollucite fom Karibib (see Ahrens, 1) which had been treated with hydrofluoric acid. Sr 4077 is very clearly evident and its intensity may be contrasted with the extreme weak in-

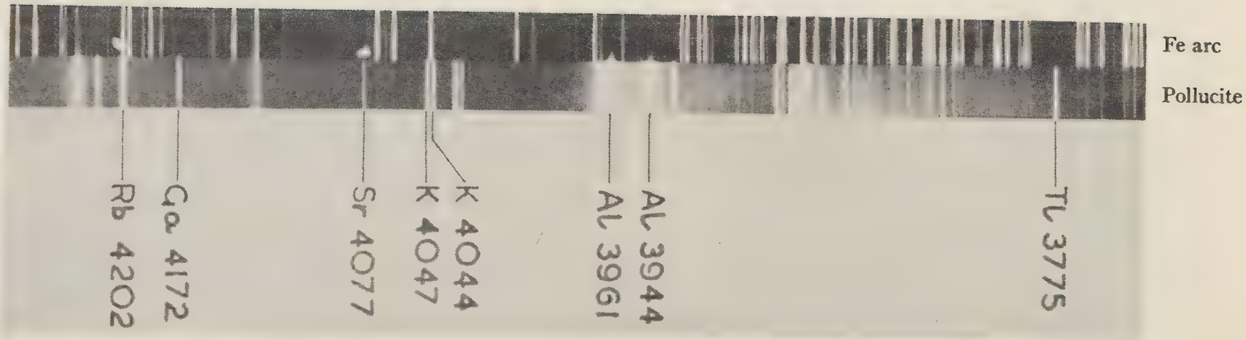

FIG. 1. Spectrum of residue of a specimen of pollucite (Karibib, South West Africa) after treatment with hydrofluoric acid. Note strong relative intensities of Sr 4077 and $\mathrm{Al}\begin{cases}3944\\3961\end{cases}$ compared with the weak intensities of these lines in Figure 2. It is probable that the emission of Sr 4077 is from radiogenic strontium (Sr^{87}).

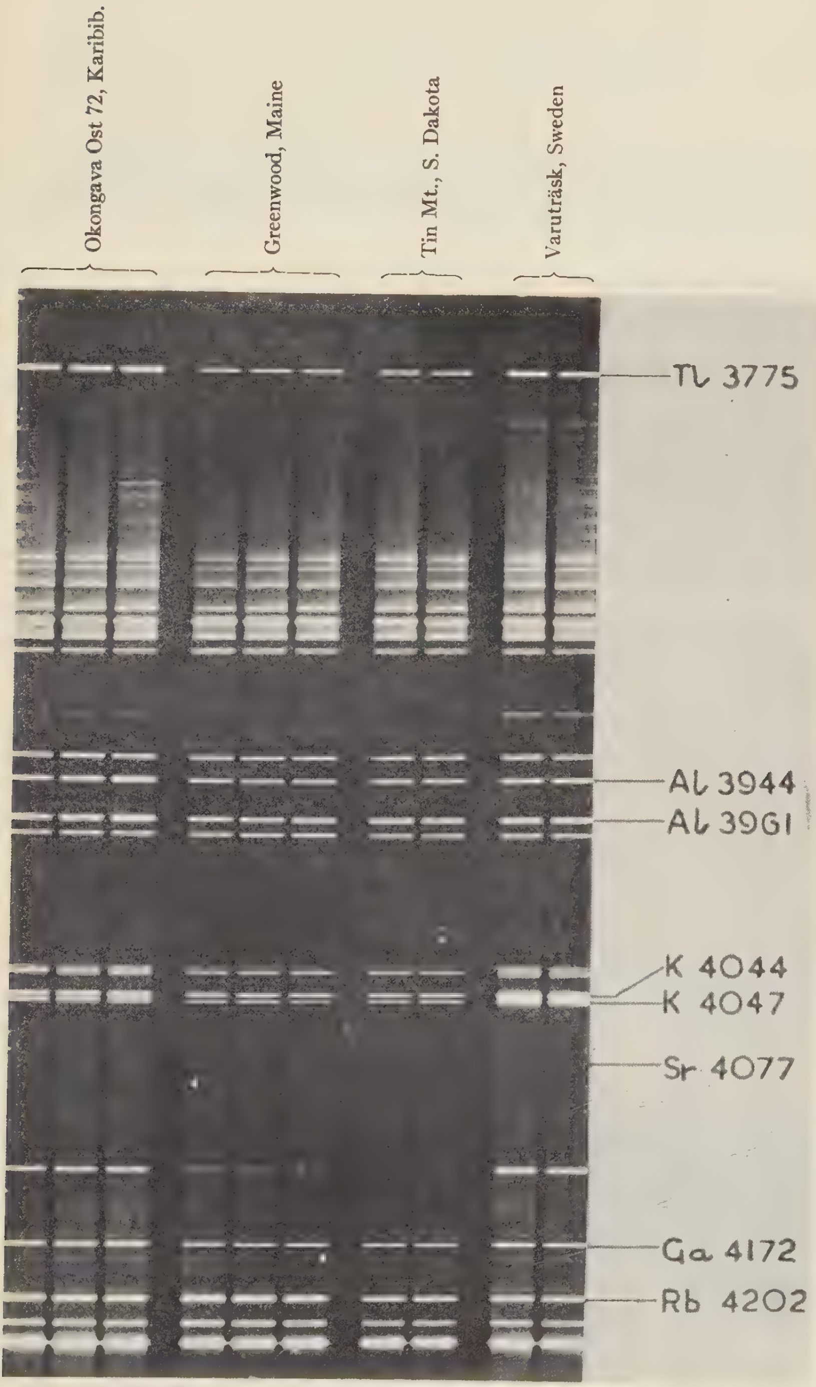

FIG. 2. Duplicate and triplicate spectra of different specimens of pollucite. The presence of gallium, potassium, rubidium and also the rare element thallium, several properties of which are similar to the alkali metals of higher atomic weight, is clearly evident in each case.

tensity of Sr 4077 in the different spectra on Figure 2. Note also the difference in intensities between $\text{Al}\left\{\begin{matrix}3944\\3961\end{matrix}\right.$ on Figure 1 (relatively intense) and on Figure 2 (relatively faint); Al is relatively involatile when silicates are arced, but by conversion to the fluoride it is made volatile.

A blank examination on the hydrofluoric acid failed to reveal the presence of any of the elements sought.

(*b*) *Quantitative analysis:*

A specimen of pollucite from Karibib, the analysis of which was known (Ahrens, 1), served as a standard for the estimation of gallium (semi-quantitative), thallium, rubidium, potassium and lithium. A description of the quantitative spectrochemical technique for estimating Rb and Tl is described in the literature (Ahrens, 3) and a similar method may be employed for the estimation of potassium and lithium. Figure 2 shows the spectra of the different specimens which have been arced in duplicate or in triplicate; inspection of this Figure shows that agreement between the duplicate and triplicate analyses is reasonably close in each case.

Results and Discussion

(*a*) *Qualitative:*

Of all the elements sought qualitatively, Sr alone could be detected, and was present in all three specimens. In this respect the spectrum of pollucite is relatively "pure" when compared with the spectra of other pegmatitic minerals and one probable reason for this purity is that the lattice of pollucite does not contain a site capable of accommodating medium size ions, that is, ions in six-fold co-ordination as in mica, for example.

The presence of traces of strontium will be discussed under a separate sub-heading (Radioactivity of rubidium).

(*b*) *Quantitative:*

The quantitative results are given in Table 1.

Table 1

Locality	$\%Tl_2O$	$\%Rb_2O$	$\%K_2O$	$\%Li_2O$	$\%Ga_2O_3$
Greenwood, Maine, U.S.A.	0.0019	0.68	0.16	0.008	0.0005
Tin Mt., S. Dakota, U.S.A.	0.0019	0.25	0.19	0.006	0.0005
Varuträsk, Sweden	0.0080	0.37	2.5	0.053	0.0010

The results of these analyses will be discussed under three sub-headings.

(1) *Abundance of rubidium:*

Including the three analyses given in this paper, seven analyses of rubidium in pollucite are now available, and these are given in Table 2.

TABLE 2

Locality	%Rb_2O	Author
Tin Mt., Black Hills, U.S.A.	absent	Wells & Stevens (4)
Tin Mt., Black Hills, U.S.A.	0.25	Ahrens (This paper)
Norway, Maine, U.S.A.	0.23	Ahrens (1)
Greenwood, Maine, U.S.A.	0.68	Ahrens (This paper)
Karibib, S.W. Africa	0.54	Ahrens (1)
Varuträsk, Sweden	0.37	Ahrens (This paper)
Varuträsk, Sweden	1.60	Quensel (5)

With the exception of the first analysis, these analyses indicate that rubidium is relatively enriched in pollucite which appears to contain about the same quantity as is commonly found in green microclines (amazonite). For analyses of rubidium in amazonite, see Goldschmidt (6), Tolmacev, (7) and Ahrens (3).

After lepidolite, which is the mineral richest in rubidium, pollucite (and amazonite) appears to be richest in rubidium, although relatively large quantities may on occasion also be encountered in muscovite and biotite.

It is surprising that Wells and Stevens were unable to detect any rubidium in their specimen from Tin Mountain.* They analysed their specimen chemically for the alkali metals and examined different alkali metal rich fractionates spectroscopically and in each case rubidium was found to be absent.

(2) *Abundance of thallium:*

Five analyses of thallium in pollucite are now available; three in this paper and two in the previous publication (1), and the mean Tl_2O content of these five analyses is 0.0028%. This value is about the same as the mean Tl_2O content of fifteen amazonite specimens, which is 0.0023% (3).

---

* Their specimen was not the same one as that analysed by me.

Together with amazonite, pollucite is probably the mineral second richest in rubidium, lepidolite being the richest.

(3) *Ratio Rb_2O/Tl_2O:*

The mean weight ratio Rb_2O/Tl_2O in potassium minerals is about 110 (3) and the limits of variation of this ratio are 30 (minimum) and 650 (maximum). In pollucite where Rb^+ and Tl^+ replace Cs^+ instead of K^+ as in potassium minerals, the Rb_2O/Tl_2O ratios of five specimens that have been analysed are:

Greenwood	350	This publication
Tin Mt.	130	
Varuträsk	45	
Karibib	50	Previous publication on the minor constituents in pollucite (1).
Norway (Maine)	180	

The mean ratio for these five specimens is 150 and is very similar to the mean ratio for the potassium minerals. Because the Rb_2O/Tl_2O ratios are about the same for potassium minerals and for pollucite, there is little doubt that Rb^+ and Tl^+ replace K^+, and Cs^+, with the same or very nearly the same relative facilities.

(*c*) *The presence of strontium and the radioactivity of rubidium:*

In the earlier publication on pollucite (1) it was suggested that the presence of a trace of strontium in the Karibib pollucite could be ascribed to the radioactive disintegration of rubidium; $Rb^{87} \rightarrow \beta$ particle $+ Sr^{87}$. Hahn and co-workers (8) have isolated strontium from a specimen of pollucite, examined it on the mass-spectrograph, and found Sr^{87} predominant with only a very small amount of $Sr.^{88}$ The results of the analyses of the specimens described in this paper corroborate the above evidence that Sr in pollucite is largely radiogenic, because in each of the three specimens of pollucite traces of strontium could be detected; furthermore, although no accurate estimates of the strontium contents were made, approximate determinations showed that in each case the quantity of strontium was about equal to that expected, if it were radiogenic. Thus, although the specimen of pollucite from Maine contained 0.68% Rb_2O, whereas the specimen from Tin Mountain contained 0.25%, the strontium content of the former appeared to be slightly less than that of the latter. This is in agreement with the relative ages of the two specimens in question; the age of the specimen from Maine is about 300,000,000 years (from Sr/Rb measurements on lepidolites), whereas the age of the pollucite from Tin Mountain is very much greater, and is probably about 1,300,000,000 years, as determined from Pb/U ratios of uranium minerals from the Black Hills. (A preliminary note on the use of Sr/Rb ratios for age determinations has been published (9) and a detailed account is in the press.)

In none of the specimens could barium be detected (limit of detection about 0.0001% Ba); this absence of barium provides indirect corroborative evidence of the radiogenesis of strontium.

ACKNOWLEDGMENTS

I would like to express my gratitude to Dr. Michael Fleischer of the U.S. Geological Survey for kindly providing the three specimens of pollucite.

REFERENCES

(1) AHRENS, L. H., *Am. Mineral.*, **30**, 616 (1945).
(2) RANKAMA, K., *Bull. Com. Geol. Finlande*, No. 133 (**1944**).
(3) AHRENS, L. H., *Trans. Geol. Soc. S. Afr.*, **48**, 207 (1945).
(4) WELLS, R. C., AND STEVENS, R. E., *Ind. Eng. Chem., Anal. Ed.*, 9, 236 (**1937**).
(5) QUENSEL, P., *Geol. För. Stockholm Förh.*, **60**, 612 (1938).
(6) GOLDSCHMIDT, V. M., BAUER, H., AND WITTE, H., *Nachr. d. Ges. d. Wiss. Göttingen, Math.-Phys. Kl.*, Vol. **1**, No. 4, 39 (1934).
(7) TOLMACEV, J., AND FILIPPOV, A., *Compt. Rend. Acad. Sci., U.R.S.S.*, **5**, 323 (1935).
(8) HAHN, O., STRASSMANN, F., MATTAUCH, J., AND EWALD, H., *Naturwiss.*, **30**, 541 (1942).
(9) AHRENS, L. H., *Nature*, **157**, 269 (2 March 1946).

HEXAGONAL FOUR-INDEX SYMBOLS

J. D. H. Donnay, *The Johns Hopkins University, Baltimore, Maryland.*

Introduction

The purpose of this paper is to present a mathematical derivation of some properties of the four-index notation, for faces and zones, in the hexagonal system. No such treatment seems to be available in English, although adequate presentations can be found in other languages.

I. Face Symbol

In the hexagonal crystal system, a face is referred to the Bravais axes (Fig. 1) by means of the four-index symbol $(hk\bar{i}l)$, in which $i=h+k$.

Proof.—Let a straight line AB intersect the negative a_3-axis in a point C. Let its intercepts be $OA=a/h$, $OB=a/k$, $OC=a/i$. The equation of the line AB is

$$x/(a/h) + y/(a/k) = 1;$$

that of the line OC, the bisector of the angle AOB, is

$$x = y.$$

The co-ordinates, OM and ON, of the point C are thus $x=y=a/(h+k)$. Since the triangles OMC and ONC are equiangular, hence equilateral, the intercept OC is equal to either co-ordinate of the point C,

$$OC = a/i = a/(h+k),$$

so that $i=h+k$.

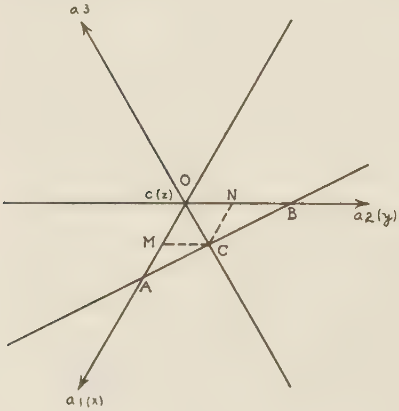

Fig. 1

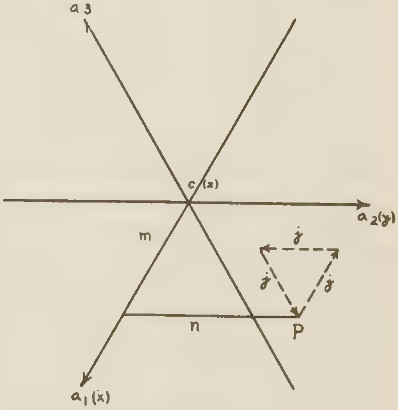

Fig. 2

II. Zone Symbol

A zone may likewise be expressed, in the four-index notation, by a symbol $[uv\bar{j}w]$, in which $j=u+v$.

Proof.—Let a point P in the $(a_1a_2a_3)$-plane (Fig. 2) be designated by the co-ordinates m, n, 0 (expressed in terms of the unit length a), which refer to the axes a_1, a_2, a_3, respectively. It is permissible to decrease (or increase) each of these co-ordinates by one and the same number, since the sum of the three vectors thus introduced is equal to zero. The point P can, therefore, be represented by the co-ordinates $m-j$, $n-j$, $\bar{j}$, in which j is equal to any number, positive or negative. In particular, j may be chosen equal to $(m+n)/3$, so that the sum of the three co-ordinates

$$u = m - [(m+n)/3], \quad v = n - [(m+n)/3], \quad j = -(m+n)/3,$$

becomes equal to zero. The zone symbol $[mn0w]$ may, therefore, be written $[uv\bar{j}w]$, with $j=u+v$.

Remarks.—To pass from the four-index notation (axes a_1, a_2, a_3, c) to the three-index notation (axes a_1, a_2, c):

(1) In the case of a face symbol $(hk\bar{i}l)$, drop the third index and obtain (hkl);

(2) In the case of a zone symbol $[uv\bar{j}w]$, add j to the first three indices, so as to make the third index zero, and obtain $[u+j\cdot v+j\cdot w]$.

III. Equation of Zone Control

The equation of zone control is the relation between the indices of a zone $[uv\bar{j}w]$ and those of a face $(hk\bar{i}l)$ contained in the zone. Using the three-index notation, the face symbol is written (hkl) and the zone symbol $[u+j\cdot v+j\cdot w]$. It is known that the equation of zone control can then be expressed

$$h(u+j) + k(v+j) + lw = 0. \tag{1}$$

This can be written

$$hu + kv + (h+k)j + lw = 0$$

or, since $i=h+k$,

$$hu + kv + ij + lw = 0. \tag{2}$$

Because $j=u+v$, the latter equation may also be written

$$(h+i)u + (k+i)v + lw = 0. \tag{3}$$

The indices of a face $(hk\bar{i}l)$ situated at the intersection of two given zones $[u_1v_1\bar{j}_1w_1]$ and $[u_2v_2\bar{j}_2w_2]$ are found by means of equation (1). They must satisfy the equations:

$$(u_1+j_1)h + (v_1+j_1)k + w_1l = 0,$$
$$(u_2+j_2)h + (v_2+j_2)k + w_2l = 0.$$

The three indices h, k, l are therefore obtained by cross-multiplication:

$$\begin{array}{c|ccccccc|c} (u_1+j_1) & (v_1+j_1) & & w_1 & & (u_1+j_1) & & (v_1+j_1) & w_1 \\ & & \times & & \times & & \times & & \\ (u_2+j_2) & (v_2+j_2) & & w_2 & & (u_2+j_2) & & (v_2+j_2) & w_2 \\ \hline & & h & & k & & l & & \end{array} \qquad (4)$$

and the superabundant index is $\bar{\imath}=-(h+k)$.

The indices of a zone $[uv\bar{\jmath}w]$ containing two given faces $(h_1k_1\bar{\imath}_1l_1)$ and $(h_2k_2\bar{\imath}_2l_2)$ are found by means of equation (3). They must satisfy the equations:

$$(h_1+i_1)u+(k_1+i_1)v+l_1w=0,$$
$$(h_2+i_2)u+(k_2+i_2)v+l_2w=0.$$

The three indices u, v, w are therefore obtained by cross-multiplication:

$$\begin{array}{c|ccccccc|c} (h_1+i_1) & (k_1+i_1) & & l_1 & & (h_1+i_1) & & (k_1+i_1) & l_1 \\ & & \times & & \times & & \times & & \\ (h_2+i_2) & (k_2+i_2) & & l_2 & & (h_2+i_2) & & (k_2+i_2) & l_2 \\ \hline & & u & & v & & w & & \end{array} \qquad (5)$$

and the *necessary* additional index is $\bar{\jmath}=-(u+v)$.

To check whether a given face $(hk\bar{\imath}l)$ is contained in a given zone $[uv\bar{\jmath}w]$, use equation (2).

Remarks.—Note that $(h+i\cdot k+i\cdot l)$ is *not* the three-index symbol of $(hk\bar{\imath}l)$ and that $[uvw]$ is *not* the three-index symbol of $[uv\bar{\jmath}w]$. In equation (2) the quantities h, k, i, l, on the one hand, u, v, j, w, on the other, play similar roles. This mathematical symmetry of equation (2) explains why it can be written in both forms (1) and (3). It also accounts for the fact that the same type of calculations permits finding the indices of a zone between two faces and those of a face at the intersection of two zones.

IV. Examples of Calculations

In beryl a face n is located at the intersection of two zones, between the faces $m(10\bar{1}0)$ and $v(21\bar{3}1)$ on the one hand, between the faces $a(11\bar{2}0)$ and $u(20\bar{2}1)$ on the other hand. What are its indices?

According to (5) we have

$$\begin{array}{cccccc} \multicolumn{6}{l}{\text{Indices of the first zone:}} \\ 2 & 1 & 0 & 2 & 1 & 0 \\ & \times & \times & \times & & \\ 5 & 4 & 1 & 5 & 4 & 1 \\ \hline & 1 & \bar{2} & 3 & & \end{array} \qquad \begin{array}{cccccc} \multicolumn{6}{l}{\text{Indices of the second zone:}} \\ 3 & 3 & 0 & 3 & 3 & 0 \\ & \times & \times & \times & & \\ 4 & 2 & 1 & 4 & 2 & 1 \\ \hline & 3 & \bar{3} & \bar{6} & & \end{array}$$

The symbols of the two intersecting zones are $[1\bar{2}13]$ and $[1\bar{1}0\bar{2}]$.

According to (4) we have

Indices of the face *n*:

$$\begin{array}{ccccccccccc}
0 & & \bar{3} & & 3 & & 0 & & \bar{3} & & 3 \\
 & & & \times & & \times & & \times & & & \\
1 & & \bar{1} & & \bar{2} & & 1 & & \bar{1} & & \bar{2} \\
\hline
 & & & 9 & & 3 & & 3 & & &
\end{array}$$

The symbol of the face *n* is $(31\bar{4}1)$.

According to (2) the face $(31\bar{4}1)$ belongs to the zones $[1\bar{2}13]$ and $[1\bar{1}0\bar{2}]$ since

$$\begin{array}{cccc}
3 & 1 & \bar{4} & 1 \\
\times & \times & \times & \times \\
1 & \bar{2} & 1 & 3 \\
\hline
3 & -2 & -4 & +3=0
\end{array}
\qquad\qquad
\begin{array}{cccc}
3 & 1 & \bar{4} & 1 \\
\times & \times & \times & \times \\
1 & \bar{1} & 0 & \bar{2} \\
\hline
3 & -1 & +0 & -2=0
\end{array}$$

V. Addition and Subtraction Rule

In the three-index notation it is known that any face $(ph_1 \pm qh_2 \cdot pk_1 \pm qk_2 \cdot pl_1 \pm ql_2)$, where p and q are any integers, lies in a zone with the faces $(h_1k_1l_1)$ and $(h_2k_2l_2)$. The validity of this "addition and subtraction rule" is obviously unaffected by the use of the fourth, superabundant, index.

In the preceding example the indices of the face *n* could have been obtained simply as follows (taking $p=q=1$):

$$\begin{array}{cccc}
1 & 0 & \bar{1} & 0 \\
2 & 1 & \bar{3} & 1 \\
\hline
(3 & 1 & \bar{4} & 1)
\end{array}
\qquad\qquad
\begin{array}{cccc}
1 & 1 & \bar{2} & 0 \\
2 & 0 & \bar{2} & 1 \\
\hline
(3 & 1 & \bar{4} & 1)
\end{array}$$

By virtue of the duality principle between faces and zones, the addition and subtraction rule also holds good for four-index zone symbols. For instance the zone $[0\bar{1}15]$ passes through the intersection of the zones $[1\bar{2}13]$ and $[1\bar{1}0\bar{2}]$, since its indices are obtained by subtraction as follows:

$$\begin{array}{cccc}
1 & \bar{2} & 1 & 3 \\
1 & \bar{1} & 0 & \bar{2} \\
\hline
[0 & \bar{1} & 1 & 5]
\end{array}$$

VI. Graphical Determination of a Zone Symbol from the Gnomonic Projection

In the three-index notation, the indices of a zone axis in the direct lattice (a_1, a_2, c) are the same as the indices of the plane perpendicular to the given zone axis in the reciprocal lattice (a_1^*, a_2^*, c^*). This follows from the very definition of the reciprocal lattice. The plane in question—the *zone plane*—contains all the normals to the faces in the zone. Its trace on the plane of the gnomonic projection is therefore the *zone line.*

The gnomonic projection is a representation of the reciprocal lattice (Mallard's Theorem). Indeed, since the scale of the projection is arbitrary, it is permissible to choose the plane of the gnomonic projection at a distance c^* above the origin; the gnomonic poles $(hk1)$ then constitute a net of the reciprocal lattice, namely its first layer. The natural axes of co-ordinates (P_1, P_2) of the gnomonic projection (Fig. 3) are parallel to the axes (a_1^*, a_2^*) of the reciprocal lattice. The zone plane passes through the origin; therefore, in order to find its indices in the reciprocal lattice, it is convenient to translate it parallel with itself until its intercept on the c^* axis is $-c^*$ or $c^*/\bar{1}$. After translation, the intercepts of the zone plane on the a_1^* and a_2^* axes of the reciprocal lattice are equal to the intercepts of the zone line on the P_1 and P_2 axes of the gnomonic projection. Let a^*/m and a^*/n be these intercepts, which can be determined graphically. The symbol of the zone plane in the reciprocal lattice is $(mn\bar{1})^*$. The symbol of the zone axis in the direct lattice (referred to the three axes a_1, a_2, c) is therefore $[mn\bar{1}]$. If the four axes, a_1, a_2, a_3, c, are used, the symbol may be written $[mn0\bar{1}]$ or preferably $[uvj\bar{1}]$, where u, v, j are the functions of m and n defined above (Section II). The necessity for carrying out the transformation $[mn0\bar{1}]$ to $[uvj\bar{1}]$ can be avoided and the latter symbol determined directly by graphical means, thanks to the following mathematical artifice.

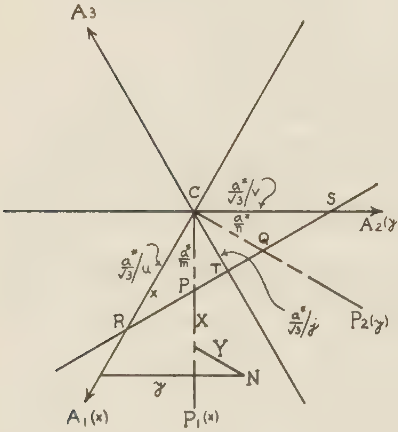

FIG. 3

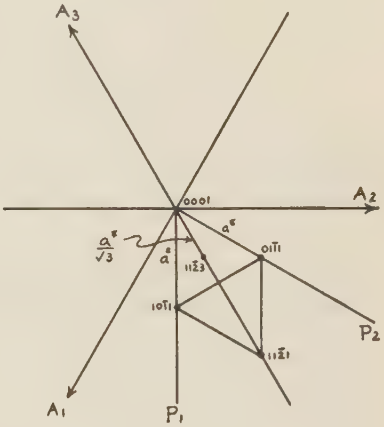

FIG. 4

Theorem.—In the plane of the gnomonic projection (Fig. 3) a zone line that intercepts a^*/m, a^*/n on the axes P_1, P_2 will intercept A/u, A/v, $A/\bar{j}$ (where $A=a^*/\sqrt{3}$) on the axes A_1, A_2, A_3.

Proof.—This theorem is easily proved by effecting a change of co-ordinates in the gnomonic plane. Let the old axes be P_1, P_2, with co-ordinates X, Y. Let the new axes be A_1, A_2, with co-ordinates x, y. The relation between the old and the new co-ordinates of any point N (Fig. 3) are

$$X + Y \sin 30^\circ = x \cos 30^\circ,$$
$$y - Y \cos 30^\circ = x \sin 30^\circ,$$

which can be written in the symmetrical forms

$$X = (2x - y)\sqrt{3}/3, \qquad Y = (2y - x)\sqrt{3}/3. \tag{6}$$

The equation of the zone line PQ in the old co-ordinate system is

$$X/(a^*/m) + Y/(a^*/n) = 1.$$

In the new co-ordinate system, it becomes, by virtue of relation (6) and after simple rearrangements,

$$x/\{(a^*/\sqrt{3})/[m - \tfrac{1}{3}(m + n)]\} + y/\{(a^*/\sqrt{3})/[n - \tfrac{1}{3}(m + n)]\} = 1$$

or

$$x/(A/u) + y/(A/v) = 1.$$

The intercepts on the axes A_1, A_2 are thus seen to be A/u and A/v. The intercept on the A_3 axis must be $A/\bar{j}$, with $j=u+v$ (the proof of this is the same as that given in Section I).

Graphical method.—The indices $[uv\bar{j}\bar{1}]$ of a zone line RS (Fig. 3) are obtained by measuring the intercepts A/u, A/v, $A/\bar{j}$ on the axes A_1, A_2, A_3. The unit length to be used, $A=a^*/\sqrt{3}$, is equal to one third the long diagonal of the reciprocal lattice mesh (a^*, a^*) built on the axes P_1, P_2 (see Fig. 4). It is equal to the distance of the pole $(11\bar{2}3)$ from the center of the gnomonic projection.

VII. Example

Given (Fig. 5) the poles $(10\bar{1}2)$ and $(01\bar{1}3)$ in gnomonic projection, find the symbol of the zone defined by these two faces.

Through the pole $(10\bar{1}1)$ pass a line parallel to the A_3 axis to obtain the unit length $A=a^*/\sqrt{3}$ on the A_1 axis. Measure the intercepts of the zone line RS on the axes A_1, A_2, A_3. They are: $CR=3A$, $CS=3A/4$, $-CT=-3A/5$. They can be written: $CR=A/(1/3)$, $CS=A/(4/3)$, $-CT=-A/(5/3)$. The intercept on the vertical axis is $-c^*$ by construction (see Section VI). The indices of the zone plane in the reciprocal lattice are therefore $(14\bar{5}\bar{3})^*$. The zone indices in the direct lattice are the same, $[14\bar{5}\bar{3}]$.

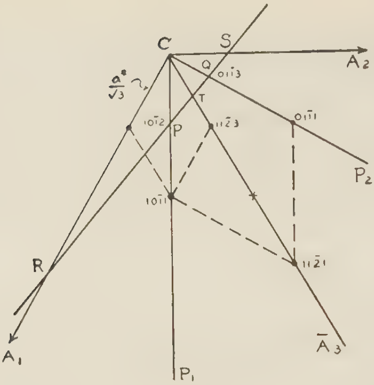

FIG. 5

VIII. REMARKS

The axes A_1, A_2, A_3 are *not* co-ordinate axes of the direct lattice. They are indeed parallel to the axes a_1, a_2, a_3 that pass through the origin. Their unit length, however, is $A = a^*/\sqrt{3}$, whereas the unit length a of the direct cell, expressed in terms of reciprocal lattice unit lengths, is $a = c^*a^*/V^* = c^*a^*/c^*a^{*2} \sin 60° = 2/a^*\sqrt{3}$ and not $a^*/\sqrt{3}$ as Wolfe implies (1944, pp. 52–53 and Fig. 4).

The four-index notation of hexagonal zones explained in Section II is due to Weber (1922). An excellent presentation is found in Terpstra's textbook (1927, pp. 201–204),[1] including the derivation of the equation of zone control in the four-index notation.

REFERENCES

HEY, MAX, H. (1930), On face- and zone-symbols referred to hexagonal axes: *Mineralog. Mag.*, **22**, 283–290.

TERPSTRA, P. (1927), *Leerboek der geometrische kristallografie*, 302 pp. P. Noordhoff, Groningen.

WEBER, LEONHARD (1922), Das viergliedrige Zonensymbol des hexagonalen Systems: *Zeits. Krist.*, **57**, 200–203.

WOLFE, C. W. (1944), Hexagonal zone symbols and transformation formulae: *Am. Mineral.*, **29**, 49–54.

---

[1] One misprint in Terpstra: on page 202, last line of the text, a minus sign is omitted. Read $\bar{\omega} = -(m+n)/3$.

ANALYSIS OF RAMSAYITE AND LORENZENITE

TH. G. SAHAMA, *Institute of Geology, Geochemical Laboratory, University of Helsinki, Finland.*

On an expedition to Southern Greenland in the year 1897 Flink discovered a new mineral from Narsarsuk, Julianehaab District, which he named lorenzenite. Later,[1] he published a detailed crystallographic, optical, and chemical study of this mineral. Of the mineral, occurring in a nepheline syenite, he gave the following chemical analysis, made by the eminent Swedish analyst R. Mauzelius:

SiO_2	34.26%
TiO_2	35.15
ZrO_2	11.92
Na_2O	17.12
K_2O	0.37
H_2O	0.77
	99.59%

The material being very rare, Mauzelius had only 0.5727 g. of the mineral available for the analysis.

In the year 1922 A. E. Fersman's expedition found a related mineral in the nepheline syenite of the Kola Peninsula. This mineral, called ramsayite, was first described by E. Kostyleva and later by W. Gerassimowsky and a general mineralogical summary of it is given in the general description of the Kola Peninsula minerals edited by Fersman.[2] Previously Kostyleva pointed out that the two minerals, lorenzenite and ramsayite, show very marked similarities in the crystal forms as well as in their chemical composition. She suggested that they represent the same mineral species. The best analysis of ramsayite thus far, made by K. Beloglazov, is as follows:

SiO_2	34.06%
TiO_2	46.26
Al_2O_3	0.90
FeO	1.03
MnO	0.02
CaO	0.35
Na_2O	16.20
K_2O	0.28
Rare earths	0.32
Loss on ignition	0.33
	99.75%

---

[1] Flink, G., On the minerals from Narsarsuk on the Firth of Tunugdliarfik in Southern Greenland: *Medd. om Grönland*, Bd. **24,** 1 (1901).

[2] Fersman, A. E., Minerals of the Khibina and Lovozero Tundras: *Lomonossov Institute of the Acad. Sci. USSR, Moscow and Leningrad* (**1937**).

The first description of ramsayite by Kostyleva appeared in 1923. The refractive indices given by her deviated considerably from those of lorenzenite given by Flink. However, Barth and Berman[3] showed in the year 1930 that the refractive indices given by Flink were erroneous and that the true indices of ramsayite and lorenzenite were practically identical. Later Kraus and Mussgnug[4] determined the dimensions of the orthorhombic unit cell and found exactly the same values for both minerals.

Thus, the only circumstance in which ramsayite and lorenzenite differ from each other is in the chemical composition; lorenzenite, according to the analysis by Mauzelius, containing zirconium apparently in the place of titanium in the lattice. Zirconium has, however, not been found in ramsayite.

In a previous paper dealing with the chemistry of the mineral titanite,[5] I have presented a general mineralogical classification of the titanite group. In connection with this work I was interested in ramsayite. Professor Pentti Eskola placed at my disposal a very beautiful specimen of the mineral from the collections of the Institute of Geology of the University of Helsinki. The analysis by Beloglazov given above being somewhat incomplete, I asked Mr. Oleg v. Knorring, M. A., to make a chemical analysis of this specimen of ramsayite. In addition, Mr. Oiva Joensuu, M. A., made a number of spectroscopic determinations of those elements which could not be determined chemically. This analysis was made in order to determine whether water and fluorine could be thought to play similar roles in the ramsayite lattice as seems to be the case in titanite. In order to compare lorenzenite in this respect with ramsayite and titanite, I asked Professor Arne Noe-Nygaard of Copenhagen for some lorenzenite specimens. He very kindly sent me three samples of the mineral. From one of these samples I separated a very pure fraction of lorenzenite, amounting to about 3.3 g. Mr. v. Knorring and Mr. Joensuu analyzed this mineral also.

The results of the analyses of ramsayite and lorenzenite made by v. Knorring and Joensuu are given in Table 1. Table 2 contains the corresponding molecular numbers. As to the methods used, I refer to my previous paper on titanite mentioned above. Because of the fact that both ramsayite and lorenzenite are easily fusible on heating, the determination of H_2O+ was carried out by employing the Penfield tube, without using any fluxing material, as is necessary for titanite.

---

[3] Barth, T., und Berman, H., Neue optische Daten wenig bekannter Minerale (Die Einbettungsmethode): *Chem. d. Erde*, Bd. **5**, 22 (1930).

[4] Kraus, O., und Mussgnug, F., Identität von Lorenzenit und Ramsayit: *Naturwissenschaften*, Jahrg. **29**, 182 (1941).

[5] Sahama, Th.G., On the chemistry of the mineral titanite: *Bull. Comm. géol. Finl.*, No. **138**; *C.R. Soc. géol. Finl.*, No. **XIX** (1946) (In print).

TABLE 1. ANALYSIS OF RAMSAYITE AND "LORENZENITE"

	Ramsayite Kola	"Lorenzenite" Narsarsuk, Greenland
SiO_2	34.64	35.40
TiO_2	45.01	43.16
Nb_2O_5	2.14	3.89
Ta_2O_5	0*	0*
V_2O_5	0.01	0.01
Al_2O_3	0.21	0.00
Fe_2O_3	0.00	0.00
Cr_2O_3	0.00	0.00
FeO	0.42	0.34
MgO	tr.	0.00
Sc_2O_3	0.003	0.003
ZrO_2	0.11	0.07
CaO	0.08	0.19
SrO	0.007	0.010
BaO	0.00	0.00
Na_2O	16.79	16.23
K_2O	tr.	0.00
Y_2O_3	<0.01	0.02
La_2O_3	<0.01	0.01
Ce_2O_3	0.05	0.04
MnO	0.024	tr.
F	0.07	0.38
Cl	0.00	0.00
H_2O+	0.48	0.42
H_2O-	0.20	0.17
−0	0.03	0.16
Sum	100.22	100.18

* If present less than 0.1 per cent.

The ramsayite and lorenzenite specimens given in Table 1 show very similar compositions, representing almost ideal sodium titanium silicates. Only the values of niobium are comparatively high, higher than in titanites. This observation for ramsayite is in complete agreement with the observation made by Borowsky and Blochin.[6] They found in ramsayite about 2.8 per cent Nb_2O_5, but no tantalum.

---

[6] Borowsky, I. B., and Blochin, M. A., The analysis of minerals by the x-ray spectroscopical method: *Bull. Acad. Sci. l'USSR, Cl. Math. Nat.*, Sér. Géol., No. 5, p. 929 (1937). (Russian with English summary).

STUDIES ON SILICON CARBIDE

LEWIS S. RAMSDELL, *Mineralogical Laboratory, University of Michigan.*

ABSTRACT

This paper is divided into four parts. Part I describes a new system for naming the types of SiC based on the symmetry and number of layers in the unit cell. Part II presents several methods for describing the structures of the various types. These reveal definite progressive series, from which the possible existence of new types may be predicted. Part III discusses the structure of type 51*R* (old type V). Part IV describes the morphology and the crystal structure of the new type 87*R*.

PART I. THE NAMING OF SiC TYPES

The discovery of another form of SiC, as reported in Part IV of this paper, and the probability that still others will yet be found makes it highly desirable that a new system of designating the types of SiC be introduced. The present system is based primarily on the order of discovery, and has no relationship with either the symmetry or contents of the unit cells.

When crystal structure determinations first began to be made, there were three known types of SiC, arbitrarily designated as I (15-layer rhombohedral), II (6-layer hexagonal), and III (4-layer hexagonal). When a cubic form was discovered, it became type IV, and the 51-layer rhombohedral type next found was designated type V (Ott, 1928). Thibault (1944) more recently found two new rhombohedral types, with 21 and 33 layers, respectively. He renamed the cubic form β-SiC, and called all of the others α-SiC. The designation type IV (formerly cubic) he then applied to his new 21-layer structure and type VI to the 33-layer.

The author has recently found a crystal of SiC based on an 87-layer rhombohedral cell. Because of the very definite systematic relationships evident between the 15-, 33-, 51-, and 87-layer types, it seems certain that there is also a 69-layer rhombohedral cell yet to be found. Although the 21-layer rhombohedral (IV) has no companions so far, it is likely that it, too, is part of a series with still other types. It would seem rather ridiculous to go on naming these types VII, VIII, IX, etc., in the order of their discovery. Moreover, if any new scheme of naming appropriate to the actual structures is developed for new types yet to be found, it should logically be applied to the types already known.

There seems no likelihood of more than one cubic form. Since this has a structure corresponding to β-ZnS (sphalerite), the choice of β-SiC seems to be satisfactory. All remaining types (α-SiC) so far found are based on either hexagonal or rhombohedral unit cells, and a proper designation should certainly indicate which. All types have identical layers, but differ in the arrangement of these layers. Each type is uniquely distinguished either by the number of layers necessary for the arrangement to repeat itself, that is, the number of layers in the unit cell, or by the number of formula weights in the unit cell. Which of these two numbers is used is more or less a matter of choice. In the hexagonal types, or in the rhombohedral types referred to a hexagonal unit, the two numbers are identical. In the actual rhombohedral unit cell, the number of formula weights is $\frac{1}{3}$ of the total number of layers included within the length of the *c* axis. However, since comparisons between types and descriptions of types are best made by using hexagonal unit cells throughout, it would seem a wiser choice to use the number of layers as the characteristic number. The designation for any type, then, would consist of the appropriate number, followed[1] by the letter "*H*" or "*R*", depending upon whether the unit cell is hexagonal or rhombohedral. Such a designation is simple, accurate, and descriptive. The 8 known types would be designated as follows:

Cubic	Hexagonal	Rhombohedral
β-SiC	4*H* (old type III)	15*R* (old type I)
	6*H* (old type II)	21*R* (old type IV)
		33*R* (old type VI)
		51*R* (old type V)
		87*R* (new, no previous designation)

All of the possible types which are predicted in Part II of this paper, would readily fit into this system of naming.

Part II. The Description of SiC Types, and the Prediction of Types as Yet Undiscovered

In his report on the 15*R* type of SiC (old type I), Ott (1925) described the structure in terms of the sequence of silicon (or carbon) atoms along the symmetry axes. The five atoms on a given axis are separated by layer intervals of 2, 4, 3, 4, and 2, and thus the sequence 24342 describes the structure. For the 33-layer rhombohedral type (Ramsdell, 1945), the author used the same method of description, and found the structure to be based on an interval sequence of 24243334242, and for the 51-layer rhombohedral type (described in part III of this paper), the sequence was found to be 24242433333424242. This method of describing the atomic arrangement becomes increasingly unwieldy, for the 87-layer rhombohedral type (part IV of this paper) has an interval sequence of 2424242424333333334242424242. Moreover, this method is not equally applicable to the hexagonal structures, for in them the symmetry axes are not all alike, the sequence along the 6-fold axis being different from that along the 3-fold axes. A much superior type of description is available.

---

[1] *The Strukturbericht* classifies general structure types as *A*, *B*, *C*, . . . followed by a number. Thus scheelite is type *H*4 and apatitie $H5_7$. By having the number precede the letter *H* in the type designations for SiC, no confusion will result.

In α-SiC, all atoms lie on the symmetry axes, and all symmetry axes lie in the $11\bar{2}0$ plane; hence, a vertical section through the unit cell along $11\bar{2}0$ gives an adequate representation of the structure (Fig. 1). If a Si (or C) atom lies on A in one layer, the next must either be to the right, on B, or to the left, on C. If to the right, the third layer might have its atom continue to the right, or it might change direction and go to the left. Because of these repeated changes in direction, a zig-zag pattern results. Such an arrangement can be described in terms of the number of layers added in each direction in succession, and in this paper will be designated as the *zig-zag* sequence, in contrast to the *interval* sequence previously used.[2] Thus, type $4H$ consists of two layers added to the right, then two to the left, etc., and can be described as 22. Type $6H$ adds three to the right, then three to the left, or 33. Type $15R$ has three right, then two left. This is repeated three times to form the unit cell, and the complete symbol would be 323232. Every symbol for a rhombohedral cell

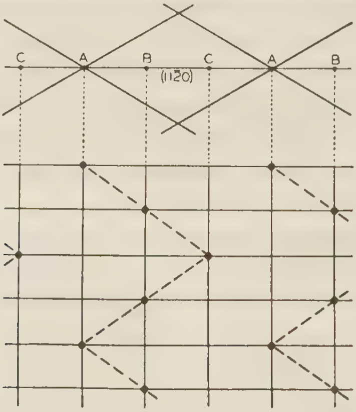

FIG. 1. $11\bar{2}0$ cross-section of α-SiC, showing zig-zag arrangement of Si (or C) atoms.

---

[2] The author had used this method in determining the number of possible structures for $51R$, but is indebted to Dr. H. T. Evans, Jr., of the Massachusetts Institute of Technology, for his suggestion that the zig-zag sequence was a better method for description of types than the interval sequence. Recently, there has also appeared an article on "The Numerical Symbol of Close Packing of Spheres" (Zhdanov, 1945), in which this method was described.

would be of this triple character, and could easily be abbreviated to a single set of figures. The following list of rhombohedral types will illustrate this method of notation.

3 . . . 2 series, rhombohedral

15*R*	32
33*R*	3332
51*R*	333332
(69*R*)	33333332
87*R*	3333333332

Not only is this a concise method of describing the structure, but it clearly reveals the basis for predicting the existence of a 69-layer rhombohedral type. Moreover, only odd numbers of 3's occur in this tabulation, and the possibility of structures involving an even number of 3's arises. To complete a unit cell, the last layer must be directly above the initial layer. This is the reason the rhombohedral sequences must be repeated three times. Likewise, with an even number of 3's, the sequences would have to be repeated twice, and the following tabulation becomes evident.

3 . . . 2 series, hexagonal

4*H*	2	2
(16*H*)	332	332
(28*H*)	33332	33332
(40*H*)	3333332	3333332
(52*H*)	333333332	333333332

Only the first of these represents a known structure, 4*H*, but the others represent possible hexagonal types as yet undiscovered. It might be noted here that the *interval* sequence originally used likewise predicts the existence of 69*R*, but does not suggest the possible hexagonal types. The complete hexagonal symbols are always doubled, and like the rhombohedral, could be abbreviated, except for the first one (4*H*). The symbol 2 alone would not be satisfactory.

The 21*R* type does not appear in the foregoing tabulations. Its zig-zag sequence is 343434, or, in abbreviated form, 34. Although no other structures of this type have so far been found, the following series is suggested:

3 . . . 4 series

Rhombohedral types	34	21*R*	Hexagonal types	4	4	(8*H*)
	3334	(39*R*)		334	334	(20*H*)
	333334	(57*R*)		33334	33334	(32*H*)
	33333334	(75*R*)		3333334	3333334	(44*H*)

In both the 3 . . . 2 and the 3 . . . 4 series, the larger cells have an increasing number of 3's. The sequence 33 is characteristic of 6*H* (old type II), which has been found to be the most abundant type present in commercial silicon carbide. Thus, not only is the 33 structure the most common, but it occurs within most of the other structures. Whole blocks of the larger cells have the 6*H* structure, and the larger cells become increasingly like 6*H*. For this reason, it is quite certain that the above series extend indefinitely, with 6*H* as the limiting case. However, the increasing resemblance to type 6*H*, both with respect to *x*-ray diffraction effects and to morphology, may make proof of this difficult. This matter will be discussed later in part IV.

Although the sequence methods already discussed give adequate mathematical description of the structures, they do not give a completely satisfactory visual picture. A graphical 2-dimensional presentation is possible in terms of the atomic configurations represented in the $11\bar{2}0$ cross-section. A remarkable simplification occurs when this is done, for it reveals that for all known types, including the cubic, there are only two basic arrangements of the atoms.

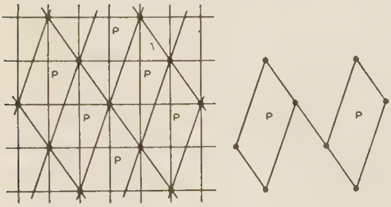

(*a*) (*b*)

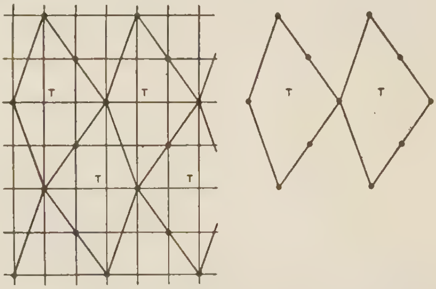

(*a*) (*b*)

FIG. 2 (*a*). Typical parallelogram arrangement (*P*) of Si (or C) atoms in $11\bar{2}0$ cross-section through cubic β-SiC, in rhombohedral orientation. (b). Single horizontal *P* layer.

FIG. 3 (*a*). Typical trapezoidal arrangement (*T*) of Si (or *C*) atoms in $11\bar{2}0$ cross-section of SiC, type 4*H*. (*b*) Single horizontal *T* layer.

The cubic form may be treated as a rhombohedron, with cubic [111] becoming hexagonal [0001]. In this orientation, the $11\bar{2}0$ cross-section shows that the silicon (or carbon) atoms are so arranged that successive layers are all added in one direction, without change. The appropriate symbol would be ∞ (Fig. 2). This arrangement consists of a series of identical parallelograms, and will be designated by the letter *P*. Single horizontal layers of *P* appear as shown in Fig. 2*b*.

Type 4*H* has a $11\bar{2}0$ plane arrangement of silicon (or carbon) atoms illustrated in Fig. 3. The repeated figure is a trapezium, and will be designated by the letter *T*. This arrangement occurs in single horizontal layers as shown in Fig. 3*b*.

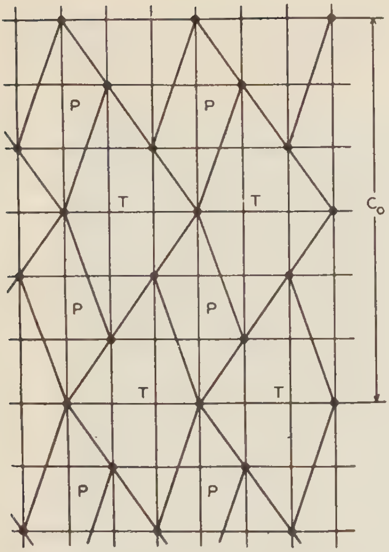

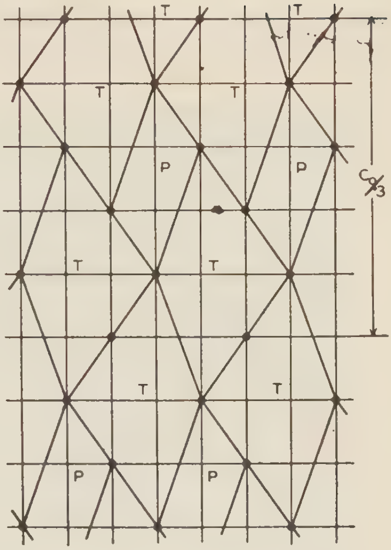

FIG. 4. $11\bar{2}0$ cross-section through type 6*H*, showing alternate *T* and *P* layers.

FIG. 5. $11\bar{2}0$ cross-section through type 15*R*, showing double *T* layers alternating with single *P* layers.

All other known types of SiC, as well as all of the undiscovered types predicted in the series previously described, are made up of horizontal layers of these two basic configurations, *T* and *P*, in various combinations. For example, the most common type, 6*H*, is made up of alternate layers of *T* and *P*, Fig. 4. Such alternate layers always occur whenever the symbol 33 occurs, and in the 3 . . . 2 and 3 . . . 4 series, whole sections of the structures are made up of these alternating *T* and *P* layers. In addition, the 3 . . . 2 series is characterized by double *T* layers (Table 1). This feature is illustrated in Fig. 5, which shows the arrangement in type 15*R*.

The 3 . . . 4 series is very similar to the 3 . . . 2, but has double *P* instead of double *T* layers. No table is shown for this, but it would be similar to Table 1. The first vertical column would be β-SiC, with nothing but *P* layers, followed by the other members. Each succeeding column would have double *P* layers interspersed with increasing numbers of alternating *T* and *P* layers. In both series the increasing resemblance to type 6*H* is very apparent.

It is quite possible that all types of SiC are limited to these two basic configurations, *T* and *P*, but the author knows no reason why this should be. Even if this limitation did hold, there are other extensive

TABLE 1. 3 . . . 2 SERIES

4*H*	15*R*	16*H*	33*R*	28*H*	51*R*	40*H*	69*R*	52*H*	87*R* . . .
T T T	T T P T T	T T P T}3 P T T	T T P T P}5 T P T T	T T P T P T}7 P T P T T	T T P T P T P}9 T P T P T T	T T P T P T P T}11 P T P T P T T	T T P T P T P T P}13 T P T P T P T T	T T P T P T P T P T}15 P T P T P T P T T	T T P T P T P T P T P}17 . . . T P T P T P T P T T

series of *T* and *P* geometrically possible, such as triple *P* and triple *T* layers interspersed with single alternating *T* and *P* layers. A very simple structure type, symbol 42, type 18*R*, would result from alternating double *P* and double *T* layers. So far, no evidence of a structure corresponding to wurzite (α-ZnS) has been discovered. This structure has a symbol 11 (for either the Zn or the S atom). Any SiC structure with a symbol including the number 1 would depart from the *T* and *P* configurations. If such structures do exist, but are so far undiscovered, the number of possibilities would be enormously increased.

PART III. THE CRYSTAL STRUCTURE OF α-SiC, TYPE 51*R*

As the name implies, silicon carbide, type 51*R* (formerly type V), has a 51-layer rhombohedral unit cell. The cell constants originally reported by Ott (1928) are as follows: hexagonal unit, $a_0 = 3.09_5$Å, $c_0 = 129.0_3$Å, $Z = 51$; rhombohedral unit, $a_r = 43.1_5$Å, $\alpha = 4°06'$, $Z = 17$. From Ott's published data, which included an oscillation photograph, the author was able to determine the structure. More recently, Dr. N. W. Thibault found an excellent crystal of type 51*R*, and very kindly made it possible for the author to obtain Weissenberg photographs from it. The 0-layer photograph (*a* axis rotation), is reproduced in Fig. 6. A complete morphological study of this crystal will soon be published by Dr. Thibault.

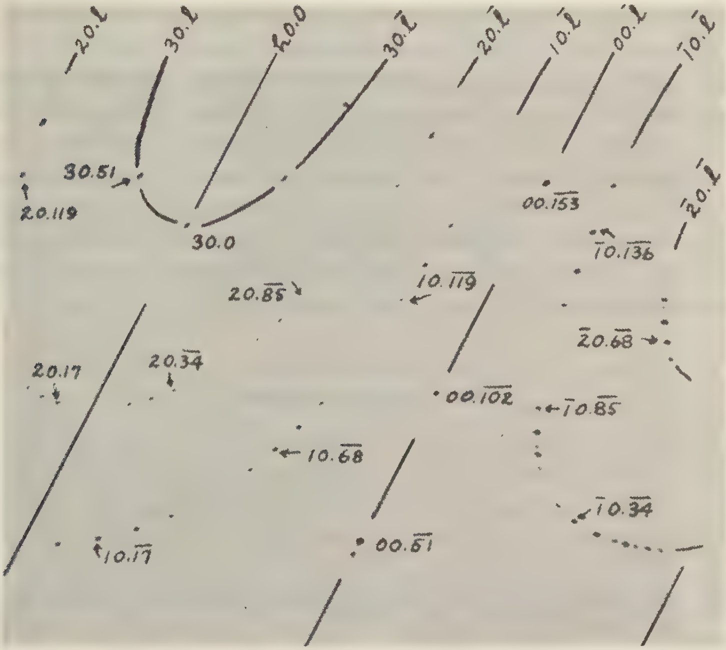

FIG. 6. Weissenberg photograph of crystal of SiC, type 51*R*. 0-level, *a* axis rotation.

Measurements from the Weissenberg photographs, together with the known relationship to the other types of SiC, give the following cell constants:* hexagonal unit, $a_0 = 3.073$Å, $c_0 = 128.17_8$Å; rhombohedral unit, $a_r = 42.76_3$Å, $\alpha = 4°07'$. The coordinates of the Si and C atoms are as follows:

Hexagonal unit cell:

17 Si at 000, 002*z*, 006*z*, 008*z*, 0012*z*, 0014*z*, 0018*z*, 0021*z*, 0024*z*, 0027*z*, 0030*z* 0033*z*, 0037*z*, 0039*z*, 0043*z*, 0045*z*, 0049*z*.

17 C at 00*p*, 002*z*+*p*, 006*z*+*p*, 008*x*+*p*, 0012*z*+*p*, 0014*z*+*p*, 0018*z*+*p*, 0021*z*+*p*, 0024*z*+*p*, 0027*z*+*p*, 0030*z*+*p*, 0033*z*+*p*, 0037*z*+*p*, 0039*z*+*p*, 0043*z*+*p*, 0045*z*+*p*, 0049*z*+*p*.

17 Si and 17 C at $\frac{2}{3}$, $\frac{1}{3}$, $\frac{1}{3}$+the above coordinates.

17 Si and 17 C at $\frac{1}{3}$, $\frac{2}{3}$, $\frac{2}{3}$+the above coordinates.

$$z = 1/51;\ p = 1/68$$

The unit cell of type 51*R* is so large that from a purely geometrical standpoint an enormous number of structures exist which could fully satisfy the requirements as to symmetry and provide the basic tetrahedral arrangement of carbon atoms about the silicon atoms.[3] In determining the structure of type 33*R*, certain limiting assumptions were made (Ramsdell 1945), which reduced the number of possible atomic arrangements to five. Each of these five was tested, and the correct one determined. The same procedure applied to 51*R* leaves 44 possible structures, from which the correct one must be selected. The labor involved in calculating intensities for such a large number of structures would be very great. As reported at the 26th annual meeting of the Mineralogical Society of America (Ramsdell 1946), the existence of a progressive series of structures, consisting of types 15*R*, 33*R* and 51*R*, seemed apparent when their interval sequences were listed.

---

* In order to be consistent with the earlier articles on SiC, the unit cell dimensions are given in Å units, although they should actually be designated as kX units.

15*R*	24 3 42
33*R*	2424 333 4242
51*R*	24242433333424242

The third set of intervals is an extrapolation of the first two, and corresponds to one of the possible arrangements for type 51*R*. The intensities calculated for this arrangement were in such excellent agreement with the observed intensities that it was felt that it must be the correct one.

However, since no actual elimination of the remaining 43 possible structures had been made, further study seemed desirable. The possibility of a quite different arrangement producing the same diffraction effects was ruled out. Certainly, cumulative experience in the field of crystal structure determinations gives no support to the idea that two different structures can give rise to similar diffraction effects for any extended series of reflections.

There remained the possibility that a very similar structure might give approximately the same series of relative intensities as the chosen one. To test this, a structure was chosen from among the rejected ones which was very similar in arrangement. Its interval sequence was 24332433333423342. This represents a structure with the least change possible. Forty-five out of the original fifty-one atoms are unchanged. The remaining six form pairs, in which the only change is a reversal of position in the two structures in the $11\bar{2}0$ plane. If these pairs slope to the right in one, they slope to the left in the other. The intensities calculated for this slightly modified structure are so distinctly different as to completely eliminate it from consideration.

---

[3] For type 51*R* the total number of interval sequences is 43,690, being equal to $2^n/3$, where n is the number of Si atoms on any vertical symmetry axis—in this case, 17. Actually many of these sequences are congruent, and the number of different sequences is much smaller than 43,690. So far, the author has found no means of predicting the number of different sequences, but it would undoubtedly be in the thousands.

The use of the zig-zag sequence in describing the structures reveals more clearly than the interval sequence why this apparently very minor change just referred to results in such marked intensity changes. The abbreviated symbol for 51*R* is 333332, whereas the symbol for the modified structure is 3932. In other words, it changes the addition of successive layers from 3 right, 3 left, 3 right, to 9 in one direction. In terms of the $11\bar{2}0$ cross-section, as described in Part II, the structure is changed from TTPTPTPTPTPTT to TTPTPPPPPPPTPTT. There is no reason known to the author why this latter structure is not a possible one, but it very definitely is not in the established 3 . . . 2 series, to which type 51*R* clearly belongs.

These computations would probably never have been made had the existence of type 87*R* been known at the time. The recent discovery of this new type, reported in part IV of this paper, establishes so firmly the existence of a progressive series of structures, that there should be no hesitancy in accepting the structure as valid, without any further study of the many rejected structures.

Recently, two Russian scientists have reported on an investigation of type 51*R*, and found the same structure (Zhdanov, Minervina 1945). The only types known to them were 4*H*, 6*H*, and 15*R*, whose structure symbols are 22, 33, and 32. On the assumption that the zig-zag sequence symbol for any other type of SiC must be limited to the numbers 2 and 3, they found for type 51*R* only two possible rhombohedral arrangements, 22222223 and 333332. The calculated intensities for the former did not correspond, while those for the latter agreed so well with the data published by Ott, that they accepted it as the correct structure. Even had they been familiar with the existence of type 21*R*, with the symbol 34, it would have made no difference, for there is no combination of 3 and 4 which can give rise to a rhombohedral 51-layer structure. Their determination was based on a restriction much more limiting in its character than that used by the author—namely, that the sequence intervals must be limited to 2, 3, and 4. This restriction limited the number of possible structures to 44, as contrasted with the two possibilities which they considered. Since 51*R* does belong to the 3 . . . 2 series, their limitation happened to be all right, and their determination turned out to be correct. However, it seems quite obvious that their restriction is not a general one, and cannot be applied to any type not in the 3 . . . 2 series.

If the type 21*R* had not been discovered, there would not be any suggestion whatever of the possibility of a 3 . . . 4 series. For this reason, the author feels that it would be very unwise to propose any limitations as to further possible types. Various simple structures not included in the 3 . . . 2 and 3 . . . 4 series are geometrically possible, as well as an enormous number of more complicated arrangements.

IV. THE MORPHOLOGY AND STRUCTURE OF α-SiC, TYPE 87*R*

Morphology

The only example of the new type 87*R* so far found is a very small, dark blue crystal, about 0.4 mm. long, 0.25 mm. wide, and 0.15 mm. thick. It is tabular parallel to (0001) and elongated parallel to one of the *a* axes. The two pinacoids are the largest faces present. They are well developed and give excellent reflections on the goniometer. No attempt has been made to determine by etching which is the upper and which the lower pinacoid (Thibault, 1944). The remaining faces are much smaller, and in general less well developed. None gives as good signals on the goniometer as do the pinacoids, and for some the signals are diffuse, or spread over a considerable angular range. Of the six trigonal pyramid zones, only four have measurable faces. Seven trigonal pyramids have been definitely established, with one more probable, and several other quite doubtful. No evidence of second order faces has been found. The distribution of faces is shown in Table 2. Table 3 gives the morphological data, and the angle table is given in Table 4. With the exception of $10\bar{1}1$, the faces present correspond to planes whose *x*-ray reflections are very strong.

TABLE 2. DISTRIBUTION OF FACES ON CRYSTAL OF α-SiC, TYPE 87*R*

$(10\bar{1}l)$	$(01\bar{1}l)$	$(\bar{1}10l)$	$(\bar{1}01l)$	$(0\bar{1}1l)$	$(1\bar{1}0l)$
$1.0.\bar{1}.43$	—	$\bar{1}.1.0.43$	$\bar{1}.0.1.44$	—	—
$1.0.\bar{1}.28$	—	$\bar{1}.1.0.28$	$\bar{1}.0.1.29$	—	$1.\bar{1}.0.29$
$1.0.\bar{1}.13$	—	—	$\bar{1}.0.1.14$	—	$1.\bar{1}.0.14$
$1.0.\bar{1}.1$	—	$\bar{1}.1.0.1$	$\bar{1}.0.1.\bar{1}$	—	$1.\bar{1}.0.\bar{1}$
$1.0.\bar{1}.\overline{14}$	—	—	$\bar{1}.0.1.\overline{16}$?	—	—
		—	$\bar{1}.0.1.\overline{28}$	—	—
		$\bar{1}.1.0.\overline{44}$	$\bar{1}.0.1.\overline{43}$	—	$1.\bar{1}.0.\overline{43}$

On the crystals of types 21*R* and 33*R*, Thibault found faces which were characteristic, their angles being quite different from those of any other type. But for the crystal of 87*R*, the only measurable faces present are

TABLE 3. MORPHOLOGICAL DATA, α-SiC, TYPE 87R

Form	No. Times Observed	Quality	Angle between Form and Base		
			Range	Weighted Average	Calcd.
0001	2	A			
$1.0.\bar{1}.43$	4	C–E	62°07′–62°25′	62°21′	62°22′
$1.0.\bar{1}.28$	3	B–E	71°06′–71°42′	71°12′	71°11′
$1.0.\bar{1}.13$	1	B	80°59′	80°59′	81°02′
$1.0.\bar{1}.1$	4	B–D	89°15′–89°23′	89°19′	89°18′
$0.1.\bar{1}.14$	3	B–E	80°19′–80°34′	80°23′	80°21′
$0.1.\bar{1}.29$	2	D	70°35′–70°44′	70°39′	70°33½′
$0.1.\bar{1}.44$	2	D–E	61°42′–61°51′	61°48′	61°52′

TABLE 4. ANGLE TABLE, α-SiC, TYPE 87R
Hexagonal—R, ditrigonal pyramidal—$3m$
$a:c=1:71.151_5$ $\alpha=2°25'$
$p_0:r_0=82.09:1$ $\lambda=119°59'$

Form		ϕ	ρ	A_1	A_2
c-$\bar{c}$	0001	+30°00′	0°00′	90°00′	90°00′
ζ-$\bar{\zeta}$	$1.0.\bar{1}.43$	+30°00′	62°22′	39°53½′	90°00′
ϵ-$\bar{\epsilon}$	$1.0.\bar{1}.28$	+30°00′	71°11′	34°56½′	90°00′
β-$\bar{\beta}$	$1.0.\bar{1}.13$	+30°00′	81°02′	31°11½	90°00′
α-$\bar{\alpha}$	$1.0.\bar{1}.1$	+30°00′	89°18′	30°00½′	90°00′
τ-$\bar{\tau}$	$0.1.\bar{1}.44$	−30°00′	61°52′	90°00′	40°12½′
x-$\bar{x}$	$0.1.\bar{1}.29$	−30°00′	70°33½′	90°00′	35°15′
ν $\bar{\nu}$	$0.1.\bar{1}.14$	−30°00′	80°21′	9°00′	31°22½′

ones whose angles are very close to those commonly found on type 6H crystals, and careful measurement is necessary to make the distinction. The closeness of the angles is shown in the following list, which gives the calculated values for ρ. In cases where good goniometer signals can be obtained, this situation would present little difficulty, but where signals are poor, and possibly only a few faces present, the variation from type 6H might be overlooked. For higher members of the 3 . . . 2 series, this closeness of angles would become increasingly evident. Consequently, the discovery of new members of the series on the basis of goniometric measurements along will be increasingly difficult.

6*H*		87*R*	
10.0	90°00′	10.1	89°18′
10.1	79°59½′	10.13	81°02′
		$\overline{14}$	80°21′
		16	79°00′
10.2	*70°33½′*	10.28	71°11′
		$\overline{29}$	*70°33½′*
10.3	62°06′	10.43	62°22
		$\overline{44}$	61°52′
10.4	*54°47′*	11.58*	*54°47′*
		$\overline{59}$*	54°21′
10.5	48°34½′	$10.\overline{71}$*	49°11′
		10.73*	48°23½′

* Not present on crystal, but possible.

ρ values in italics are identical for both types.

Crystal structure of 87*R*

Weissenberg photographs of excellent quality were obtained from the crystal of SiC, type 87*R*. Reproductions of the 0-level and 1-level photographs, with rotation about an *a* axis, are shown in Fig. 7*a*, *b*. The space group is *R*3*m*, and the unit cell dimensions as obtained from the 0-level films are as follows: Hexagonal—$a_0 = 3.073$Å, $c_0 = 218.65_7$Å; $Z = 87$; rhombohedral—$a_{rh} = 72.865$Å, $\alpha = 2°25'$; $Z = 29$.

As would be expected, certain reflections coincide exactly in position with those of the other rhombohedral types, as well as with type 6*H*. Since the length of the *c* axis in every case is an exact multiple of a common unit, certain planes must come at exactly the same angles. The reflections from these planes are the ones which have common positions on the Weissenberg films. In the rhombohedral types, the value of *l* for these planes is always a multiple of the number of formula weights in the unit cell. Some of these common planes are as follows:

15*R*	21*R*	33*R*	51*R*	87*R*	6*H*
$10\cdot\overline{5}$	10·7	$10\cdot\overline{11}$	$10\cdot\overline{17}$	$10\cdot\overline{29}$	10·2
10·10	$10\cdot\overline{14}$	10·22	10·34	10·58	10·4
$10\cdot\overline{20}$	10·28	$10\cdot\overline{44}$	$10\cdot\overline{68}$	$10\cdot\overline{116}$	10·8
10·25	$10\cdot\overline{35}$	10·55	10·85	10·145	10·10
etc.	etc.	etc.	etc.	etc.	etc.
00·15	00·21	00·33	00·51	00·87	00·6
11·15	11·21	11·33	11·51	11·87	11·6

The characterizing difference between the Weissenberg photographs of the successive rhombohedral types lies in the increasing number of $hk\cdot l$ reflections occurring *between* the common reflections in fixed positions. This is illustrated in the diagrams of Fig. 8. These diagrams represent small portions of the rows of $10\cdot l$ reflections from the Weissenberg

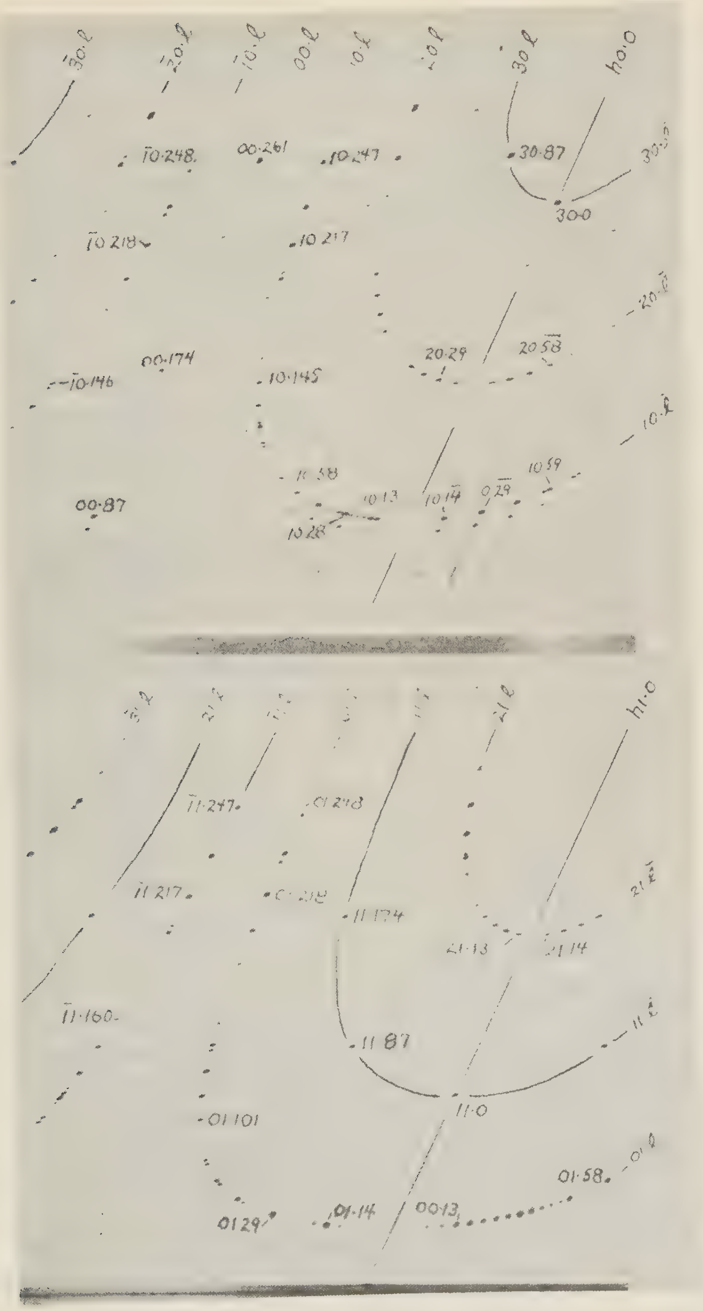

FIG. 7. Weissenberg photographs of crystal of SiC, type 87*R*; *a* axis rotation. (*a*) 0-level. (*b*) 1-level.

photographs. For each type, two of the common reflections occurring in fixed positions are shown. These are the ones at the extreme right and left of each row. In between are the additional reflections characteristic of each type. Each reflection is designated by its l value, and the observed intensities are approximately indicated by the vertical height of the line, with a spot indicating a very weak or missing reflection.

The indexing of the films presents no serious difficulties. Since the unit cell is rhombohedral, the $10\cdot l$ reflections cannot have $l=3n$. For $87R$, the $10\cdot\overline{29}$ reflection must come at exactly the same position of the film as $10\cdot\overline{2}$ for $6H$, and $10\cdot 58$ at the same position as $10\cdot 4$ of $6H$. Although $10\cdot\overline{29}$ does coincide in position with $10\cdot\overline{2}$, $10\cdot 28$ is so close to the position of $10\cdot 2$ that it is very uncertain which is which at the start. Likewise, $10\cdot 58$ and $10\cdot\overline{59}$, both strong reflections, are practically indistinguishable. The calculated values for the distances from the zero line of $10\cdot 28$ and $10\cdot\overline{29}$ differ by only 0.12 mm., those for $10\cdot 58$ and $10\cdot\overline{59}$ by 0.13 mm. However, for higher values of l, the separation of such pairs becomes increasingly greater, and no difficulty is encountered, for example, in distinguishing $10\cdot 217$ and $10\cdot\overline{218}$, or $10\cdot 247$ and $10\cdot\overline{248}$. From these identifiable reflections, it is easy to work back down to the lower values.

Although, as explained later, the characteristics of the x-ray pattern are such as to furnish definite proof of the fact that the structure must belong to the 3 . . . 2 series, intensities have been calculated for some of the reflections. A structure based on the zig-zag sequence 3333333332 has theoretical intensities that agree with the observed intensities with the same high degree of correlation which has been found for the other types of SiC. A comparison of the observed and the calculated intensities for the first 30 reflections from type $87R$ is given in Table 5.

An interesting feature of the Weissenberg photographs of type $87R$ is the resemblance to photographs of type $6H$. It is now apparent that this is also true, but to a much less extent, of the photographs of $51R$ and $33R$, but it was not until the films of $87R$ were available that this was noticed. This is illustrated in Fig. 9, which shows diagrammatically some of the reflections of type $6H$ compared with the strongest reflections of $87R$. The pairs of reflections joined by dashed lines come at identical positions, and the others at approximately the same positions. In some cases, single reflections of $6H$ are opposite pairs of $87R$ reflections. The variations in intensity in the comparatively few reflections of $6H$ are closely followed in the reflections of $87R$ which occur at the same position, while in between, where $6H$ has no reflections, the reflections of $87R$ are either comparatively weak or absent.

TABLE 5. COMPARISON OF OBSERVED AND CALCULATED INTENSITIES FOR SOME OF THE REFLECTIONS OF TYPE 87*R*

10·*l*	Calcd. I	Obser. I	10·$\bar{l}$	Calcd. I	Obser. I
10·1	1.1	vvw	10·$\bar{2}$	1.1	vvw
4	1.8	vvw	$\bar{5}$	1.4	vvw
7	3.2	vvw	$\bar{8}$	2.2	vvw
10	8.4	w	$\overline{11}$	6.2	vw
13	100	vs	$\overline{14}$	262	vvs
16	135	vs	$\overline{17}$	10	mw
19	24	m	$\overline{20}$	2.5	vvw
22	19	m	$\overline{23}$	1.0	a
25	33	m	$\overline{26}$	0.7	a
28	515	vvs	$\overline{29}$	417	vvs
31	92	ms	$\overline{32}$	0.7	a
34	17	m	$\overline{35}$	1.1	vvw
37	10	w	$\overline{38}$	2.4	vvw
40	12	w	$\overline{41}$	12	w
43	390	vvs	$\overline{44}$	365	vvs

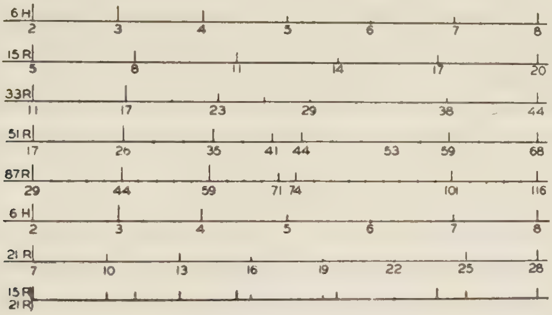

FIG. 8. Comparison of some of the 10.*l* reflections from various types of SiC. The reflections at the extreme right and left of each row occur in identical positions for all types. In between are varying number of reflections, characteristic of each type. Heights of lines indicate approximate relative intensities for important reflections. Other reflections are either absent, or comparatively weak.

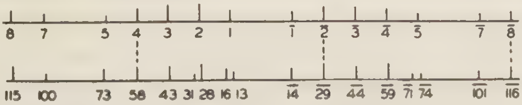

FIG. 9. Diagrammatic comparison of some type 6*H* reflections with the strongest reflections of 87*R*. Reflections from 87*R* not indicated are comparatively weak or absent.

This situation is, of course, due to the fact that of the 87 layers in the unit cell of *87R*, 81 correspond exactly to the *6H* arrangement. Consequently, there are large blocks of the *87R* structure which are identical to *6H*. This close resemblance of the Weissenberg pattern of *87R* to that of *6H* implies membership in either the 3 . . . 2 or the 3 . . . 4 series. The fact that only in the former could an 87-layer rhombohedral cell occur clearly establishes the structure.

Types *51R* and *33R* include relatively smaller blocks of the *6H* structure, and their resemblance to *6H*, as revealed by the Weissenberg photographs, is not so pronounced (Fig. 8).

Since type *6H* is the limiting case for the 3 . . . 2 series (and the 3 . . . 4 series as well), it would be expected that the higher members should increasingly resemble *6H*, both morphologically and with respect to *x*-ray data. If single small crystals are available, consisting entirely of one type, recognition of several additional members of the series, such as *105R* and *123R*, might be possible. The Weissenberg patterns should offer a better opportunity for detection than a morphological study.

In the recognition of possible new types of SiC by means of Weissenberg photographs, care must be taken to avoid confusion with crystals which represent a coalescence of types (Thibault, 1944). Such crystals would likewise have extra reflections in between the common reflections in fixed positions. An example of this is illustrated in the bottom row of Fig. 8, which represents an imaginary coalescence of *15R* and *21R*. In such a case, the reflections $10\cdot\bar{5}$ and $10\cdot\overline{20}$ of *15R* would coincide with $10\cdot 7$ and $10\cdot 28$ of *21R*. In between would be $10\cdot\bar{8}$, $10\cdot\overline{11}$, $10\cdot\overline{14}$, and $10\cdot\overline{17}$ of *15R*, and $10\cdot 10$, $10\cdot 13$, $10\cdot 16$, $10\cdot 19$, $10\cdot 22$, and $10\cdot 25$ of *21R*. This would make a total of ten reflections in between the fixed positions. Type *33R* likewise has ten reflections in between the corresponding fixed positions ($10\cdot\overline{11}$ and $10\cdot\overline{44}$ for *33R*). But these two sets of ten reflections would be easily distinguishable. Those for *33R* would be regularly spaced, while the coalescence of *15R* and *21R* would have an uneven distribution. This is clearly shown in the bottom line of Fig. 8.

This would hold true for any possible coalescence of types. Two sets of regular spacings of differing magnitude cannot combine to form a single set of smaller equal spacings. The reflections would form irregular groups. However, in the special case where one set of spacings was an exact multiple of the other, the larger spacings would all coincide with certain ones of the smaller, and the coalescence might be overlooked. This might be the case with a coalescence of β-SiC (which treated as rhombohedral would be type $3R$) with any other rhombohedral type, and might also occur in coalescences between possible hexagonal types.

The 3 . . . 2 series was first recognized when the structure of type $51R$ was determined. At that time, there seemed to be no evidence as to how far the series might extend. It now seems certain that it extends indefinitely. Indeed, type $6H$ is really the limiting case for the series, with the number of 3's in the symbol indefinitely large. Because of the increasing resemblance to $6H$, both morphologically and with respect to x-ray data, the chances of discovering any large number of additional types in the 3 . . . 2 series seems remote.

SUMMARY

Like all of the other rhombohedral types of SiC, the space group of $87R$ is $R3m$. The unit cell constants are as follows:

Hexagonal—$a_0=3.073$Å, $c_0=218.65_7$Å, $Z=87$.

Rhombohedral—$a_r=72.90_7$Å, $\alpha=2°25'$, $Z=29$.

The atomic positions for the hexagonal cell are:

29 Si at 000, $002z$, $006z$, $008z$, $0012z$, $0014z$, $0018z$, $0020z$, $0024z$, $0026z$, $0030z$, $0033z$, $0036z$, $0039z$, $0042z$, $0045z$, $0048z$, $0051z$, $0054z$, $0057z$, $0061z$, $0063z$, $0067z$, $0069z$, $0073z$, $0075z$, $0079z$, $0081z$, $0085z$.

29 C at $00p$, $002z+p$, $006z+p$, $008z+p$, $0012z+p$, $0014z+p$, $0018z+p$, $0020z+p$, $0024z+p$, $0026z+p$, $0030z+p$, $0033z+p$, $0036z+p$, $0039z+p$, $0042z+p$, $0045z+p$, $0048z+p$, $0051z+p$, $0054z+p$, $0057z+p$, $0061z+p$, $0063z+p$, $0067z+p$, $0069z+p$, $0073z+p$, $0075z+p$, $0079z+p$, $0081z+p$, $0085z+p$.

29 Si and 29C at $\frac{1}{3}$, $\frac{2}{3}$, $\frac{2}{3}+$the above coordinates.

29 Si and 29C at $\frac{2}{3}$, $\frac{1}{3}$, $\frac{1}{3}+$the above coordinates.

$$z=1/87;\ p=1/116$$

The rhombohedral types of SiC, $15R$, $33R$, $51R$, ($69R$, not yet discovered) and $87R$ belong to a definite series, in which the higher members become increasingly like the simple $6H$ type, both morphologically and with respect to x-ray data. This is because incorporated in the structures are increasing numbers of layers identical to $6H$. Type $21R$ belongs to a different series, which likewise converges toward $6H$ as the limiting case. It is so far the only member of this series to be found. There seem to be no reason why others may not be found in either of the known series, or in yet other series.

REFERENCES

OTT (1925), Das Gitter des Karborunds (SiC): *Zeits. Krist.*, **61,** 515–531.

——— (1928), Eine neue Modifikation des Karborunds: Probleme der modernen Physik: *Arnold Sommerfeld Festschrift*, 208–214, S. Hirzel, Leipzig.

RAMSDELL (1945), The crystal structure of α-Sic, type VI: *Am. Mineral.*, **30**, 519–525.

——— (1946), The crystal structure of α-SiC, type V (abstract): *ibid.*, **31**, 205.

THIBAULT (1944), Morphological and structural crystallography and optical properties of silicon carbide: *Am. Mineral.*, **29**, 249–278; 327–362.

ZHDANOV (1945), The numerical symbol of close packing of spheres and its application in the theory of close packings: *Compt. Rend.* (URSS), **48**, 39–42.

——— AND MINERVINA (1945), Analysis of the crystal structure of SiC V (51-layered packing): *ibid.*, 182–184.

URANINITE CRYSTALS WITH A NEW FORM FROM PORTLAND, CONNECTICUT*

Austin F. Rogers, *Stanford University.*

Abstract

Euhedral crystals of uraninite from one of the pegmatites at this locality are octahedra modified by the cube, the dodecahedron, and a new form, the tetrahexahedron {520}. The latter is determined on a matrix specimen by measurement on the microscope stage of the plane angle formed on the (520) face by its intersections with (111) and $(11\bar{1})$, which may be expressed as the interzonal angle $[2\bar{5}3] \wedge [\bar{2}53]$.

The uraninite crystals occur on a matrix of feldspar which proves, on optical examination, to be albite with the approximate composition $Ab_{95}An_5$. The albite is a replacement of microcline, which is present in very small amounts as a relict mineral.

Besides the usual cleavages parallel to {001} and {010}, the albite shows fair cleavage parallel to {110}, (no cleavage parallel to $\{1\bar{1}0\}$), and both albite and pericline twin-lamellae, as well as pericline parting.

Introduction

The specimen here described was obtained from Ward's Natural Science Establishment some years ago. It is labeled "Collins Hill, Portland, Conn." An account of the minerals of Strickland's Quarry at Portland has been given by Shannon (1). In view of the present interest in uraninite it seems an appropriate time to describe the specimen.

The specimen consists mainly of buff-colored cleavable feldspar which proves, when examined in thin sections, to be albite. Scattered about the feldspar there is a little pale-green muscovite; some smoky quartz, a little secondary autunite, a few specks of garnet, a fair-sized euhedral crystal of columbite, and, most important of all, the crystallized uraninite.

The Uraninite

The specimen, reduced in size by careful trimming, furnished several euhedral crystals of uraninite varying from 2 to 5 mm. as well as a number of feldspar cleavages. Figure 1 is a photograph of a portion of the specimen after trimming.

The uraninite crystals are octahedra modified by the cube and dodecahedron. One crystal on the matrix (*u* in Fig. 1) shows a few faces of a tetrahexahedron {*hk*0}. This must be a new form since no tetrahexahedra for uraninite are listed in either Goldschmidt's *Atlas* or the seventh edition of Dana's *System of Mineralogy.*

---

* Paper read by title at the 27th annual meeting of the Mineralogical Society of America, Chicago, Dec. 26–28, 1946.

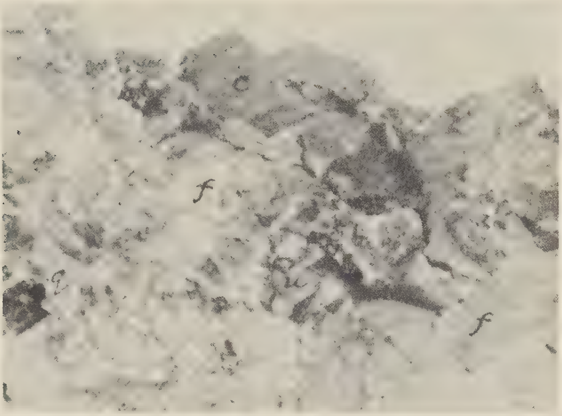

Fig. 1. (×2) Uraninite (*u*) crystal on matrix of feldspar (*f*) (albite, $Ab_{95}An_5$), with columbite (*c*), and quartz (*q*).

In order to keep the museum specimen intact it became necessary to measure the plane angle of the (*hk*0) face on the stage of a microscope. The polarizing microscope with rotating stage may be used as a goniometer with an accuracy intermediate between that attained with a contact goniometer and a reflection goniometer.

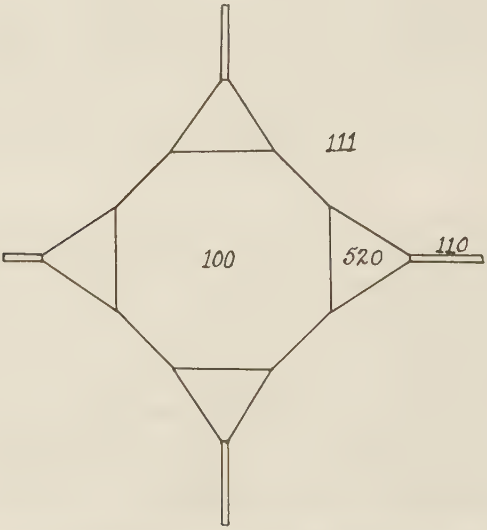

Fig. 2. Front elevation of a portion of idealized uraninite crystal with the forms: {111}, {100}, {520}, and {110}.

Figure 2 is a front elevation of a part of the best crystal. The triangular face is (*hk*0); the most likely form is either {210} or {310}. Figure *3a* is a plan view of the crystal. Figure *3b* is a supplementary drawing made from the plan. The plane angle *etf* on measurement proves to be 21°9′, which is the average of ten values varying from 20°20′ to 22°0 . The calculated value of the interzonal angle $[2\bar{5}3]\wedge[\bar{2}53]$ is 21°2′, which is proof that the {*hk*0} form is {520}.* One has the impression that this is an unusual isometric form, but it is known on the following minerals: copper, diamond, garnet, gold, fluorite, magnetite, perovskite, pyrite, silver, sperrylite, sphalerite (?), and sylvite, according to the data of Goldschmidt's *Atlas*. The zone-symbol of the edge *et* is $[2\bar{5}3]$ and the zone-symbol of the edge *ft* is $[\bar{2}53]$.

The use of plane angles or interedge angles in the determintion of minerals has been emphasized by the writer in a recent paper on braunite (2).

The matrix crystal also shows line faces between (100) and (520), between (100) and (111), and between (520) and (111).

The common forms on uraninite are the octahedron, the cube, and the dodecahedron. The trapezohedron {411} was found on crystals from Cardiff township, Ont., by Parsons (3) and the trapezohedron {533} on crystals from Grafton Center, N. H., by Shaub (4). The complete form-system† for uraninite, then, is: {111}, {100}, {110}, {411}, {533}, and {520}.

According to Dr. J. D. H. Donnay‡ the space group of a crystal of the hexoctahedral class with these forms is O_h^5-Fm3m. Strunz (5*a*) also gives this space group.

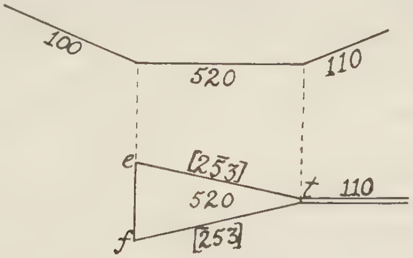

FIG. *3a*. Plan view of a portion of uraninite crystal.
FIG. *3b*. Supplementary projection showing (520) face in its true shape. Plane angle *etf* = $[2\bar{5}3]\wedge[\bar{2}53]$.

---

* For {210} the corresponding interzonal angle $[1\bar{2}1]\wedge[\bar{1}21]$ is 25°12′, and for {310} the interzonal angle $[1\bar{3}2]\wedge[\bar{1}32]$ is 17°58′.

† V. Goldschmidt's name for the totality of forms known for a given crystal species.

‡ Personal communication, Oct. 30, 1946.

The uraninite shows some evidence of imperfect octahedral cleavage or parting, probably the former since there is no sign of any twinning. Seaman (5), who emphasizes cleavage in the determination of minerals, makes no mention of cleavage or parting for uraninite.

The specific gravity of one of the uraninite crystals weighing a little over a gram is approximately 10.0 as determined on a beam balance.

The uraninite gives a bright green $NaPO_3$ bead test in R.F. It also gives a pale yellow NaF bead which fluoresces a bright yellow in the ultraviolet light given off by a silica-glass mercury lamp (6). This sodium fluoride bead test is probably the best blowpipe test for uranium. Heated in a closed tube the uraninite gives a very small amount of water.

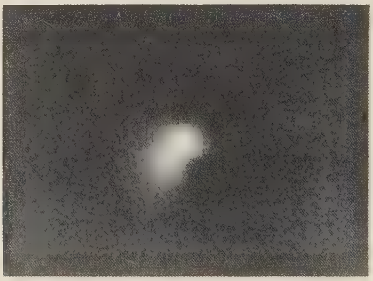

FIG. 4. Radiograph of specimen of Fig. 1.

A spectrographic analysis made by Mr. Kenneth C. Peer of the Multiphase Laboratories of San Francisco gave the following:

U—major constituent
Pb—a few tenths of 1%
Fe—a few tenths of 1%
Si—>a few tenths of 1%, <1%
La—faint trace
Th—present
Zr—a few hundredths of 1%
Al—a few hundredths of 1%
Sr—<0.001%
Ca—<0.001%
Ba—a few hundredths of 1%
Na—trace
Cr—<0.001%
Cb—a few hundredths of 1%
Ta—trace
Ti—a few thousandths of 1%, or less

The uraninite is readily soluble in hot nitric acid. NH_4OH added to the solution gives a yellow precipitate.

The specimen shown in Fig. 1 on a 24-hour exposure to a Wratten photographic plate gave the radiogram reproduced as Fig. 4 at the spot marked "u" which is the uraninite crystal measured.

Additional evidence of radioactivity was furnished by a test with a Geiger-Müller counter. Using a lead shield with an opening placed over "u" in the photograph of Fig. 1, the "clicks" were very noticeable and less evident when placed over "c", the columbite.

The Feldspar

The feldspar proves to be almost as interesting as the uraninite. At sight it greatly resembles microcline, but thin sections prove it to be albite. A few patches of microcline, with the characteristic gridiron structure, oriented parallel to the main albite section are interpreted as evidence that the albite has replaced microcline (see Fig. 5). There is nothing in the thin sections to suggest antiperthite.

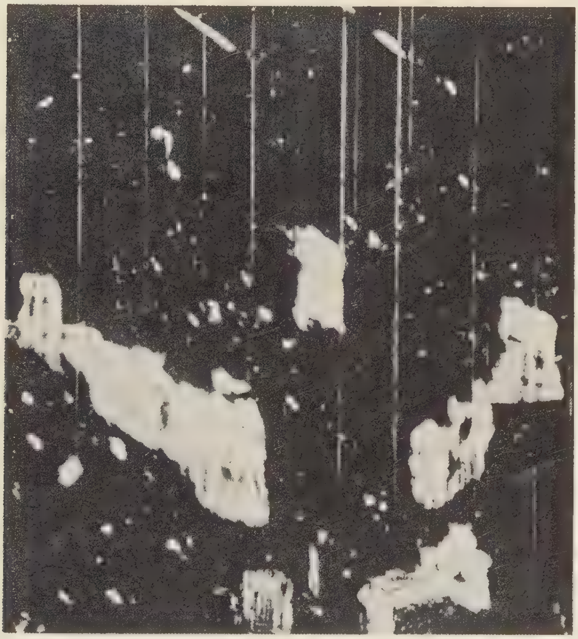

Fig. 5. (×60) Photomicrograph of a thin section of the feldspar cut parallel to (001) to show newly formed albite ($Ab_{95}An_5$) with relict microline.

The feldspar shows perfect (001) and (010) cleavage and imperfect (110) cleavage but no $(1\bar{1}0)$ cleavage. The absence of the $M(1\bar{1}0)$ cleavage, which is usually mentioned for plagioclase feldspars, was verified by the measurement of the $c\ (001) \wedge b(010)$ cleavage angle on a reflection goniometer with four different cleavage fragments. For example, in the specimen represented in Fig. 6 the angle $c\ (001) \wedge b(010)$ is about 86° and so the cleavage face m is (110) and not $M\ (1\bar{1}0)$. If this were $M\ (1\bar{1}0)$, the angle $c\ (001) \wedge b(010)$ would be about 94°. The intersection of the (010) and (110) cleavages determines the c [001] zone-axis and thus enables one to orient the feldspar, as has been emphasized by the writer, (7, p. 206). Faint albite twin-lamellae are noticed on the (001) cleavage face and pericline twin-lamellae are noticed on some portions of the (010) cleavage faces as shown in Fig. 6.

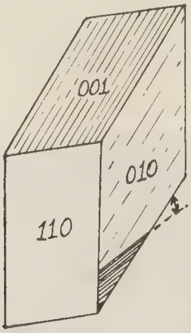

FIG. 6. Albite ($Ab_{95}An_5$) cleavage fragment showing cleavage parallel to {001}, {010}, and {110}, with albite twin-lamellae on (001) and pericline twin-lamellae on (010). The angle of the rhombic section is indicated by the arc.

The angle of the rhombic section, *i.e.*, the angle between the trace of the (001) cleavage and the outcrop of the pericline twin-lamellae measured on the (010) cleavage, is +24°0′ (the average of five measurements varying from +22°50′ to +25°0′). This places the albite at $Ab_{95}An_5$ according to the curve of Schmidt (8) which is reproduced as Fig. 223 on page 245 of Rogers and Kerr (9). This is verified by the extinction angle of +16°0′ (average of ten readings varying from +14°10′ to +16°50′) measured on a thin section cut parallel to the (010) cleavage with the (001) edge as a reference line. There is additional verification in the extinction angle of −13°52′ (average of ten readings varying from −13°5′ to −15°0′), obtained in an oriented section cut normal to the (001:010) = [100] edge. According to Duparc and Reinhard's (10) curve the extinction angle of a section of $Ab_{95}An_5$ cut normal to [100] is −13°0′.

The specific gravity of a specimen of the albite weighing about 18 g. is 2.62, which furnishes a good check on the optical determinations.

ACKNOWLEDGMENTS

I am indebted to Mr. Kenneth C. Peer for the spectrographic analysis, to Mr. James F. McGee for the test with the Geiger-Müller counter, to Mr. Frank L. Hess, formerly of the U. S. Bureau of Mines, for a specimen of antiperthite from Tyee River, Va., which was kindly furnished by Mr. V. V. Kelsey of Tyee River, to Mr. Alexander Tihonravov, Department Technician, for the photographs, and to Professor Charles F. Park, Jr., for a critical reading of the manuscript.

References

1. Shannon, E. V., *Am. Mineral.*, **5,** 51–54 (1920)
2. Rogers, A. F., *Am. Mineral.*, **31,** 561–568 (1946).
3. Parsons, A. L., *Univ. Toronto Studies*, Geol. Series, **32,** 17 (1932).
4. Shaub, B. M., *Am. Mineral.*, **23,** 334–341 (1938).
5. Seaman, W. A., *Mineral Classification According to Cleavage and Crystal Habit*, 4th ed., Houghton, Mich. (**1935**).

5*a*. Strunz, H., *Mineralogische Tabellen*, p. 108, Akad. Verlagsgesellschaft Becker and Erler Kom.-Ges., Leipzig, 1941. (Alien Property Custodian, Edwards Brothers, Ann Arbor, Michigan, 1944).

6. Northrup, M. A., *Industrial and Engineering Chemistry*, Anal. Ed., **17,** 664–670 (1945).
7. Rogers, A. F., *Jour. Geology*, **21,** 206 (1913).
8. Schmidt, E., *Chemie der Erde*, **1,** 400, Fig. 511 (1919).
9. Rogers, A. F., and Kerr, P. F., *Optical Mineralogy*, 2nd. ed., N.Y. (**1942**).
10. Duparc, L., and Reinhard, M., *Mémoires de la Soc. de Phys. et D'Hist. Nat. de Genéve*, **40,** 23, Fig. 10 (1924).

URANINITE AND PITCHBLENDE*

AUSTIN F. ROGERS, *Stanford Univerity.*

ABSTRACT

It is proposed to use the name uraninite for the crystalline (isometric), essentially uranium dioxide (UO_2) mineral, with specific gravity varying from 8.0 to 10.5 and with low water content, and the name pitchblende for its massive or colloform amorphous equivalent (mineraloid) with specific gravity varying from 6.8 up to 8.5 and water content varying from about 2 per cent to 5 per cent.

Uraninite and pitchblende are usually treated as synonyms, sometimes one name being used, sometimes the other.

Some mineralogists have attempted to distinguish (*A*) the distinctly crystalline mineral from (*B*) the massive, often colloform, mineral or mineraloid of lower specific gravity and higher water content. The writer (1), for example, mentions uraninite as the crystalline equivalent of pitchblende. Ellsworth (2) in an important paper, "Rare-Element Minerals of Canada", lists uraninite and pitchblende separately and makes the following statement: "Uraninite is usually crystallized in forms of the cubic system, whereas pitchblende never shows indications of crystal form. Thus it seems advisable to consider these as two different minerals."

Emmons (3) evidently considers uraninite and pitchblende to be distinctive minerals, for he makes the following statement: "Uraninite, pitchblende (a uranium oxide), and carnotite ($K_2O \cdot UO_3 \cdot V_2O_5 \cdot 8?H_2O$) are the chief uranium minerals . . . ."

In the latest edition of Dana's *Textbook of Mineralogy* Ford (4, pp. 45–46) distinguishes (1) crystallized uraninite from (2) massive uraninite, but includes them both under uraninite. Palache, Berman, and Frondel (5, pp. 613–614) adopt the same procedure in the new (7th) edition of *The System of Mineralogy.*

This is the conservative attitude of many mineralogists, but since a fairly sharp distinction can be made between (*A*) and (*B*) it seems reasonable to separate them and to use distinctive names.

Kirsch (6) distinguishes "1. Kristallisierte Pechblenden" and "2. Unkristallisierte Pechblenden." For 1 he uses the name *ulrichite* in honor of the Austrian mining specialist, C. Ulrich, with bröggerite, cleveite, and nivenite as varieties, and for 2 he uses the name *uranpecherz.*

It seems better to use the well-known name uraninite for the crystalline mineral with higher specific gravity and lower water content and pitchblende for the massive mineraloid* with lower specific gravity and higher water content.

---

* Paper read by title at the 27th annual meeting of the Mineralogical Society of America, Chicago, Dec. 26–28, 1946.

Uraninite usually occurs in granite pegmatites, and pitchblende is, for the most part, found in metalliferous veins, but it should be emphasized that intrinsic characters and not geological occurrence should be used in distinguishing and determining minerals and mineraloids.

Of these two important uranium minerals, pitchblende is the more common. It occurs at Jachymov (Joachimstal), Bohemia; Great Bear Lake, Canada; and in the Belgian Congo. Uraninite occurs in pegmatites in Ontario, New England, Norway, Karelia, and India.

Yagoda (8) in an important paper makes a sharp distinction between crystaline uraninite and massive pitchblende. The former has a P_α value (the number of escaping rays per sq. cm. per sec.) varying from 338 to 271, whereas the latter (pure pitchblende) has a P_α value varying from 278 to 246.

I am much indebted to Dr. Yagoda for the opportunity to discuss uranium minerals with him during his recent visit to Stanford University.

References

1. Rogers, A. F., *Introduction to the Study of Minerals and Rocks,* 2d. ed., p. 324, N.Y.' (**1921**).
2. Ellsworth, H. V., *Canada Dept. of Mines Geological Survey,* Econ. Geol. Series, no. 11, p. 45, p. 131 (1932).
3. Emmons, W. H., *The Principles of Economic Geology,* 2nd ed. p. 468, N.Y. (**1940**).
4. Ford, W. E., *A Textbook of Mineralogy* by E. S. Dana, 4th ed., N.Y., pp. 645–646 (**1932**).
5. Palache, C., Berman, H., and Frondel, C., *The System of Mineralogy of J.D. and E. S. Dana,* 7th ed., vol. 1, pp. 613–614, N.Y. (**1944**).
6. Kirsch, G., Tschermak's *Min. u. Pet. Mitth.* **38,** 223–228 (**1925**).
7. Niedźwiedzki, J., *Centralblatt für Min., Geol., u. Paleon.* (**1909**) pp. 661–663.
8. Yagoda, H., *Am. Mineral.* **31,** 92 (1946).

---

* This useful term was introduced by Nied´wiedzki (7).

NOTES AND NEWS

STABILITY ON STORAGE OF THE HIGH REFRACTIVE INDEX LIQUIDS OF C. D. WEST

Brynjolf Bruun and Tom. F. W. Barth,
Mineralogisk Institutt, Oslo, Norway.

The set of high index liquids proposed by C. D. West* consists of mixtures of yellow phosphorus, sulfur, and methylene iodide. They cover a range from 1.74 to 2.06, and have proved themselves decidedly superior to any other immersion substance for this index range. The optical properties (as well as some physico-chemical properties), and directions for preparing them have been given by West, together with remarks on the storage and stability relations as far as he could judge after only 9 months experience with the liquids.

At the Mineralogisk Institutt in Oslo these liquids were successfully prepared in December 1936, and have since greatly facilitated the determination of optical properties of various minerals. The liquids were stored under a layer of water in glass stoppered bottles as described by West.

Table 1. Variation with Time of Refractive Index of Phosphorus Liquids

Dec. 9, 1936; initial value	1.801	1.811	1.824	1.830	1.845	1.852	1.864	1.875	1.906	1.933
Apr. 17, 1939; after 2¼ years	1.8018	1.8111	1.8144	1.8309	1.8417	1.8522	1.8548	1.8756	1.9060	1.9335
Dec. 9, 1941; after 5 years	1.8027	1.8113	1.8143	1.8310	1.8410	1.8521	1.8546	1.8762	1.9052	1.9336
May 18, 1945; after 8½ years	1.804	1.813	1.823	1.832	1.845	1.855	1.857	1.878	1.906	1.936
Dec. 9, 1936; initial value	1.945	1.975	1.980	1.986	2.002	2.004	2.036	2.047	2.049	2.059
Apr. 17, 1939; after 2¼ years	1.9455	1.9753	1.9800	1.9862	2.0021	2.0045	2.0264	2.0373	2.0500	2.0590
Dec. 9, 1941; after 5 years	1.9437	1.9766	1.9816	1.9864	2.0056	2.0086	2.0266	2.0409	2.0520	2.0619
May 18, 1945; after 8½ years	1.945	1.976	1.982	1.988	2.007	2.010	2.027	2.046	2.051	spoiled

The indices were measured in sodium light at 19° C. by minimum deviation using a hollow 51° prism. The figures are correct to the third decimal, but the fourth decimal is uncertain.

It should be of some interest to mineralogists that during all this time (a period of 5 years) the refractive indices of the several liquids have remained reasonably constant as demonstrated by Table 1. A closer inspection of the table shows the following:

---

* West, C. D., Immersion liquids of high refractive index: *Am. Mineral.*, **21**, 245 (1936).

For liquids of the lower range, from 1.80 to 1.95, the variation of the index is almost negligible and frequently within the limits of measurement.

For liquids from 1.97 to 2.06 the index increases slowly but apparently systematically at a rate of about 0.0008 per year.

Thus the stability of the phosphorus liquids on storage is very satisfactory, and it can be concluded that in this respect also, these liquids are excellently suited as immersion media. For the index range covered they are, indeed, in every respect preferable to any other immersion substance thus far known.

Postscript:

Thus far we had gotten on December 9, 1941. Although Norway was occupied by Germany our idea was to send the manuscript to the U. S. with which we at that time still had postal connection.

Well—Pearl Harbor and the American-German war put a stop to all plans. In nazi occupied Norway conditions went from bad to worse; in November 1943 the university was raided by German Police Forces, everybody was jailed and the majority of the students deported to Germany's barbaric concentration camps.

The refractive index liquids, however, remained in their drawer until V-E-Day. In May 1945 they were remeasured by Mr. Chr. Oftedahl. Table 1 has been expanded so as to include his results too.

August 1945.

Post Postscript:

The M.S. sent from Norway to America in August 1945 apparently never reached its place of destination. The mail was at that time subject to censorship and often uncertain. Here it comes.

August 1946.

BERYLLIUM IN PEGMATITES*

Kenneth De P. Watson, *University of British Columbia, Vancouver, B. C.*

Recently, notes have been published on spectrographic investigations of beryllium in pegmatites[1] and in wallrocks of pegmatites.[2] Some fragmentary information on this subject was obtained by the writer in 1944 during a study of some muscovite-bearing pegmatites in the Big Bend area near Golden, British Columbia. In the course of field-work near the head of Yellow Creek, beryl was found in a pegmatite once worked for muscovite. In an attempt to determine whether the presence of this beryl might be suggested by the occurrence of beryllium as a minor element in other minerals nearby,[3] two samples of muscovite, one of biotite, and one of feldspar from the pegmatite, and samples of kyanite and garnet from the adjacent wallrock were selected carefully and were spectrographed. Traces of beryllium were detected in all samples except in one of muscovite and one of feldspar.[4] For comparison, samples of muscovite, biotite, feldspar, quartz, kyanite, and garnet from the Blue River area about 50 miles west of Yellow Creek were spectrographed. Field examination by S. S. Holland of some pegmatites in this region had not revealed any occurrence of beryl. A trace of beryllium was found in the sample of muscovite from Blue River, but it was absent in the samples of the other five minerals. In summary, these meager data suggest that the number of minerals which contain traces of beryllium is greater in the area in which beryl occurs than in the area in which it may be absent.

---

* Published with the permission of the Chief Mining Engineer, British Columbia Department of Mines.

[1] Perry, Eugene S., and Cooke, S. R. B., Spectrographic prospecting for beryllium in pegmatites of western Montana: *Am. Mineral.*, **31,** 499–502 (1946).

[2] Stoll, W. C., The presence of beryllium and associated chemical elements in the wallrocks of some New England pegmatites: *Econ. Geol.*, **40,** 136–141 (1945).

[3] Quirke, T. T., and Kremers, H. E., Rare element prospecting in pegmatites: *Econ. Geol.*, **38,** 173–187 (1943).

[4] Analyzed by Chief Analyst and Assayer, British Columbia Department of Mines.

BULLETIN 950, "CONTRIBUTIONS TO GEOCHEMISTRY, 1942–1945," of the Geological Survey, U. S. Department of the Interior, may be obtained from the Superintendent of Documents, U. S. Government Printing Office, Washington 25, D. C., for forty cents. It includes the following fifteen papers:

Analyses of petroleum coke-ashes. Roger C. Wells. Pp. 3–6.

Studies on the peroxide method for determining vanadium in minerals and ores. Margaret D. Foster. Pp. 7–14.

Separation of small amounts of chromium from vanadium with ethyl acetate. Margaret D. Foster. Pp. 15–18.

A field test for vanadium. Joseph M. Axelrod. Pp. 19–24.

Significance of internal structure in gelatinizing silicate minerals. K. J. Murata. Pp. 25–34.

Symmetrical arrangement of atoms in aluminosilicates and random arrangement of two kinds of objects in a regular array. William G. Schlecht. Pp. 35–82.

A study of methods for the determination of vanadium. Victor North. Pp. 83–90.

Determination of beryllium in ores. Rollin E. Stevens and Maxwell K. Carron. Pp. 91–100.

A system for calculating analyses of micas and related minerals to end members. Rollin E. Stevens. Pp. 101–120.

Composition of roscoelite. Roger C. Wells and W. Wallace Brannock. Pp. 121–128.

A field test for the detection and estimation of tungsten. Victor North and F. S. Grimaldi. Pp. 129–132.

An easily cleaned measure for powders used in spectrography. Cyrus Feldman. Pp. 133–134.

Gravimetric determination of tungsten with brucine. F. S. Grimaldi and Norman Davidson. Pp. 135–138.

A volumetric method for the determination of carbon dioxide. Joseph J. Fahey. Pp. 139–142.

Gamma-ray studies of potassium salts and associated geologic formations. H. Cecil Spicer. Pp. 143–161.

BERMAN MEMORIAL LABORATORY

The Berman Memorial Laboratory in the Department of Mineralogy and Petrography, Harvard University, was dedicated on the evening of November 1, 1946. The laboratory, which is thoroughly modern and has the latest equipment for teaching and research in *x*-ray diffraction, was made possible through gifts by the host of friends left by the late Harry Berman. The dedication was attended by several of the country's leading mineralogists and scientists in allied fields.

At the time of Dr. Berman's death in August 1944 he was on leave from Harvard University, where he was Associate Professor of Mineralogy and Curator of the Mineralogical Museum. He was killed while on a war mission in the British Isles when the transatlantic plane in which he was flying crashed in landing at Prestwick, Scotland.

BOOK REVIEWS

FRITZ EPHRAIM'S INORGANIC CHEMISTRY. Fourth English Edition. By P. C. L. Thorne and E. R. Roberts. Nordeman Publishing Company, Inc., New York, N. Y. Pp. xii and 921. Figs. 95; 1943. Price: $8.75.

The first German edition of this book, which was published by Ephraim in 1922, introduced several innovations. The results of the modern investigations of atomic and crystal structure were taken into account in a systematic way. Much attention was paid to the complex or coordination compounds. A given chemical compound was described together with compounds to which it shows significant interrelations, rather than, as had been customary, in a chapter devoted to one of the elements involved. For instance, calcium carbide is treated not with other calcium or carbon compounds but under the heading "carbides, silicides, and borides: intermetallic compounds." In this way a great deal of information has been presented as concisely as possible. These characteristics and the quality of presentation earned for the numerous German and English editions a leading place among modern textbooks of advanced inorganic chemistry.

The new English edition contains some additions to the broad factual material. Much emphasis has been placed on the electronic interpretation of the structure of inorganic compounds. The authors met a difficult situation in this respect, for widely divergent points of view have been applied to this problem since the appearance of the first edition. In order to arrive at a consistent presentation it would have been necessary either to discriminate among the different theories or to show the connecting links between them. One example, of interest to the mineralogist, namely, the electronic structure of silicates, may be chosen to show how the authors dealt with this problem.

In view of the emphasis on the interrelations between the individual substances, one would expect that the structure of orthosilicate ion $(SiO_4)^{4-}$ be treated in a way analogous to that of the sulfate ion $(SO_4)^{2-}$. The latter is considered in the book from two very different points of view. On p. 231, SO_4^{2-} is derived, as in the former editions, from S^{6+} and four O^{2-} ions and is chosen as an example of a strong deformation of an easily polarizable anion by a strongly polarizing cation. It should be pointed out, that the polarizing power of the ions increases with increasing ionic charge and with decreasing size and the values given on this page for 19 cations and 8 anions run parallel with their (active) polarizing ability and not, as is stated, with their (passive) polarizability. As the measure of the latter, the ionic refraction has to be considered, which for ions of noble gas character of a given charge increases with increasing size.

On p. 575, one finds in the present edition for the first time another description of SO_4^{2-} ion based on the "resonance" considerations of L. Pauling which are reproduced throughout the book in connection with many other compounds. Since these resonance formulas are also given in great detail in the new book by the mineralogist P. Niggli, which is reviewed below, it is not out of place to explain their origin and purpose. The idea of single, double, and triple bonds, which originated in the chemistry of carbon compounds, has been represented by G. N. Lewis (1916) by one, two, and three pairs of electrons respectively shared by the bonded atoms.

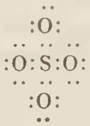

$$\begin{array}{c} \overset{\cdot\cdot}{:\mathrm{O}:} \\ :\overset{\cdot\cdot}{\underset{\cdot\cdot}{\mathrm{O}}}:\overset{\cdot\cdot}{\underset{\cdot\cdot}{\mathrm{S}}}:\overset{\cdot\cdot}{\underset{\cdot\cdot}{\mathrm{O}}}: \\ \underset{\cdot\cdot}{:\mathrm{O}:} \end{array}$$

The formula proposed for SO_4^{2-} on the basis of this covalent theory is reproduced here. This formula was in agreement with another aspect of the theory, an octet of electrons around each atom, and was considered as a satisfactory scheme until Pauling arrived at the conclusion that the internuclear distance S—O does not correspond to the value this formula led him to expect. The latter expectation is based on the postulate of the additivity of "covalent radii." According to this, a single-bond S—O distance should be exactly the sum of half of the S—S distance in the S_8 molecule and of half of the O—O distance in H—O—O—H. Since the distance in SO_4^{2-} is shorter than this sum, a dynamic electron distribution is assumed, such that part of the four S—O bonds have part of the time a "double bond character" represented by four electrons. It is known that the carbon-carbon distance in $H_2C=CH_2$ is shorter than in H_3C-CH_3. There are many possible structures which can be written in this way for SO_4^{2-}; seven of them take up half of p. 575. None of them is supposed to have any reality but the whole is regarded as a "resonance hybrid." This scheme can hardly be considered a simple one and since it is not possible to estimate the contribution of the single resonating structures to the hybrid without arbitrariness, the main goal of the whole method, namely, a quantitative explanation of the S—O distance, cannot be achieved.

The authors do not make any attempt to correlate the SO_4^{2-} treatments on pp. 231 and 575. Furthermore, in spite of the analogy between SO_4^{2-} and SiO_4^{4-}, the discussion of the internal structure of the silicates on p. 826 ff. has little in common with either of the two descriptions of SO_4^{2-}. The formulas $(SiO_3)^{2-}$, $(Si_2O_7)^{6-}$ of the German edition of 1934 are replaced by $(SiO_3)^{II}$, $(Si_2O_7)^{VI}$, etc. On the other hand, while in the 1934 edition the binding within these complexes is represented throughout as Si—O and is called in the English 1939 edition binding of Si and O *atoms*, in the present edition the statement is made that according to the results of W. L. Bragg the silicates have to be regarded as consisting of Si^{4+} and O^{2-} *ions*. Consequently in the subsequent text, Si- and O-atoms are replaced by Si- and O-ions. This constitutes an improvement; unfortunately the remaining text has been left without change, which leads to contradictions. For instance the statement that oxygen neighboring two Si^{4+} "has no free valency and hence is fully saturated towards other ions, the linkage being homopolar as is the linkage of carbon in organic chains" is inconsistent with the assumption of ionic binding as well as with the facts. In the chain structure of enstatite ($MgSiO_3$) the O^{2-} with two Si^{4+} neighbors are *not* "fully saturated," they are approached by one Mg^{++}, although at a distance of about 0.3 Å larger than the distance between Mg^{++} and O^{2-} when the latter has only one Si^{4+} neighbor. These facts can be easily explained from the point of view of polarization and tightening of O^{2-} by adjacent cations but can not be understood from the homopolar (covalent) point of view or on the basis of the idea of definite ionic radii.

The polarization of O^{2-} by Si^{4+} is not mentioned in connection with the structure of silicates although on p. 231 the polarizing power of Si^{4+} is expressed by the high value 26 as compared with the polarizing power of F^- 0.6 which according to p. 39 deforms the K^+ in KF appreciably. The undersigned agrees fully with the statement on p. 39 that "the polarization, distortion and alteration in volume of the ion due to the presence of adjacent ions alters its properties." If so, is it justified to give in the table on p. 36–37 apparent radii of Si^{4+} (0.39 Å) and of S^{6+} (0.34) derived from the experimental distances Si—O and S—O by subtraction of a *constant* value for O^{2-}? This procedure must appear still less appropriate if one realizes that the free O^{2-} is not stable and can exist in compounds only due to the stabilizing influence of adjacent positive ions. It is therefore understandable that the degree of tightening of O^{2-}, which can be measured by the very sensitive optical refraction, depends to a high degree on the surrounding electric fields. Thus it appears most natural to compare the S—O distance in SO_4^{2-} with the Si—O distance in the analogous SiO_4^{4-} and not with the S—S and O—O distances in S_8 and H_2O_2. Since S^{6+} must attract and tighten O^{2-} stronger than does Si^{4+}, one can understand that in SO_4^{2-} the distance, the molar refraction and dispersion are smaller than in SiO_4^{4-}. Thus the assumption of many resonating forms is not necessary for the explanation of the properties of SO_4^{2-}. It deserves to be stated in this connection that the additivity of "covalent radii" is not generally true even in cases which are usually considered as closely analogous: although diamond, silicon and SiC all have the same crystal structure, the Si—C distance (1.883) is smaller by 0.060 Å than the arithmetic mean of the C—C (1.541) and the Si—Si (2.346) distances.

The valence bond theory which originated in the chemistry of carbon compounds has been known for a long time to encounter serious difficulties in the cases of many inorganic compounds. It suffices to mention here B_2H_6 which has a composition analogous to C_2H_6 although boron is tri- but carbon tetra-valent. The attempt to make this theory more satisfactory by introduction of electron pairs and octets and the newest additional assumptions strongly emphasized in the present edition, like resonance, one-electron, three-electron and even no-electron bonds do not improve the situation. (See the following review). Thus it is difficult to avoid the conclusion that the very foundations of the theory of covalency have to be revised and that considerations based on it should be taken with reserve.

The experimental facts, however, are presented in the book in a reliable and interesting way and the newest edition of Ephraim can be warmly recommended in this respect. The carefully prepared index of 33 pages adds to the value of the volume as a reference book.

KASIMIR FAJANS,
Dept. of Chemistry,
Univ. of Michigan

GRUNDLAGEN DER STEREOCHEMIE. By PAUL NIGGLI. Lehrbücher und Monographien aus dem Gebiete der Exakten Wissenschaften. Chemische Reihe. Volume I. Verlag Birkhäuser, Basel. Pp. 283, Figs. 207. 1945. Price: 32.50 Swiss francs.

The well known mineralogist and crystallographer explains in the introduction the purpose of presenting in this volume the Principles of Stereochemistry. He distinguishes three periods in the development of this branch of chemistry.

1. Van't Hoff postulated that the four valences of a carbon atom are directed from the center to the corners of a tetrahedron. Thus he fixed the directions of the hypothetical valence forces and not the real position of the atomic centers. In many cases when the carbon has only three adjacent atoms, e.g., in 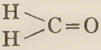 $\begin{matrix}H\\H\end{matrix}\!>\!C=O$ or two, e.g., in $O=C=O$, the valence tetrahedron does not show a direct relation to the atomic positions but can be correlated with them if appropriate assumptions are made. However, in the case of benzene, difficulties arise.

2. Alfred Werner introduced the purely geometric idea of the coordination number of an atom as the number of its nearest neighbors. In the case of the complex compounds, the coordination number is often higher than the normal valency. Werner's distinction between principal and secondary valences did not find justification in the experimental facts.

3. The results of the *x*-ray analysis of crystals have shown that even in such simple compounds as NaCl, one must strictly distinguish between valency and coordination number. This made it necessary, according to Niggli, to develop a stereochemistry which in the first instance investigates systematically all the geometrically possible forms and only then discusses the forces which are responsible for the stability of some selected configurations. This plan has been followed by the author and his associates in a series of papers and the present book gives a review of the results obtained.

The titles of the book's four main chapters and some subtitles will indicate the questions which the author intends to answer.

I. Symmetry relations within configurations of points:
    A. General concepts. Equivalent points. . . . Isomers and formulas expressing the symmetry. . . . Symmetry of vibrations within a given configuration.
    B. Molecular configurations.
    C. One-, two-, and three-dimensional configurations in crystals.
    D. Formulas for configuration of points in crystals.
II. Structural groups within configuration of points.
    A. Homogeneous groups (formed by one kind of points).
    B. Regular heterogeneous groups within A_mB_n.
    C. Structural groups within A_mB_n with variable coordination numbers of a given component.
    D. Structural groups of multiple heterogeneity.
III. Chemical combination of atoms.
    A. Formation of ions and electron pair bond.
    B. Hydrogen bond. One- and three-electron bond.
    C. Relations between the different kinds of binding. Resonance.
IV. Stereochemistry as the study of group formation of atoms.
    A. Molecular configurations in the broader sense. . . . Heteropolar covalent molecules with one positive center. . . . Isomerism. Polymerism. . . . Pseudocrystalline State. . . . Anions of pyro- and poly-acids.

B. Crystalline configurations. . . . Salt-, molecular- and metallic crystals. . . . Complexity of the kinds of binding in crystalline compounds. . . . The concept of type in stereochemistry.

In the purely geometrical Chapters I and II, the interrelations are discussed in a systematic and exact way. The 147 figures, most of them of remarkable clearness, help considerably in the understanding of the text. Several symbols are introduced which characterize the geometric relations.

One of the goals of such a thorough and critical analysis of the geometrical relations should be to assist the physicist and chemist in the choice between existing theories of interatomic forces and to prepare a foundation for the further development of this problem. Chapter III in which one could expect a discussion of this kind contains merely a report on some current views of electronic structure without any attempt to show their relation to the problems of stereochemistry.

The discussion starts on p. 169 with the very appropriate example of CO_2. As the first possibility, the formulation $O^{2-}C^{4+}O^{2-}$ is given and it is stated that the assumption of a complete transfer of electrons from C to O which this formula is commonly thought to indicate, is not adequate. Therefore several covalent resonance formulas (see preceding review) are discussed. A new method of presentation of groups of shared and unshared electrons by numbers instead of points is described. However, the question which is sterochemically of main interest, how the combination of all these resonating forms can lead to the linear structure of CO_2, is not mentioned and would be indeed difficult to answer. The same applies to the internuclear distance. The next example is SO_4^{2-} for which, as in Ephraim, seven covalent forms are reproduced but without explanation of the observed tetrahedral form. Even for $SiCl_4$ twelve covalent forms fill p. 182 although this compound is known to give chloride ions with great ease when in contact with water. This alone would be sufficient to justify the formula $Si^{4+}(Cl^-)_4$. Naturally, due to the strong polarizing field of Si^{4+}, the Cl^- in this compound are tightened to a higher degree than in Na^+Cl^-, as has been unambiguously shown by the molar refraction data. It can furthermore be shown that the formulations $Si^{4+}(Cl^-)_4$ and $S^{6+}(O^=)_4$ explain the tetrahedral shape of these groups. The equilibrium positions of the anions Cl^- and O^{2-} around the central cation are the result of the attraction exerted by the latter and the repulsive forces between the anions themselves. Consequently the anions tend to occupy positions as far as possible from each other, and these are given by the corners of a regular tetrahedron. In a similar way the linear structure of CO_2 follows at once from the formula $O^{2-}C^{4+}O^{2-}$. Naturally the O^{2-}, although its electronic shell is assumed in this formulation to have the quantum configuration of the neon atom, is still more strongly deformed and tightened by the intense field of the small C^{4+} than it is in the silicates by the larger Si^{4+}. Thus from the electric point of view, the formula $O^{2-}C^{4+}O^{2-}$ does not mean a complete transfer of electrons from C to O. Due to the ionic polarization, such complete transfer does not take place even in the typically ionic molecules like NaCl.

The individuality of the two O^{2-} as a definite quantum state is strongly supported by the fact that CO_2 adds a third O^{2-} in an alkaline solution with greatest ease to become a symmetrical planar carbonate ion with OCO angles of 120°. The structure $C^{4+}(O^{2-})_3$ is in best accord with the properties of CO_3^{2-}. Its larger C—O distance as compared with CO_2 is due to the additional repulsion of the third O^{2-}.

Thus the "carbon atom" as such does not have four valences aiming at the corners of a tetrahedron and it is logical to assume that CF_4 has a tetrahedral structure due to the repulsion of the $4F^-$ surrounding C^{4+}. Finally in Be_2C, which has the fluorite structure, each C is surrounded by 8 Be and the idea of four carbon valences represented by four bonds fails completely. The only possible formulation is $(Be^{++})_2C^{4-}$. The main reason why Niggli did not arrive at all these conclusions which relate the geometry of molecules and crystals with their physics and chemistry is that he followed the trend of the last decade in strongly overemphasizing the covalent point of view. On pp. 218–19 the polarization of ions is mentioned but the author does not make use of the applications of this concept to crystal structure which is due especially to V. M. Goldschmidt. Niggli denotes (p. 224) crystallized NaCl as being held by "true" ionic binding, but ScN by covalent binding. However, the fact that ScN has NaCl structure with the coordination number six is much better understood when one ascribes to it the structure $Sc^{3+}N^{3-}$. The polarization of the ions in ScN is naturally much stronger than in NaCl but it is still stronger in $Al^{3+}N^{3-}$ which causes the ions to have the coordination number four, and is extremely strong in $B^{3+}N^{3-}$ with the coordination number three.

On the other hand Niggli recognizes clearly that one has to distinguish strictly between the experimental coordination scheme and the hypothetical valence scheme. Thus he recommends (p. 168) calling the angle of 180° in CO_2 the angle between coordination directions and not the "valence angle." It is of interest to note that for representing the valence scheme of CO_2 the author uses in Fig. 149 the classical spatial diagram with two double bonds and not the resonance structures discussed on pp. 170–172. On p. 203 Niggli writes: "it is not yet possible to see whether it is justified to ascribe to the resonance forms such great importance as is done by Pauling." The reader may be helped in answering this question by the present reviews as well as by the fact that the resonance forms given on p. 180 for B_2H_6 with one-electron bonds have been recently generally abandoned. The undersigned considers the formula

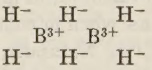

$$\begin{array}{ccccc} H^- & & H^- & & H^- \\ & B^{3+} & & B^{3+} & \\ H^- & & H^- & & H^- \end{array}$$

as the best representation of this molecule, which for many years was an enigma of the covalent theory.

Chapter IV is a combination of the points of view of geometric character with those pertaining to the nature of chemical binding. It contains many facts of interest for the crystallographer as well as for the chemist. The praise of the figures of Chapter I and II cannot be fully extended to those in Chapter IV. Many of them are photographs of models and some contain such a large number of spheres representing the atoms and wires indicating axes as well as bonds that they can hardly help in the understanding of the structures.

The text does not contain specific references to the literature, which however are given at the end of the book in three parts, each arranged alphabetically. Not all authors' names mentioned in the text are to be found in the references.

The main value of the book consists in the extension to molecules of the exact geometric relations developed during the last thirty years in the field of atomic structure of crystals.

Kasimir Fajans,
Dept. of Chemistry,
Univ. of Michigan

RÖNTGENOGRAPHISCH—ANALYTISCHE CHEMIE. MÖGLICHKEITEN UND ERGEBNISSE VON UNTERSUCHUNGEN MIT RÖNTGENINTERFERENZEN IN DER CHEMIE. By E. BRANDENBERGER. Lehrbücher und Monographien aus dem Gebiete der Exakten Wissenschaften. Chemische Reihe. Volume II. Verlag Birkhäuser, Basel. Pp. 287, Figs. 120; 1945. Price: 28.50 Swiss francs.

According to the author the book is a counterpart to that of P. Niggli reviewed above and is intended to deal with the methods and possibilities of chemical and especially stereochemical investigations by means of x-ray diffraction. The titles of the eight main chapters and a few subtitles indicate the general content of the book.

I. The nature of the crystals. Molecular and crystalline compounds.
II. Methods of x-ray investigation of crystalline substances.
III. Crystalline and amorphous phases.
IV. X-ray diffraction patterns as criterion of crystalline types—Methods of determination of crystalline types by x-rays.
V. Roentgenographic analysis of mixtures and exploring of the composition of complex systems.
VI. X-ray and electron diffraction patterns as criterion of the state of the crystal—in respect to particle size, mosaic structure, texture, condition of the surface, etc.
VII. X-ray diffraction as means of investigation of transformations and chemical reactions in solid state.
VIII. X-ray diffraction as criterion of the constitution of solids (determination of crystal structure by x-rays). General procedure of a crystal structure determination. . . . Crystal-chemical characterization of atoms and ions and their importance for crystal structure determinations. . . .

As can be seen, the author deals with many sided applications of x-ray diffraction in crystals to chemical problems. The x-ray spectra of the elements as a means of qualitative or quantitative chemical analysis are not treated, as the title of the book "Roentgenographic—analytical chemistry" might lead one to expect. The subtitle given above "Possibilities and Results of Investigations by X-ray Diffraction in Chemistry" comes closer to the content of the book. The selection of the topics is very appropriate and their presentation instructive and interesting. Paper, print and figures are excellent. The references to the literature are given in an original way. At the end of each of the Chapters II to VI follows a list of references including the full title of the papers involved. Chapter VII contains such a list after each of the four subdivisions. For instance, on pp. 176–197 are treated "tarnishing and analogous processes." In the text, no author's name is given in this section; however, pp. 198–199 contain 29 references. Their order is neither alphabetical nor chronological but after each title a short explanation is given concerning the method of investigation the paper is suppose to illustrate. The paper of W. H. Taylor, "The structure of analcite" is characterized as "Example of investigation by x-ray diffraction of a dehydration process and of a base exchange." Thus the book can serve as a guide for the selection of appropriate methods of investigation. In view of the increasing importance of the applications of x-ray methods it should prove to be very useful.

It deserves mentioning that the implications of Table VI, in which ionic radii are given with two decimal places, do not conform to the present knowledge and to the critical remarks in the book of Niggli (pp. 225–226) about the lack of exact additivity of internuclear distances. For instance, 1.12 Å is given as the radius of Hg^{2+} for the coordination number six. This value was derived in 1926 on the assumption of additivity from an approximate evaluation of the Hg^{2+}—F^- distance in HgF_2. However, the coordination number of Hg^{2+} in HgF_2 is not six but eight. In the molecular structure of $HgCl_2$, Hg^{2+} has six neighbors, but the octahedron formed by the six Cl^- is far from regular, the Hg^{2+}—Cl^- distances being 2.23, 2.27, two at 3.34 and two at 3.63, which by subtraction of 1.81 for Cl^- would give for Hg^{2+} values between 0.42 and 1.82 Å. Obviously, due to the high polarizability of Cl^- and Hg^{2+} and the high polarizing power of Hg^{2+} the ions interpenetrate each other strongly and are far from spherical. A similar situation is found in $HgBr_2$ and in cinnabar. A definite "radius" of Hg^{2+} for the coordination number six does not apply to any compound of known structure. It would have been more instructive and more exact to give the present experimental value 2.40 Å of the internuclear distance in HgF_2 and the above facts about $HgCl_2$ than a hypothetical radius of Hg^{2+}.

KASIMIR FAJANS,
Dept. of Chemistry,
Univ. of Michigan

THE ART OF GEM CUTTING by H. C. DAKE AND R. M. PEARL. Pp. 128, figs. 55, 6″×9″, paper. Mineralogist Publishing Company, Portland, Oregon. 1945, Price $1.50.

The Art of Gem Cutting is designed primarily for the "amateur" gem stone cutter and is an extension of an earlier edition first issued in 1938. Following a brief description of gem cutting as a hobby, the methods for cabochon and facet cutting are given in detail in parts I and II. The fundamentals of the scientific aspects of gemology are discussed in part III. Part IV is entitled Special Lapidary Technic and includes short articles by H. L. Luoma, E. P. Van Leuen, Ralph Dietz, and E. F. Montgomery. This inexpensive publication contains much useful information and should appeal greatly to the amateur gem cutter.

EDWARD H. KRAUS